Remote stereocontrol of chiral NHC metal complexes by stereodynamic Aib foldamers and application to enantioselective hydrosilylations

A thesis submitted to The University of Manchester for the degree of Master of Philosophy

in the Faculty of Science and Engineering

YEAR OF SUBMISSION 2021

Heng Zhong

School of Natural Sciences/Department of Chemistry

Supervisor: Dr Simon Webb

Contents

Abbreviations

AcOH – Acetic acid

Aib - α-Aminoisobutyric acid

Boc – *Tert*-butyloxycarbonyl

BQPA - *N*, *N*-bis(quinolin-2-ylmethyl) -*N*-(pyrid-2-ylmethyl) amine

^{t}Bu – *Tert*-butyl

Cbz – Carboxybenzyl

CD – Circular dichroism

COD – Cyclooctadiene

DCM – Dichloromethane

DIPEA – Diisopropylethylamine

Dipp – 2,6-diisopropylphenyl

DMF – Dimethylformamide

DMSO – Dimethyl sulfoxide

EDC·HCl - *N*-Ethyl-*N*′-(3-dimethylaminopropyl) carbodiimide hydrochloride

EtOAc – Ethyl acetate

EtOH - Ethanol

GPCR - G-protein coupled receptors

Hex – Hexane

HOBt – Hydroxybenzotriazole

Leu – Leucine

M – Left-handed screw sense

Me – Methyl

MeOH – Methanol

MTBE –Methyl tert-butyl ether

NBD – Norbornadiene

NEt_3 – Triethyl amine

NMR – Nuclear magnetic resonance

OEC – Oxygen equilibrium curve

P – Right-handed screw sense

PE – Petroleum ether

Phe – Phenylalanine

PMA – Phosphomolybdic acid

PPh_3 – Triphenyl phosphine

RT – Room temperature

TFA – Trifluoro acetic acid

TLC – MS – Thin layer chromatography mass spectrometry

TPPO – triphosphine oxide

TMS – Trimethylsilane

UV – Ultra-violet

Val – Valine

VT – Variable temperature

Abstract

A series of Aib_4-imidazolium bromide salts have been prepared by alkylation of 1-substituted imidazole compounds with the corresponding α-aminoisobutyric acid foldamer. These salts are precursors for the synthesis of series of rhodium(I) complexes containing bulky oligomer and alkyl functionalized N-heterocyclic carbenes (NHCs). The novel rhodium(I) complexes [RhCl(COD)(NHC)] [COD = cyclooctadiene, NHC =1-R_1-3-R_2-imidazolin-2-ylidene; R_1= Me, Ph, Mes; R_2 = N_3Aib_4Et, Cbz-L-(αMeVal)Aib_4Et], contain on one nitrogen a bulky alkyl substituent and on the other an Aib foldamer substituent. The catalytic activity of the Aib rhodium(I) complexes in the hydrosilylation of carvone with H_2SiPh_2 and terminal alkynes with $HSiMe_2Ph$ have been investigated, and the dependence on the N-terminal functional groups of the Aib foldamer portion has been determined.

Declaration

That no portion of the work referred to in the thesis has been submitted in support of an application for another degree or qualification of this or any other university or other institute of learning.

Copyright Statement

i. The author of this thesis (including any appendices and/or schedules to this thesis) owns certain copyright or related rights in it (the "Copyright") and s/he has given the University of Manchester certain rights to use such Copyright, including for administrative purposes.

ii. Copies of this thesis, either in full or in extracts and whether in hard or electronic copy, may be made only in accordance with the Copyright, Designs and Patents Act 1988 (as amended) and regulations issued under it or, where appropriate, in accordance with licensing agreements which the University has from time to time. This page must form part of any such copies made.

iii. The ownership of certain Copyright, patents, designs, trademarks and other intellectual property (the "Intellectual Property") and any reproductions of copyright works in the thesis, for example graphs and tables ("Reproductions"), which may be described in this thesis, may not be owned by the author and may be owned by third parties. Such Intellectual Property and Reproductions cannot and must not be made available for use without the prior written permission of the owner(s) of the relevant Intellectual Property and/or Reproductions.

iv. Further information on the conditions under which disclosure, publication and commercialisation of this thesis, the Copyright and any Intellectual Property and/or Reproductions described in it may take place is available in the University IP Policy (see http://documents.manchester.ac.uk/DocuInfo.aspx?DocID=2442 0), in any relevant Thesis restriction declarations deposited in the University Library, the University Library's regulations (see http://www.library.manchester.ac.uk/about/regulations/) and in the University's policy on Presentation of Theses.

Acknowledgements

I would like to express my gratitude to all those who helped me during the writing of this thesis. My deepest gratitude goes first and foremost to Dr Simon Webb, my supervisor, for his constant encouragement and guidance. He has walked me through all the stages of the writing of this thesis. Without his consistent and illuminating instruction, this thesis could not have reached its present form.

I also owe a special debt of gratitude to all the members of the Webb group, who all welcomed me so warmly in September and have been a pleasure to work and socialise with. I should finally like to express my gratitude to my beloved parents who gave me a lot of encouragement.

1 Introduction

Foldamers are a class of folded oligomer that adopt well-defined conformations. Some foldamers are non-static and show a dynamic equilibrium of conformers. These dynamic foldamers have promising properties for the biomimicry of allosteric proteins and receptor proteins. Chemical signals can be translated through foldamer conformational changes into chemical outputs such as reactivity changes and/or spectroscopic signals. Allosteric enzymes for example show exquisite selectivity and rely on communication of information through long distances to its active site. Some synthetic dynamic foldamers can mimic this shape change of enzymes by conformational changes in intramolecular hydrogen-bonds whose properties are determined by terminal functional groups. For example, 2-aminoisobutyric acid (Aib) foldamers are well-established class of synthetic dynamic helical foldamers that can transfer chiral information through changes in helical conformation, both in solution and membranes. In this project, Aib foldamers will be designed as artificial enzymes. The foldamer will be attached to a metal catalyst in order to study the influence of helical chirality on the reactivity and selectivity of this catalysts. The catalysts will be tested with diastereoselective and enantioselective reactions and the results will be used to evaluate the extent of chemical information transmission down the helical foldamer.

1.1 Dynamic helical foldamers

Nature relies on large molecules to perform complicated chemical operations, such as catalysis, specific binding, molecular recognition and information storage. The polymers that undertake these critical tasks, mainly proteins and sometimes RNA, are unique because they adopt specific compact conformations that are thermodynamically and kinetically stable. Most of the backbone atoms of the folding molecules are fixed in spatial positions. Functional groups are arranged in a precise three-dimensional geometry and the folding pattern can generate active sites widely spaced along the polymer backbone.[1]

Foldamer is used as the term to describe those extended synthetic molecules (oligomers or polymers) that have strong tendency to fold into well-defined compact conformations. An important foldamer example is protein, and its compact conformation arises from the assembly of elements of regular secondary structures

such as helices, sheets and turns. Many artificial foldamers of diverse backbones (*e.g.* oligopeptides, oligonucleotides, oligoureas, polyisocyanates, nucleic acids, hydrocarbon chains) can mimic structural motifs such as helices, sheets, columns and cavities in solution and have key conformational characteristics providing them with biomimetic functions. [1,2]

Helices, for example in polymers, are well-defined conformations constructed by small units based on self-assembly and/or superamolecular assembly through non-covalent bonding interactions such as hydrogen bonding, π – π stacking, ion-dipole, electrostatic interactions, and their combinations.[3] The structure of the helices and their helical screw senses can be clearly revealed by techniques such as scanning force microscopy (SFM), atomic force microscopy (AFM) and transmission electron microscopy (TEM) combined with circular dichroism (CD).

A helix has an intrinsic, rigid helical shape and can be separated into *P* (right-handed) and *M* (left-handed) enantiomeric forms.[3] Some natural and artificial polymers which consist of enantiomerically pure chiral monomers prefer a single-handed helix, such as right-handed DNA double helix.[2] In early investigations of artifical helices, one helical column oligomer built from chiral monomers was found to be stable in apolar solvents, where the helical oligomer stabilized by solvate molecule[3] The screw sense of the helical oligomer is represented by the complexed guest solvate molecules. A number of achiral monomers are also reported to build up stable but racemic helical oligomers or polymers. Polyisocyanate is the example which can fold into a one-handed helix configuration in water by interactions between the polyisocyanates and an optically active amine.[2]

The interconversion of polyisocyanates between enantiomeric conformations is described as a dynamic phenomenon. Dynamic foldamers have low energy barriers for helical reversal.[2] However, only a few classes of achiral polymer can interconvert rapidly between enantiomeric conformers in solution. The inverting helices are considered as configurationally achiral, because even though the global conformation (e.g. *M* and *P* screw senses) is chiral, there are no configurationally stable stereochemistry elements.[2]

Controlling the interconversion between conformations in dynamic foldamers by applying stimuli is an attractive feature to build stimuli responsive biomimetic

systems. Therefore, many efforts have been put into investigating control of the helical sense of the dynamic structures. Meijer *et al*. reported dynamic helical foldamers composed of OPVUT (oligo(p-phenylenevinylene, OPV) equipped with ureidotriazine) monomers had one helical sense favoured in a chiral solvent although the efficiency is low (Figure 1a).[4] Weschel *et al*. reported a dynamic oligourea foldamer based on hydrogen-bonds between urea residues that adopts high population of *M* screw sense enantiomer in organic solvent. The major conformer can change from *M* to *P* by adding phosphate which will interact with terminal group of helix. (Figure 1b).[2]

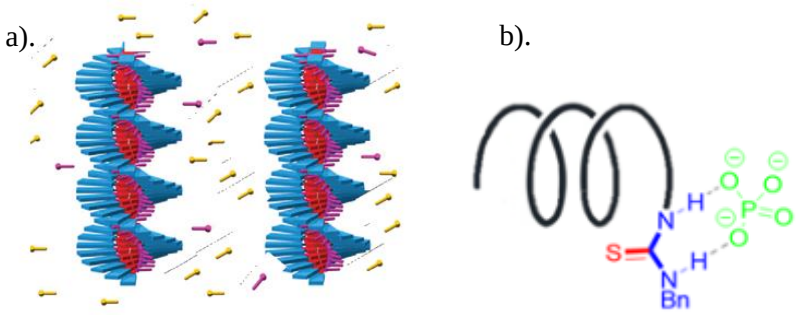

Figure 1. a). Chiral helical OPVUT oligomers (blue and red) induced by R-citronellol (pink) in methyl cyclohexane (yellow); b). M conformer favored oligurea foldamer induced by interaction of terminal thiourea and phosphate.

For helical foldamers built from achiral monomers, an intramolecular chiral controller is the most efficient way to amplify one helix enantiomer over the other. Regardless of the influence of solvent, an oligomer of achiral monomer units adopting a helical structure exists as a rapidly interconverting racemic mixture of *M* and *P* enantiomers (Figure. 2a). Introduction of a terminal chiral controller can induce an equilibrium bias

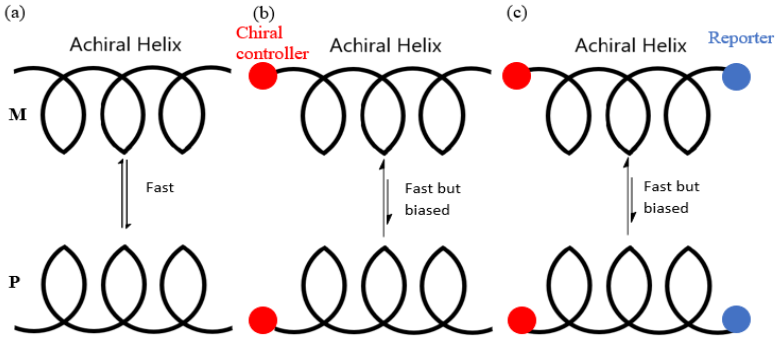

Figure 2. Control and detection of helical preference in an achiral oligomer a). equilibrium in helical conformers without bias; b). helical preference induced by terminal chiral controller; c). detection of helical preference.

and increase the proportion of one preferred helical conformer. (Figure 2b) With a reporter (Figure 2c) e.g. at the other terminal, the resulting propagation preference can be directly reported by UV or NMR spectroscopy.[2]

1.2 2-Aminoisobutyric acid foldamers

2-Aminoisobutyric acid (Aib) is an achiral amino acid monomer that can provide oligomers that fold into 3_{10} helices. In nature, peptaibols are biologically active peptides that are rich in Aib and function as antibiotics and antifungal agents. These peptaibols embedded in the bilayers create ion channels, so understanding their helical conformation helps to clarify the biological activity of these Aib-rich peptides.[6]

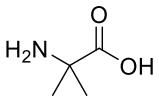

Figure 3. α-Aminoisobutyric acid (Aib)

Aib is a non-proteinogenic achiral amino acid with a *gem*-dimethyl α-carbon (Figure 3). Aib foldamers are artificial oligopeptides made of the achiral Aib monomer, which can adopt 3_{10} helical conformations (Scheme. 1) due to the Thorpe-Ingold effect. 'C^{α}-tetrasubstitution tends to bring the nearby atoms on both sides of the substituted carbon in close proximity' through bond angle compression.[3,7] The 3_{10} helix is characterised by an intramolecular hydrogen-bonding pattern (C=O of residue i and NH of i + 3). Each 3_{10} helix is enclosed in a ring connected by a hydrogen bond and contains three residues, 10 atoms which include hydrogen atom. Aib foldamers made of only non-chiral Aib monomers have no preference for *M* or *P* screw sense (racemic mixture of *M* and *P* enantiomers) and their conformational interconversion happens on a timescale of milliseconds or less over an energy barrier of inversion of screw sense ($\Delta G^{\ddagger}$ = 46 kJ mol^{-1} at -8 ^{o}C).[3,6,7] This value is much lower than that observed for α-

helices. Influencing the screw-sense preference therefore provides a molecular switch, with the message carried being chiral information.[3]

Helicity is distinct other secondary structures, such a linear, zig-zag, or random coil alternative, while screw sense is used to refer to each enantiomeric conformation of the entire helical secondary structure.

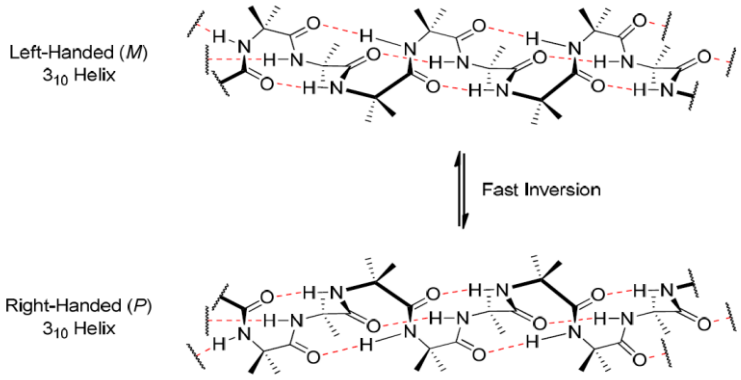

Scheme 1. Interconversion between (*M*) and (*P*) enantiomers of an Aib homo-oligomer adopting a 3_{10}-helix.

1.3. Control of Aib foldamer conformation

1.3.1. Quantification of helical excess for Aib foldamers with a screw sense preference

The induction of a screw sense preference in an Aib oligopeptide has been investigated both in solution and in the crystal state by incorporating a chiral controller at a terminus (N- or C-) or at an internal position of an Aib oligopeptide.[8] The incorporation of a chiral controller induces a local conformational preference that is relayed along the foldamer, leading to a change in the distribution of *M* and *P* helix population as the resulting diastereoisomers have different energies. The absolute screw sense preference can be obtained by X-ray diffraction. Relative values of screw sense preference are obtained from comparison of NMR and/or CD spectra of foldamers with different chiral controllers.

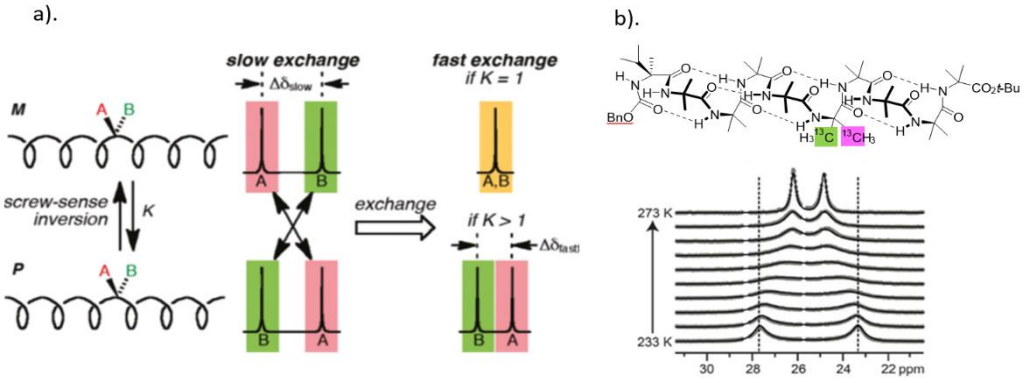

Figure 4. (a) Coalescence of equally and unequally populated pair of enantiomeric conformers; (b) ^{13}C NMR spectra of Cbz-L-ValAib$_4$Aib**Aib$_4$OtBu in CD_3OD, where Aib is the labelled monomer.

Webb, Clayden and their research teams have developed NMR spectroscopy methods to quantify the helical excess for those compounds. The methods are necessary to evaluate the efficiency of stereochemical information transfer along the helix in solution and in membrane. A screw sense preference in Aib foldamers carrying a terminal chiral controller can be detected by the NMR spectra of nuclei (*i.e.* ^{1}H of glycinamide CH_2, ^{13}C of Aib with labeled $^{13}CH_3$, ^{19}F of Aib of 2,2-difluoroAib) which become diastereotopic in the helical environment. This is called AB system, as A and B are used to distinguish two nuclei.[2,13] When the AB system consists of two methyl groups, the helical excess can be calculated from the chemical shift difference of the carbon signals.[13] The mechanism can be explained using the case of Aib oligomers without a chiral controller. If the screw sense of the helix inverts slowly (at low temperature 233 K), the two methyl groups will show two resolvable signals for each carbon, with chemical difference $\Delta\,\delta_{slow}$ (in Hz). If the screw sense of the helix inverts rapidly (e.g. at higher temperature 273K) on the NMR timescale, the two signals will coalesce (Figure.4a upper), namely $\Delta\delta_{fast}$ is 0. The situation is different if the two helical conformers are equilibrium but not in equal population. The spectrum of slowly interconverting is similar to the equally populated system, while at fast interconversion (e.g. raising temperature from 233 K to 273 K) will lead not to single signal, but to two new signals with chemical difference $\Delta\,\delta_{fast}$ (Figure.4a bottom).[13] Figure 4b shows part of ^{13}C NMR spectra of Cbz-L-ValAib$_4$Aib**Aib$_4$OtBu in CD_3OD and with temperature increasing, the labelled ^{13}C signals showed the trend of coalescence. Therefore, the ratio of $\Delta\,\delta_{fast}$ / $\Delta\,\delta_{slow}$ =([*P*] - [*M*]) / ([*P*] + [*M*]), where *K* = [*P*] / [*M*]

(provided anisochronicity is temperature-independent). The quantity of $\Delta\delta_{fast}$ / $\Delta\delta_{slow}$ is termed as the 'helical excess' (by analogy to 'enantiomeric excess').[14]

This method can be applied to ^{1}H-containing, ^{13}C-containing reporters and ^{19}F-containing NMR reporters. The proton AB system commonly is glycinamide or its analogues, such as thionoglycine.[9,10] AibCH_2OH is also a ^{1}H-containing reporter can be put at the C-terminus, where methylene group displays a similar AB system and pattern as the glycine group in ^{1}H NMR spectrum. Diemer *et al*. introduced dibenzazepinyl urea to the helix terminus as a dual ^{1}H NMR and chiroptical probe (Figure. 5). Dibenzazepinyl urea contains two methylene groups that each form AB systems with proton signals locate from 4.6 to 4.1 ppm in ^{1}H NMR spectra and two phenyl groups able to report on *M* and *P* torsion using the 250 nm band in CD spectra.[11] Much like doubly ^{13}C labelled Aib** with both methyl groups labelled, singly labelled Aib residue can also show clear coalescence. When comparing different screw sense preferences, singly labelled Aib residue can show the difference between *M* and *P* (Figure. 6). For example, the foldamer with doubly ^{13}C labelled Aib displays two strong diastereotopic peaks at δ =26.01 and 24.69 ppm. At the same chemical shift, singly ^{13}C labelled Aib shows difference ratio which obviously indicates screw sense preference. However, the magnitude of the helical excess is not accurate by compare ^{13}C peaks integration. The magnitude of the helical excess should be calculated by coalescence method and screw sense preference is indicated by CD spectrum.

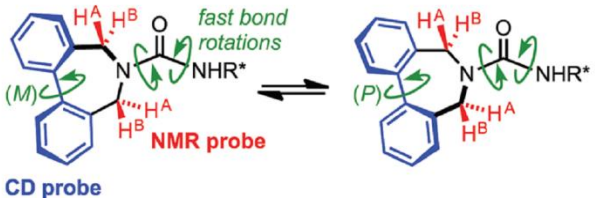

Figure 5. Terminal dibenzazepinyl urea is used as dual CD and NMR probes. R* represents the helical Aib oligomer.[11]

Each reporter group has its own advantages and disadvantages. Doubly and singly ^{13}C labelled Aib monomer are clearly identifiable in the NMR spectrum, but the probe must be synthesized from relatively expensive $^{13}C_2$-acetone. Glycinamide and 2-amino-2-methylpropan-1-ol (AibCH_2OH) can display complicated AB system but are relatively easier to synthesis. Glycine-based reporters can also be allocated at either terminal or middle of Aib foldamers. However, in the ^{1}H NMR spectrum, CH_2 signals

may be obscured by other overlapping signals. Aib foldamers containing glycine also tend to have lower solubility than related structure. [14]

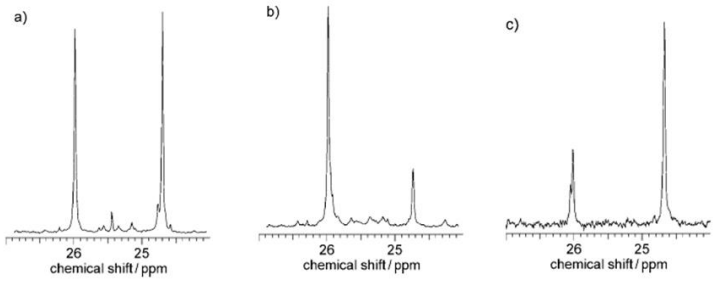

Figure 6. Portion of ^{13}C NMR spectra of Aib tetramer with C-terminal labelled Aib residue a). doubly labelled ^{13}C Aib shows two strong diastereotopic peaks at δ = 26.01 and 24.69 ppm; b). singly labelled ^{13}C Aib in *M* favoured Aib tetramer and c). *P* favoured Aib tetramer, precisely coincident with those of a) but different in ratio.

Pike *et al.* nvestigated a more versatile fluorine probe that combined the advantages of other reporters, e.g. convenience in synthesis and free from other overlapping signals. The fluorine reporters are fluorinated Aib analogues (Figure 7a) and fluorine reporter containing rigid aromatic rings to maximise anisochronicity (Figure 7b). These fluorinated reporters can display greater anisochronicity than analogues for reporting by ^{1}H NMR, but not as great as ^{13}C NMR reporters.

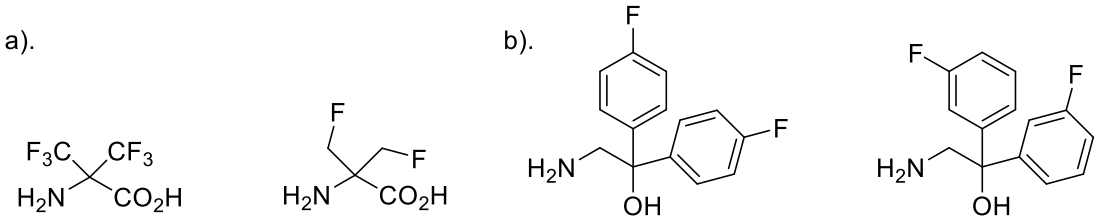

Figure 7. a). Fluorinated Aib probes and b). Fluoroarene probes.

Fluorescent probes compatible with membrane environments were developed to detect the real-time conformational changes of Aib foldamers in membranes. A bis-pyrene motif was introduced as the excited dimer (excimer) which has a broad emission (425-550 nm), has emission that varies according to the proximity of the two pyrene moieties. Conformational changes of Aib foldamers allows the two pyrene rings to move relative to each other, modulating the intensity of the excimer emission. A successful probe will exhibit a difference in the ratio of excimer to monomer emission (E/M ratio) when Aib foldamers bearing a chiral controller favour one of the screw-sense conformers. Lister *et al.* reported their bis-pyrene probes on the C-terminus of Aib_4 foldamers gave an E/M ratio of 1.05 for *M* conformer, 5.50 for *P* conformer and 2.50 for racemic mixture in organic solvent. In the bilayer, the bis-pyrene probe

displayed differences in the E/M ratio of *M* and *P* conformers of different foldamers, indicating modulation of the chiral induction by the bilayers.[15] Nonetheless, Lister *et al*. reported successful application of this pyrene probe in membrane phase, where it reflected conformational changes transmitted through an Aib foldamer to the bis(pyrene) site remote from the N-terminal binding site.[26]

1.3.2. Control of screw sense by an intramolecular 'chiral controller'

Because Aib is achiral, helical oligomers containing only Aib residues display no screw sense preference and undergo rapid conformational inversion. However, the dynamic equilibrium can show a bias towards one favoured screw-sense conformer by incorporating a chiral residue at the helix terminus. With the use of a reporter, the helical excess can be calculated through NMR and/or fluorescence spectroscopy. Screw sense preference can be also determined by CD spectroscopy. X-ray crystallography can demonstrate the bonding interactions between monomer units and interactions between terminal chiral controllers and helical chains.

In nature, the antibiotic fungal metabolites cephaibols are compounds rich in Aib and fold in right-handed helical conformation in the solid state.[17] These peptides all have a similar sequence of five or more achiral amino acids, Aib_4-Gly and chiral residues L-Phe (L-Phenylalanine) and L-Leu (L-Leucine) at N- and C-terminus, respectively. Ugo *et al*. imitated this structure and synthesized a series of compounds switching the configuration of chiral residues (e.g. replace L-Phe and D-Phe at N-terminus) to investigate how the N-terminal residues of cephaibols induce a right-handed helix. They found L-Phe is a left-handed chiral controller, while the cephaibols maintain their screw sense by matched chiral controllers working together. This was also observed in the synthetic peptides with N-terminal L-Phe and C-terminal D-Leu residue pairs. Although its screw sense is opposite from the original cephaibols, this foldamer displayed greater resistance to conformational inversion in polar solvents than those with mismatched chiral controllers (e.g. L-Phe and L-Leu).[17]

As both N- and C-terminal chiral controllers can affect the screw sense preference of the Aib foldamers, Clayden's group compared the efficiency of chiral amino acid inducers at both termini. They capped Aib_8 and $Aib_8GlyAib_8$ oligomers with different chiral controllers with the central Gly as the reporter. L-Phe (in the form of Cbz-L-Phe at N-terminus and L-PheOMe and L-$PheNH_2$ at C-termiuns) was introduced to

the oligomers, and the extent of screw sense preference is illustrated by the glycine AB system. The chemical shift demonstrated that the N-terminal Cbz-L-Phe has more propensity to control screw sense preference than its analogous residue (L-PheOMe and L-PheNH$_2$) at C-terminus. It is also found that the amide-capped C-terminal chiral residue provides a greater screw-sense bias than an ester-capped chiral residue.[6]

Oligomers composed of only the achiral amino acid Aib adopt a helical conformation stabilized by hydrogen bonds, a 3_{10} helix, without preference of screw sense. The consecutive hydrogen bond pattern in a 3_{10} helix matches that in a peptide β-turn involving four residues. Various type β-turn can induce different torsion angles around Aib residues and subsquent hydrogen bond pattern, thus propagating a left- or right-handed screw sense. Poli *et al*. investigated N-terminal tertiary L-valine and quaternary L-α-methylvaline (L-*α*MeVal) group, which induce opposite screw sense preferences through the relative opposite β-turn patterns. Using analysis by x-ray crystallography diffraction and NOESY, the influence of the chiral amino acid can be illustrated by the Newman projection of the first turn (Figure 8). A type II β-turn allows the tertiary L-Val and the first Aib to form an unhindered gauche conformation (Figure 8a) and left-handed screw sense, while the quaternary L-*α*MeVal prefers a type III β-turn for a less sterically affected (Figure 8b) right-handed screw sense.[5] The hydrogen bond pattern is transmitted through the 3_{10} helix, which allows the chiral information to be transferred from one terminus to the other.[5]

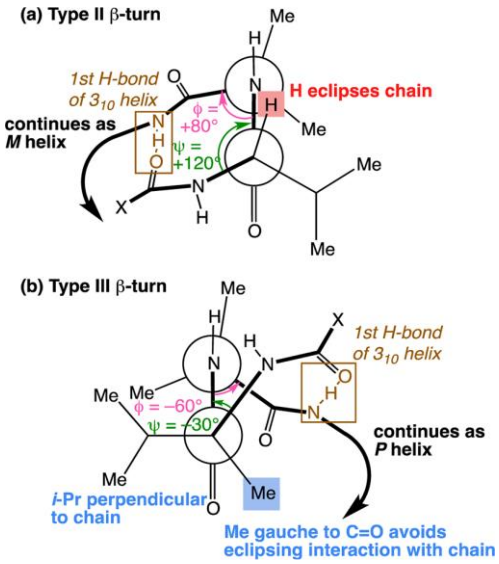

Figure 8. Newman projections of chiral controller and following residues (Aib) from the N-terminus display different types of β-turn of Aib helix. (a) Chiral controller is L-Val and (b) is L-(αMe)Val. X = Me.[5]

Based on the mechanism of β-turn induced screw sense preferences, Poli *et al*. also found N-terminal L-Phe can induce a left-handed screw-sense preference and the D-Phe is the right-handed screw sense inducer. They also reported a second chiral amino acid can reinforce the preference. Foldamer Cbz-(L-*α*-Me-Val)$_2$Aib$_4$GlyNH$_2$ which contains two quaternary L-α-methylvaline groups displayed almost perfect right-handed helix in solid state, with a helical excess of 95 %.[16]

1.3.3 Determination of how far the screw sense preference can be relayed

Chiral controllers can induce a screw-sense preference in an Aib foldamer, but each addition of an Aib residue to the oligomer increased the likelihood of a helix reversal by 3.5%.[23] In other words, there is a maximum distance that the chiral information can transmit from the terminus through the helix. Long Aib foldamers capped with two N-terminal chiral L-α-MeVal residues, which are sufficient to induce complete right-handed screw-sense preference in the first β-turn, were synthesized to find the uniform conformation persists over 60 bonds, resulting in 1,61 (1st to 61st bonds) asymmetric induction and 88 : 12 diastereoselectivity.[24,25] The helix persistence in Aib foldamers decays faster at higher temperature and in more polar solvents, while the length of the helix persistence in non-polar solvents can be around 200 monomers in theory.[25]

Interruptions in screw sense preference were also investigated. In early research, amino acid residues were placed between two sections of Aib oligomers and the term "conductor" and "insulator" were applied to describe whether the residue can transmit the screw sense preference. Glycine is an achiral amino acid and has no preference for the screw sense, but it prefers β-turn and β-sheet secondary structures and result in 17.5 % helix reversal. However, Iva, a chiral amnio acid (ethyl and methyl at the C$^{\alpha}$), was the first chiral amino acid which has no influence on the screw sense preference in the Aib foldamers.[8]

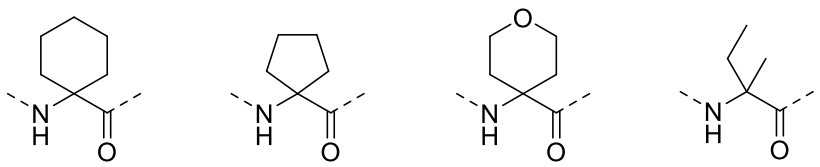

Ac$_6$c Ac$_5$c Thp Iva

Figure 9. Cα-tetrasubstituted animo acid residues

Various other Cα-tetrasubstituted amino acids (Figure 9) were tested Ac_6c for their ability to relay the screw sense as Ac_5c. The 1-aminocyclohexane carboxylic acid and 1-aminocyclopentane carboxylic acid perform as well as Aib in relaying the screw sense.

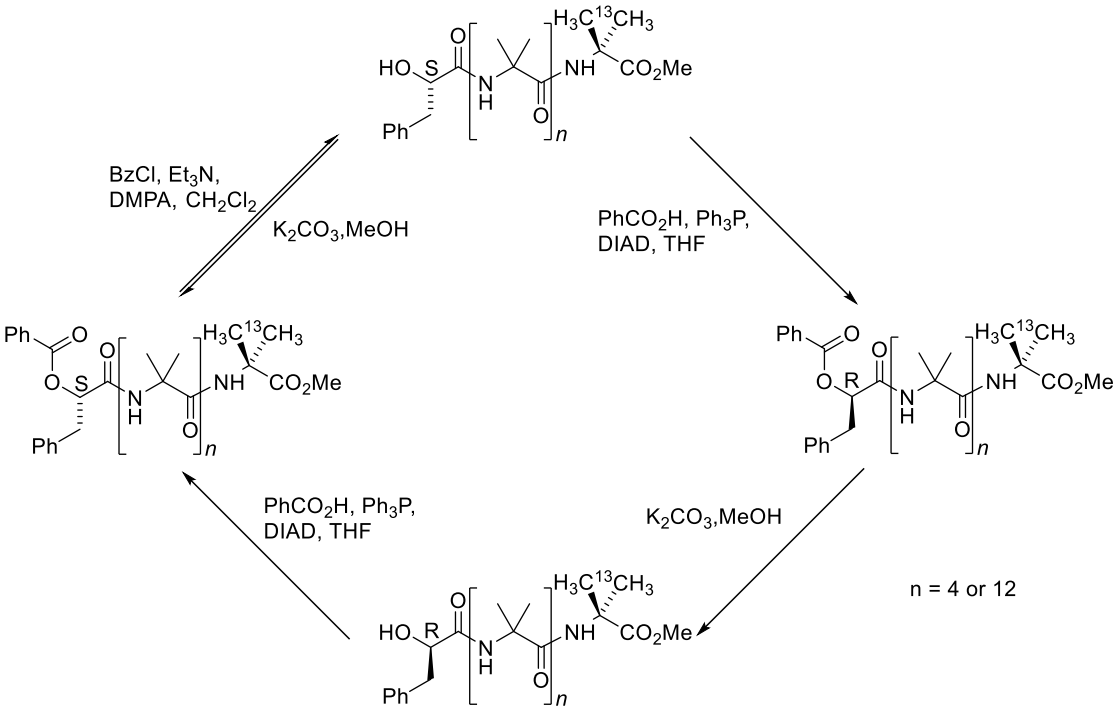

Figure 10. Aib foldamer with N-terminal chiral controller 3-phenyllactate and the route of screw sense preference switch based on Mitsunobu esterification.

The screw sense preference of Aib foldamers can be switched by incorporating N-terminal chiral controllers of switchable chirality. Using 3-phenyllactate as the chiral controller (Figure 10), the switching route is on the basis of a Mitsunobu esterification resulting in a convenient inversion of stereogenic centre between their two mirror-image forms. The screw sense preference reverses when the chiral centre changes from *S* to *R*, as shown by using singly labelled ^{13}C methyl at the remote terminus.[18]

Compared with this complicated synthetic route, light stimuli can simplify induction through a stereochemical switch. Light can trigger a conformational change in biological receptors such as rhodopsin, which transfers a signal in the vision process.[19] Clayden and co-workers designed Aib foldamers incorporating a light switchable maleamide residue to modulate screw sense preference (Figure 11). Maleamide and fumaramide are a pair of isomers which can interconvert by light irradiation. In Aib

foldamers bearing maleamide in its *Z* configururation, the maleamide works as the conductor in relaying the helicity from the L-αMeVal, while the *E*-maleamide (fumaramide) can insulate the H-bond interactions with chiral αMeVal which results in no screw sense preference in the Aib foldamers.[20]

Terminal chiral controllers can induce conformational changes of Aib helix and the

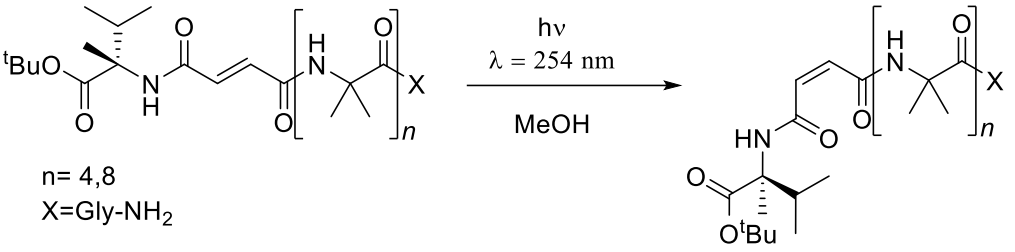

Figure 11. Aib foldamers containing photoswitchable fumaramide/maleamide residues.

chiral information can be propagated to another remote site. With a reporter at the remote site, chiral information output can be detected in the form of NMR and fluorescence signals.

1.3.4 Control of screw sense by an intermolecular 'chiral controller'

Boronic acid coordination with diols is a well exploited carboxylate sensor in biomimetic systems, as it strong yet reversible and can occur in water. Brown. *et al*. reported Aib oligomers capped with boronate binding site (Figure.12 a) could recognize diols, leading to NMR signals from the remote terminus. The boronate binding site had different affinity for various diols, thus a switch of coordinated diols can induce the changes of screw sense preference, from *M* to *P* or *vice versa*. For example, when (+)-hydrobenzoin displaces (-)-diisopropyl tartrate of the boronate site, the foldamer's screw sense preference switches from *M* to *P* (Figure.12). Furthermore, the biomolecules adenosine, guanosine, uridine and cytidine (vicinal diol molecules), can also induce different helical preference (*M, P* and racemic) in the foldamers. [21]

Alternatively, an N-terminal metal centre is also a good binding site for the coordination of chiral ligands and some can induce a screw sense preference in Aib foldamers. It is reported that a (bis(2-quinolylmethyl)(2-pyridylmethyl)amine) (BQPA) motif at the N-terminal Aib foldamers with the metal cofactor Zn^{2+} can function as a binding site for chiral carboxylic acid (Figure. 13). The metal-(BQPA)-Aib foldamer complexes sensed chiral carboxylic acids and relayed the chiral

information down the Aib helix, via the induced screw sense preference, and reported by the NMR spectra of a C-terminal AB system. The output of the terminal AB system can be analysed to calculate the *e.e.* of a chiral carboxylate acid mixture. [22,26]

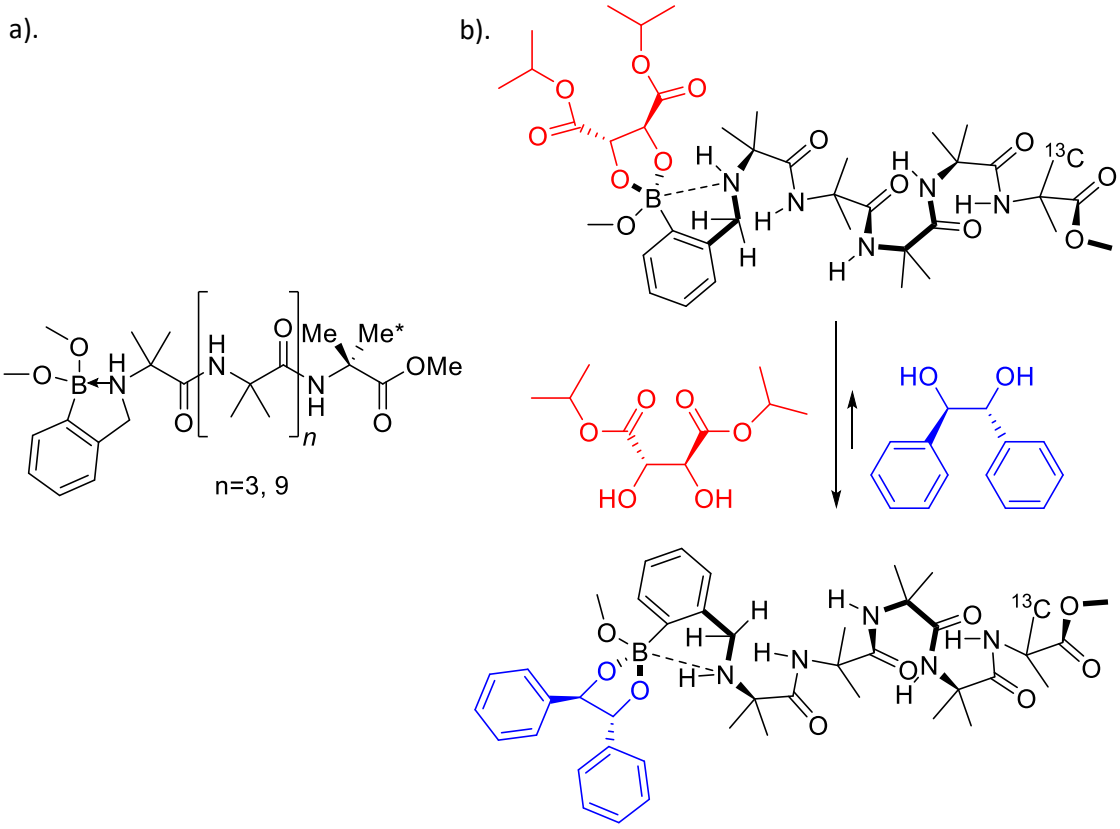

Figure 12. a). Boronate-capped Aib foldamer with C-terminal singly ^{13}C-labelled reporter and b). process of dynamic switching of screw-sense in the process of titration of diol. (+)-hydrobenzoin (HB) replaces (-)-diisopropyl tartrate (DIPT) inducing screw sense inversion.

Alternatively, an N-terminal metal centre is also a good binding site for the coordination of chiral ligands and some can induce screw sense preference in Aib foldamers. It is reported that a (bis(2-quinolylmethyl)(2-pyridylmethyl)amine) (BQPA) motif at the N-terminal Aib foldamers, with the metal cofactor Zn^{2+} can function as a binding site for chiral carboxylic acid (Figure. 13). The metal-(BQPA)-Aib foldamer complexes sensed chiral carboxylic acids and relayed the chiral information down the Aib helix, via the induced screw sense preference, and reported by the NMR spectra of a C-terminal AB system. The output of the terminal AB system can be analysed to calculate the *e.e.* of a chiral carboxylate acid mixture.[22,26]

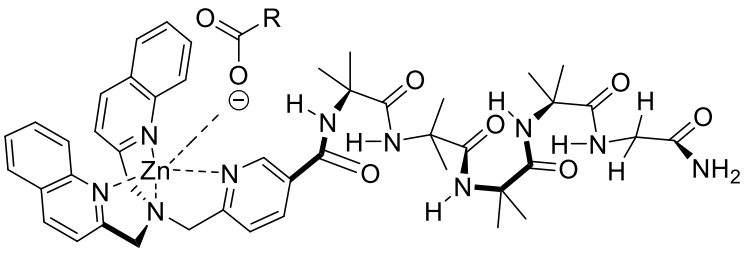

Figure 13. Structure of Zn- BQPA-capped foldamer binding a chiral carboxylate.

1.4 Incorporation into membranes and use as mimics of GPCR transmembrane proteins

A biological membrane can be defined as the external boundary of cells and separate compartments within cells. A cell membrane is essential to all living cells. It provides protection to the cytoplasm inside a cell, maintaining a chemical or biochemical environment that differs from the outside.

A biological membrane commonly consists of two layers of lipid molecules, which also contain phospholipids and many membrane-embedded proteins. In cells, lipids do not pack into micelles like detergents but rather tend to form lipid "leaflets". A bilayer is 5 to 6 nm thick and comprises two sheets or monolayers ("leaflets"). This structure arises due to the amphipathic properties of the lipid molecule, e.g. phospholipid, with polar headgroups in contact with water and apolar hydrocarbon tails toward the interior of the bilayer. These non-covalent interactions, allow membranes to be flexible and to self-seal. The formation of the bilayer is spontaneous, driven by hydrophobic interactions like the increased entropy of solvent molecules.[19,27]

Artificial phospholipid membranes are often used to simulate a membrane environment, giving an opportunity to investigate complex interactions in membranes. Since the first established bilayer model in the 1970s, there have been many approaches to produce lipid bilayer membranes, such as the painting technique, forming Langmuir–Blodgett films and lipid vesicle rupture.[28,29] The investigation of artificial lipid membranes was strongly influenced by the study of surfactants. An important parameter of surfactant structure is critical packing parameter; CPP = v / la_0, where *v* and *l* are the volume and length of the hydrophobic tail, a_0 is the optimal polar head group area. If CPP is around 1, bilayer structures will form (Figure. 14).[29]

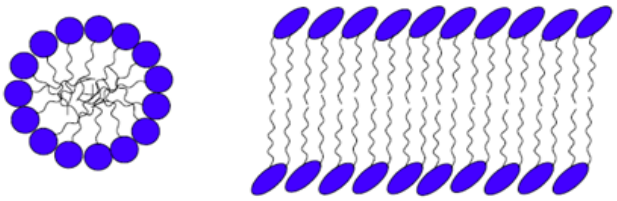

Micelle Bilayer

Figure 14. Lipid shapes of surfactant molecules

The membrane is not merely a barrier, it also a selectively permeable barrier that restricts the free passage of most molecules. Embedded membrane proteins serve as pumps selectively controlling transport of polar small molecules and ions across the membrane. There are also endocytosis and exocytosis mechanisms for large molecule import or export.

To mediate interactions between a cell and its external environment, the detection of outside molecules and conveying that information to the inside of the cell is necessary. This process is called signal transduction. This function is mediated by several proteins in the membrane, and its sole purpose is to promote communication across the membrane.

A general mechanism for signal transduction is shown in Figure 15. A ligand binds to its specific receptor on the surface of the target cell. A signal is generated by the interaction and transferred from the receptor through a transducer to a membrane-bound effector enzyme. The effector enzyme can generate a second messenger in the form of a small molecule or ion carrying the signal. Diffusion of the messenger may

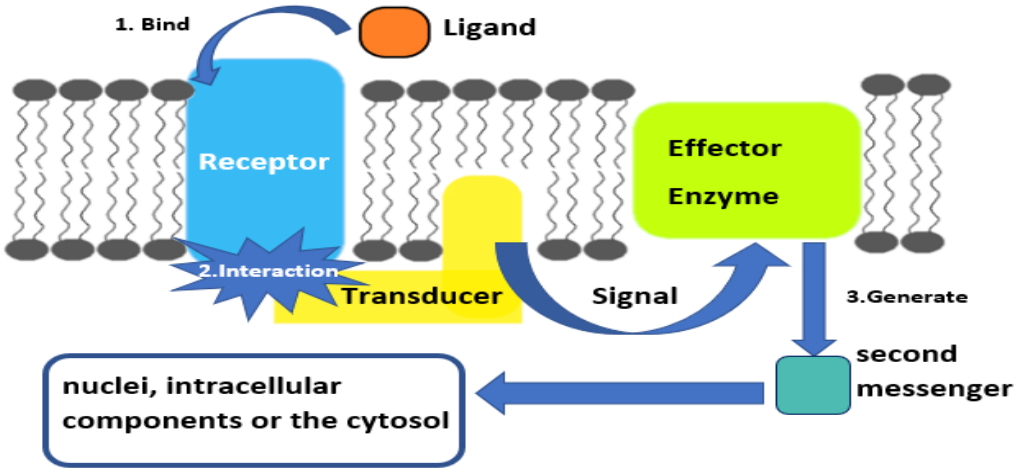

Figure 15. Signal transmission via ligand-controlled transmembrane receptors at membranes.

be to the nuclei, intracellular components or the cytosol.[19] A second messenger is often formed in G protein-mediated signal transmission. Receptor tyrosine kinases (RTK) have a relatively simpler mechanism for signal transduction as receptor, transducer and effector enzyme are within one enzyme.[31-33] Arrival of the signal triggers tyrosine phosphorylation by protein kinases (from ATP) and results in a recognisable conformational change.[33]

The G protein-mediated signal transmission mechanism is one of the most widely studied[32] in the genome, as it regulates our sense of light, smell and taste. Due to their large, complex structures, the work carried out by Lefkowitz and Kobilka into the functions of G-protein-coupled receptors (GPCRs) signalling pathway was rewarded with the 2012 Nobel Prize in Chemistry.[33]

GPCRs consist of seven transmembrane helices (Figure 16). Most of the helices are arranged almost perpendicular to the phospholipid bilayer and form bundle-like structures in which the helices are linked by loops of variable size. The orientation of the helixes and conformation of cytoplasmic loops will change when the receptor receives ligand binding and/or a sensory signal.

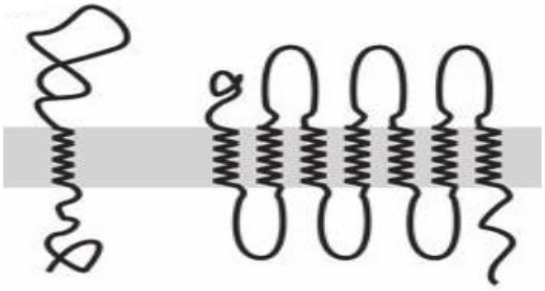

Figure 16. Transmembrane receptors : left α helix; right : seven α helixes connected by cytosolic and extracellular loops.[19] Grey rectangle : membrane.

Chemical and physical signalling ligands are received at the binding site, located at the extracellular membrane, and transmitted to intracellular G proteins. The signal transmission is based on propagation of conformational changes from the binding site through the GPCRs, thus across the bilayer, to the cytosolic terminus over 4 nm away. This releases a molecule of GDP, resulting in a cascade of different biochemical reactions, such as the regulation of adenylyl cyclase. Although the exact mechanism of signal transduction is not fully understood, artificial systems have been synthesized

that also use conformational change as a method of transferring external signals into a bilayer membrane.[19,33,34]

Rhodopsin is a sensory protein belongs to GPCRs. Rhodopsin was found in the rods of the retina from not only humans, but also seeing animals, vertebrates and bacteria. It plays an important role of virson in dime light. Rhodopsin can strongly absorb green-blue light and, therefore, appears reddish-purple, and it was given the name "visual purple". Rhodopsin changes in colour upon exposure to light due to the isomerisation of bound retinal and subsequent arrangement of its seven transmembrane helices, which converts light into a signal interior to the cell. Thus, the study of GPCRs will help understand a fundamental process of cellular signalling.

Webb, Clayden and their groups are working on the that issue by constructing dynamic helical foldamers bearing 'input' and 'output' segments at each terminus. As described earlier, a chiral controller bound to the terminus of Aib foldamers can propagate a global conformational change through the helix in order to allow end-to-end chiral information transmission over several-nanometres.

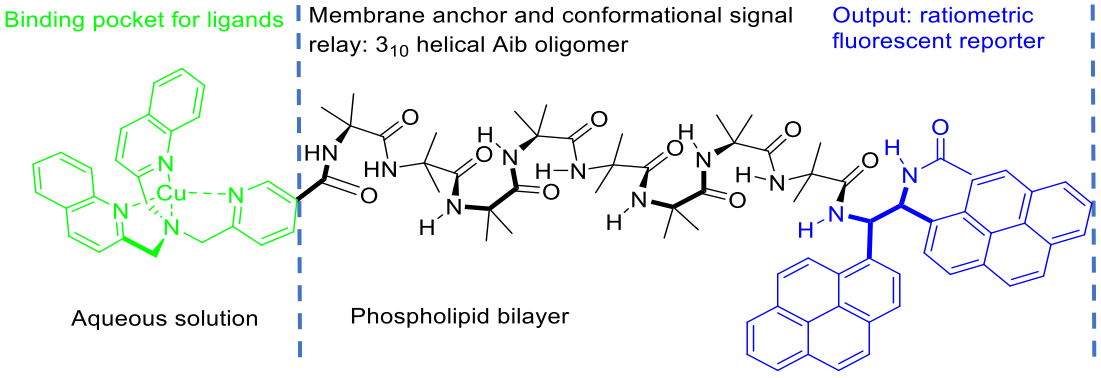

Figure 17. Structure of a synthetic GPCR mimic with copper cofactor which can bind a carboxylate ligand.

Furthermore, Aib-rich peptides have the ability to insert into phospholipid bilayers and span cell membranes,[7] for example natural Aib-rich peptides peptaibols work as membrane-disrupting fungal antibiotics.[4,8,27] Given this ability to insert into bilayers, a biomimetic Aib foldamer has been applied to the bilayers for information transmission. The Aib foldamer bore a copper (II) BQPA as the binding site at the N-terminus for the selective carboxylate acids. At the other end of the 2.6 nm helix (Figure 17), the conformational preference induced by binding a carboxylate was

reported by fluorescent pyrenes at the *C*-terminus. The selective binding of different carboxylates acid can induce different changes in the excimer emission, with a pair of carboxylates used to mimic the behaviour of an 'agonist' and an 'antagonist'. This feature is analogous to the behaviour of μ- and δ-opioid GPCR antagonists.[26]

1.5 Adding catalytic function to Aib foldamers

The successful employment of this synthetic Aib foldamer in phospholipid bilayers lead to interest in setting up more complicated systems, which are not limited to reporting on the transmission of chiral information by spectroscopy. One feature of Aib foldamers reported by Liam *et al.* was Aib foldamers with a preferred screw sense able to govern their own enantioselective extension with amino acids.[35] Therefore, the chiral controller produced an enantioselective reaction by end-to-end transmission of conformational information. The next step would be to give catalytic function to Aib foldamers, then biomimicry of enzymatic enantioselective reactions may be possible.

1.6 Introduction to N-heterocyclic carbenes (NHCs)

Carbene is a neutral molecule formed by covalent bond of a neutral carbon atom two other substituents or hydrogen atoms with general formula R_2C:. In spectroscopy, carbenes are classified as singlets and triplets, depending upon their electronic structure. In the singlet carbene, the central carbon atom is sp^2 hybridized with a lone pair of electrons; the triplet carbene has two free electrons, which can be sp^2 or linear sp hybridization. Most carbenes, e.g. alkyl carbene commonly have a triplet ground state due to the energy of triplet carbene is generally 33 kJ/mol lower than singlet. Those carbenes with nitrogen, oxygen or sulfur, and halide substituents bonded to the divalent carbon are always singlet due to substituents can delocalize electron pairs to an empty p orbital stabilizing the singlet state. They are called persistent carbenes. The well-known example is the N-heterocyclic carbene (NHC).[36]

N-Heterocyclic carbenes (NHCs) are singlet carbenes with the carbene incorporated in a heterocycle with at least on nitrogen atom. It was first investigated in 1960s and shortly thereafter, their first application as ligands of transition metal complexes was reported by Wanzlick and Öfele.[36] However, chemists seldom used these compounds due to NHCs were considered too reactive to be isolated. Since 1991, when Arduengo *et al*. isolated the first stable NHC, IAd (1,3-di(adamantyl)imidazol-2-ylidene) whose

substituents are adamantyl groups (Scheme 2), chemists have focused on finding applications across many areas of chemistry.[36]

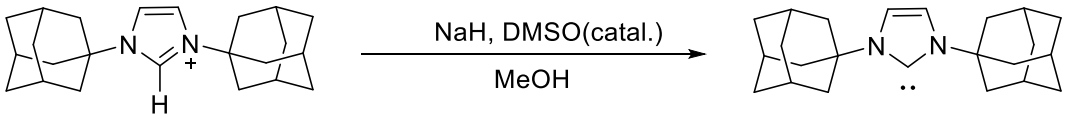

Scheme 2. Deprotonation of imidazolylidene

NHCs always have relatively independent features involved in electronic and steric stabilization. First of all, NHCs are mostly stabilized by means of bulky groups which can provide steric shielding of the carbene carbon. In other words, steric shielding of the carbene carbon increases the lifetime of the carbene. For the bis-substituted imidazolium carbenes, carbene with methyl substituents (less hindrance) is significantly less stable than adamantyl groups.[36] Second, the singlet carbene is stabilized by delocalisation of the lone pairs from two neighbouring nitrogen atoms. An NHC is obtained by deprotonating imidazolin-2-ylidene, where C-N bonds are longer and the N-C-N angle is smaller in the carbene than the imidazolium salt.[37] NHCs are different from 'traditional' carbenes, which are considered electron-deficient; they are electron-rich nucleophilic compounds, (see resonance structure, Scheme 3).

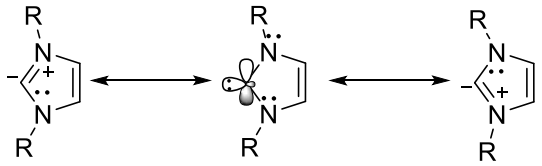

Scheme 3. Resonances of imidazolin-2-ylidene; R = alkyl groups.[37]

With respect to coordination chemistry, NHCs are considered as electron-rich, neutral sigma donor ligands due to the lone pair of electrons in a sigma orbital. NHCs can form strong stable NHC-metal bonds with soft late transition metals and early transition metals.[38,39] The degree of π-acceptor property is still unclear; results illustrate 0% to 30% π-back-bonding in the complexes' overall orbital interaction energies.[36]

The electron donating properties of NHCs can be characterized by the carbonyl stretch frequencies that are ligands on the complexes. These illustrate that NHCs are more

electron-rich ligands than trialkyl phosphines. It also shows NHCs have similar electron-donating ability arising from the substituents directly attached to the donor atoms, but phosphines span in a wider electronic range from alkyl to aryl phosphines. This reduces the effect on complex reactivity when the substituents on NHCs are replaced. Therefore, the best way to change the electronic nature of an NHC is to change the heterocycle, where the electron-donating power increases in the order benzimidazole < imidazole < imidazoline.[36]

The electronic properties of NHC ligands allow for the formation of remarkably stable metal-NHC bonds with different transition metal centres. In coordination reaction, the equilibrium between the free carbene and the carbene complex bias towards the NHC-meta complex. Complexes are often stable against air, water, light, temperature and heat. The stability is very advantageous in metal-mediated catalytic reactions, especially in oxidative conditions by stabilized low-valent intermediates. Furthermore, the electronic donating NHCs can provide catalytic activity by accelerating the formation of coordinatively unsaturated catalytically active intermediates.[35, 42]

Historically, NHCs were considered phosphine mimics, but it is interesting to compare their steric properties. The phosphine ligand is commonly described as having cone-shaped arrangement of their three substituents pointing away from metal (Figure 18 left). However, the best way to describe the steric pattern of NHCs is fan- or umbrella-shaped with the sigma NHC-metal bond and the heterocycle are in the same plane (Figure 18 right). This results in a greater steric influence from NHC ligands, as bulky nitrogen-substituents adjacent to the carbene in NHCs point toward the metal.[35,36]

Figure 18. Shape of phosphines and NHC ligands

1.6.1 Imidazolium salt synthesis

There are two different routes to synthesize imidazolium salts used to make NHCs. In the first route, *N*-alkyl-substituted imidazolium salts can be easily afforded by

alkylation of imidazole with suitable electrophiles. Alternatively, the imidazolium ring can be built up, for example by condensation reactions (Scheme 4). The latter route has become the common method for many imidazolium salts with bulky steric groups on nitrogen or multiple substituents on the backbone. It can be applied to synthesize both symmetrical and unsymmetrical *N*, *N'*-disubstituted imidazolium salts (Scheme 4). Due to the isolation of NHCs and their and applications has arisen widespread interests and research, synthetic methods of imidazolium salts have been improved recently. It is reported that the imidazolium salts can be afforded by reaction of glyoxal, formaldehyde and a primary amine in the presence of a strong acid.[45]

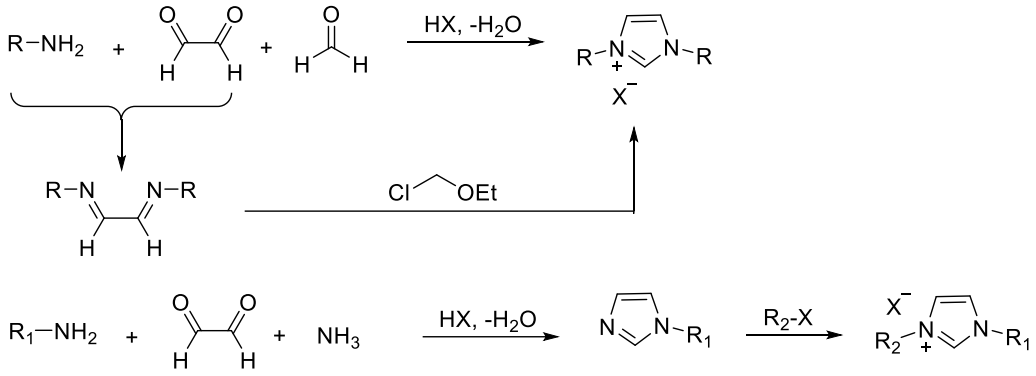

Scheme 4. Representative synthesis of symmetrical and unsymmetrical imidazolium salts

1.6.2 Applications of NHC-metal complexes

For NHC ligands to achieve high enantioselectivity in certain catalysed processes, chirality from NHC ligands is essential. The selectivity is mostly derived from steric shielding which can impede the combination of substrates and the catalyst. Chiral NHCs are also employed in the area of the asymmetric catalysis. The first asymmetric NHC ligand was reported in 1966 by Sheehan, reaching 22% e.e. In 2001 Burgess reported the first highly enantioselective reaction using an NHC-complex, but it was bidentate.[44,45] Grubbs gave an example of a monodentate NHC scaffold and achieved high asymmetric induction (Scheme 5). In numerous catalytic applications, the aromatic N-substituents are crucial for high enantioselectivity. A common way to introduce chirality in NHC ligands is through the incorporation of chiral substituents onto either the backbone of the NHC (pointing away from the metal) or the nitrogen atoms (pointing towards the metal), giving many options to tune the stereoenvironment at the metal centre.[42, 43] Chiral N-substituents can be easily prepared from primary amines (Scheme 6, chiral R group), and chiral substituents on

the carbons of backbone are commonly from the corresponding 1,2-diamines. Therefore, NHCs can be designed to fulfil the various electronic and steric requirements of chiral catalysts.[42]

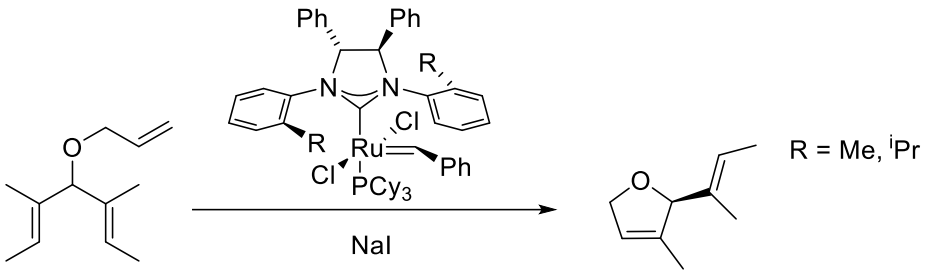

Scheme 5. Chiral NHCs employed as stereo-determining ligands of ruthenium complexes in a catalytic reaction. Dipp = 2,6-diisopropylphenyl.

The NHC-metal bond can display restricted rotation, depending on steric hindrance from the ancillary ligands, NHC substituents (steric hindrance) and the choice of heterocycle/metal (amount of π backbonding). The rotation around metal-carbon bond was commonly reported as a problem in design of chiral monodentate NHCs catalyst because such rotation will result in less rigidity in the complex and thereby lower the enantioselectivity. In such cases, the rotation must be restricted or eliminated to overcome the inherent anisotropic properties of NHC catalysts. The stereoenvionment of metal complexes is locked by big ancillary ligands, such as cyclooctadiene (COD), and bulky substituents placed on nitrogen.[46] Tricyclic NHCs are known for offering a highly rigid, sterically demanding, and C_2-symmetric chiral environment (Figure 19). However, these scaffolds always require long synthetic routes to obtain them.

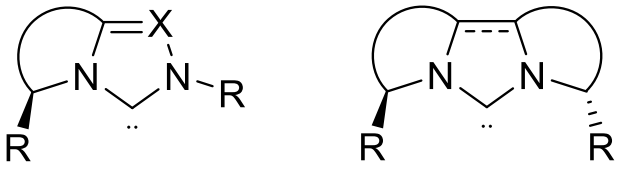

Bicyclic Tricyclic

Figure 19. Bicyclic and tricyclic chiral NHCs.

Many of the successful NHC ligands in enantioselective catalytic reactions are multidentate. They bind the metal centre through a sigma bond plus an additional arm, e.g. chelation with a heteroatom, or by a covalent bond with an NHC substituent. These chiral chelate NHC ligands introduce additional chiral information at the metal with a supplementary chelating atom (C, N, O, P, S) and chiral groups at different

positions (e.g. backbone, substituents). A large number of multidentate NHC ligands have been reported due to their important role in high enantioselective catalytic processes. The additional arm is chosen to allow (or not) its displacement during the reaction, as multiple coordination sites may not be compatible with the reaction mechanism. For example, iridium can form covalent bonds with methylene substituents on NHCs and becomes a different stereocentre. The size of the metallacycle involving the supplementary arm determines its stability (5 membered chelate rings are found to be more stable than 7 or 8 membered chelate rings).

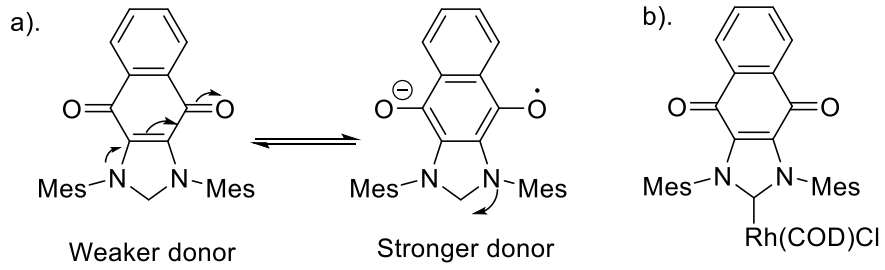

Figure 20. A hypothesized redox switchable NHC ligand based on quinone/hydroquinone system. a). FT-IR spectroscopy reveals the resonance, the neutral NHC is a relatively weak donor whereas the reduced form is relatively strong. b). Structure of rhodium complex feature redox-active quinone group.

In recent years, NHC scaffolds are reported to have promising applications in the construction of switchable catalysts.[47] Generally, a switchable catalyst depends on functional groups that respond to external stimuli (e.g. temperature, light, ions, neutral molecules). External stimuli can induce structural or electronic changes which ultimately influence the activity and/or selectivity of the catalyst. The backbone of the NHC allows it to be multiply substituted by various functional groups. For example, ferrocene on the nitrogen substituent can influence the electronics and donating properties of the NHC after a redox process. The quinone/hydroquinone system (Figure 20) is also an established redox switch and that can be annulated to the backbone of NHCs.[47] The reduction of the quinone can enhance the electron density on carbene. Another class is photoswitchable NHCs, where the electronic properties of the NHCs can be altered by UV and/or visible light. A well-developed example is based on diarylethene (DAE), where light can stimulate photocyclization of the thiophene groups (Figure 21).[48, 49] The ring-opened NHC was characterized as being relatively electron rich whereas the ring-closed NHC is electron deficient. The

photocyclizations of the corresponding Rh, Ru and Ir complexes were also characterized, but these complexes do not exhibit extraordinary switchable properties in catalytic reactions.[50]

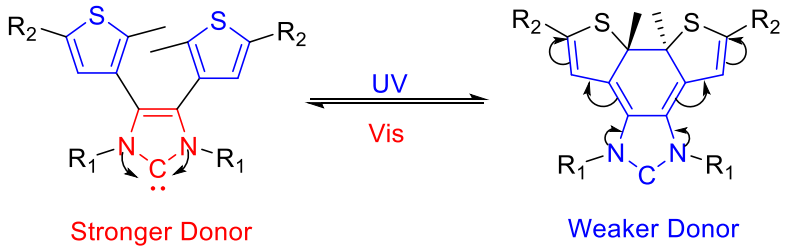

Figure 21. Diarylethene NHCs can be irritated by the UV and/or visible light.

NHCs can also be used to create Grubbs-catalyst/protein artificial enzymes. Basauri-Molina *et al*. loaded rhodium-NHC catalysts on a protein (lipase) as the active site and the rhodium catalyst showed a higher chemoselectivity in the competitive hydrogenation of olefins than ketones.[51] The rhodium-NHC was embedded in the protein scaffold which allows it to produce a pocket around the metallic center. The rhodium NHC catalyst showed intrinsically chiral and bulky character resulting in catalytic selectivity, due to the protein scaffold performs as a bulky sphere which limits some sterically demanding states. Meanwhile, NHCs performed water- and oxygen-tolerant character due to its strong σ-donating monodentate coordination towards the metal centre without influence of the remaining coordination sites needed for catalytic activity.[51]

1.6.3 Hydrosilylation by rhodium-NHC catalysts

Hydrosilylation is the reaction of addition of Si-H bonds across unsaturated bonds, in particular carbon carbon (e.g. C=C, C≡C) and carbon heteroatom (e.g. ketone) multiple bonds. The first hydrosilylation was reported 70 years ago (1947) by Leo Sommer and a Pt-catalyst was used in hydrosilylation 60 years ago.[80]

There are many rhodium complexes used to catalyse the catalytic hydrosilylation of alkenes and alkynes, e.g. $[RhH(PPh_3)_4]$, $[RhCl_3(PPh_3)_3]$. In recently years, rhodium complexes with NHC ligands have attracted considerable attention. Some Rh-NHCs (Figure 22) are efficient catalysts in the hydrosilylation of terminal alkynes and show good *trans* product selectivity.[78]

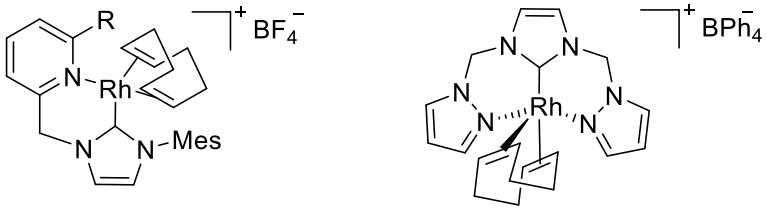

Figure 22. Bi and tri-dentate Rh(I)-NHC complexes.

Over the last decade, NHC rhodium complexes have emerged that show high efficiency in hydrosilylation of acetophenone and analogue ketones with trialkylsilanes, to give the respective silyl ethers with 63–99% yield. Cationic rhodium(I) complexes (Figure 23) were found to be active catalysts in the hydrosilylation of ketones with diphenylsilane.[79]

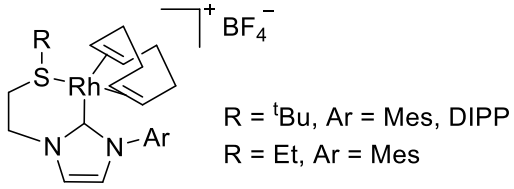

Figure 23 Structure of NHC–thioether rhodium complex.

2 Aims of project

The project aims to elaborate the previously described Aib foldamer family (Figure 24) so they can relay switchable chirality to metal catalysts, thus providing enantioselective reactions. NHCs were chosen as ligands to be placed on the C-terminus. NHCs form stable covalent bonds with metals and display great reactivity and selectivity in some well-established reactions. To the best of our knowledge, it is the first time combining dynamic Aib foldamers with NHC catalysts.

Aib foldamers with azide at the N-terminus and an NHC at the C-terminus will be complexed with the transition metal and fully characterized. The catalysts will be tested for reactivity and selectivity in catalytic reactions in organic solution. As mentioned before, the screw sense of Aib can be controlled by N-terminal chiral residues, so in the next step Aib foldamer-NHC ligands bearing chiral controller will be synthesized are compared with the azido complexes. Steric hinderance around the NHC is also a factor affecting selectivity in catalytic reaction. The difference between NHC groups with different substituents will also be synthesized and tested.

Therefore, Aib foldamer with N-terminal azide and αMe-valine (chiral controller) will be synthesized firstly. The Aib foldamer will be an N-substitute of imidazole, in other words imidazole will be attached to Aib foldamer C-terminus. The steric hinderance is modified by switching the other N-substitute by methyl, phenyl and mesityl groups. Rhodium is then loaded on the Aib-imidazole ligand.

The transmission of chiral information from foldamer N-terminus to the C-terminal NHC catalyst site will also be investigated. The efficiency of information transmission

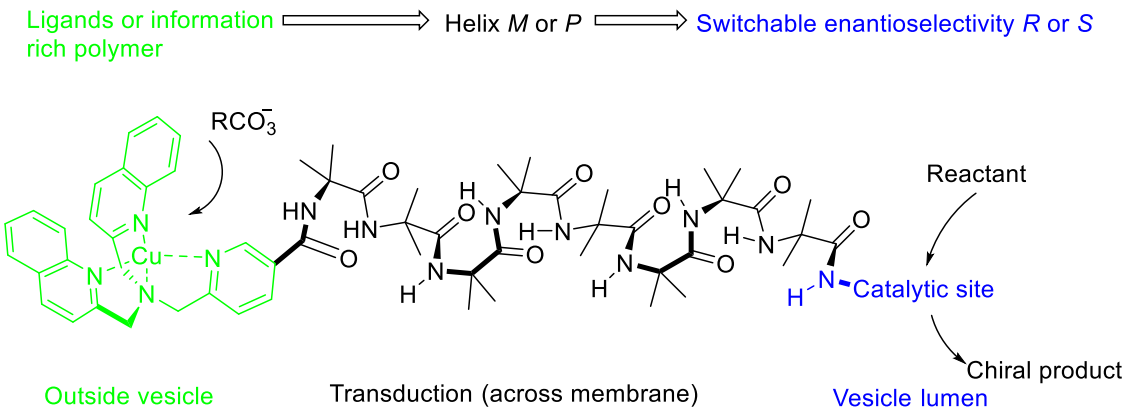

Figure 24. The transmission of dynamic chirality from Aib foldamers N-terminus to C-terminal NHC catalyst. The catalyst will be fully characterized in organic solvent and tested its reactivity and selectivity in both organic solvent and membrane.

can be directly reflected in the stereoselectivity of azido catalysts compared to catalysts with a chiral controller. Simultaneously, NMR and other spectroscopies will be applied to characterize conformational differences between foldamers with a chiral controller and those with azido N-termini. A strong screw-sense preference is expected to give chirally controlled catalysts.

If successful, the next steps will determine whether the enantioselectivity can be controlled by external chemical stimuli, for example in organic solvents, which is developed by Simon's group as shown in figure 24 green section.

Finally, since the Aib foldamer mimics the GPCRs and has been successfully applied in the membrane for chiral information. The application of the Aib-NHC catalysts in a membrane is also an aim of the project (Figure 24).

3 Results and Discussion

3.1.1 Synthesis of Aib foldamers

The synthesis of Aib foldamers was well-established in the Webb and Clayden groups.[13] The procedure starts from its azide monomer ester **1** which was obtained in excellent yield (87 %) from a S_n2 reaction of commercial reagent *tert*-butyl 2-bromo-methylpropionate with excess sodium azide in dimethylformamide (Scheme 6). It is followed by two-week-long hydrogenation of azide ester **1** with 10 % Pd/C in ethanol to afford free amine **3**, yield (95 %). Simultaneously, 2-bromo-2-methylpropionic acid was treated with excess sodium azide in dimethylformamide to give azide acid monomer **2** in also excellent yield (82 %).

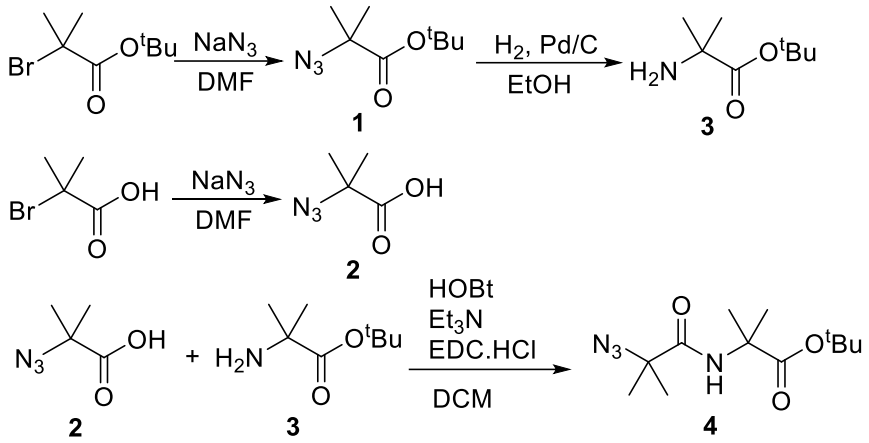

Scheme 6. Synthesis of Aib monomer and Aib dimer.

Further reaction of these monomers uses amino acid coupling. The azide acid **2** was firstly treated with coupling reagent EDC·HCl and HOBt and organic base triethylamine in dichloromethane, then 2 equivalents amine **3** was added to the reaction mixture. After 27 hours stirring purification by column chromatography to afford azide dimer **4** in good yield (54 %). In preparation for the next reaction, free amine dimer **5** is afforded by hydrogenation of azide dimer in a good yield (92 %). Repeat of the amino acid coupling between treated azide acid monomer and amine dimer **5** gave azide trimer **6** in yield (65 %). Further iteration of hydrogenation and coupling with treated azide acid monomer afforded azide tetramer **7** in excellent yield (90 %). Foldamer elongation can follow this loop of hydrogenation of azide and amino acid coupling to give progressively longer foldamers (Figure 25).

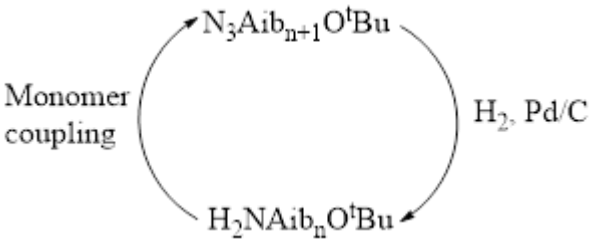

Figure 25. Elongation of Aib oligomer.

The building up of Aib tetramer and hydrolysis in this way provided a way to modify Aib oligomer and allow installation of chiral controllers and functional groups. The azido group can be reduced to amine after hydrogenation allowing chiral amino acid to coupled with it. The easter group can be hydrolysed by trifluoroacetic acid in water (Scheme 7).[13]

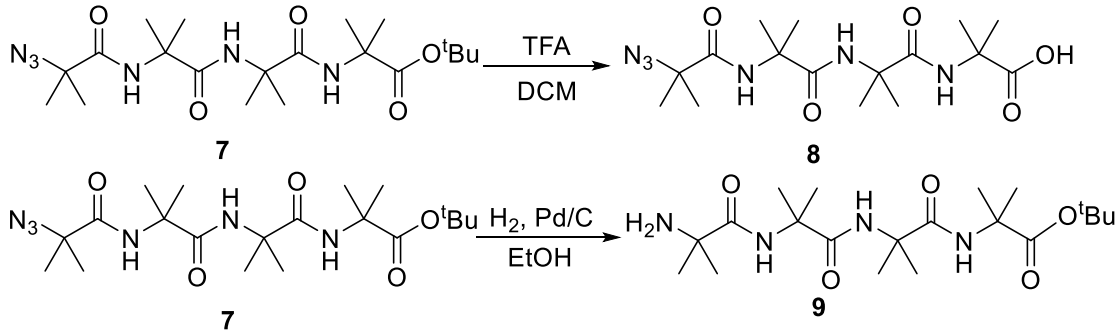

Scheme 7. Deprotection of Aib tetramer.

3.1.2 N-terminal functionalisation

Amine tetramer **9** was synthesized before functional groups were attached to the N-terminus. Firstly, a reliable reporter benzyloxycarbonyl glycine was attached to the N-terminal Aib tetramer in order to monitor the screw sense preference from the C-terminus. Then, chiral valine was introduced to the Aib tetramer to induce a screw sense preference and act as the chirality source for catalytic reactions.

Carboxybenzyl protected glycine was introduced to the Aib foldamer by the same method of monomer coupling. Due to product being poorly soluble in chloroform, the purification is simplified as precipitation and filtration yields clean glycine amide tetramer **10** (Scheme 8).[17]

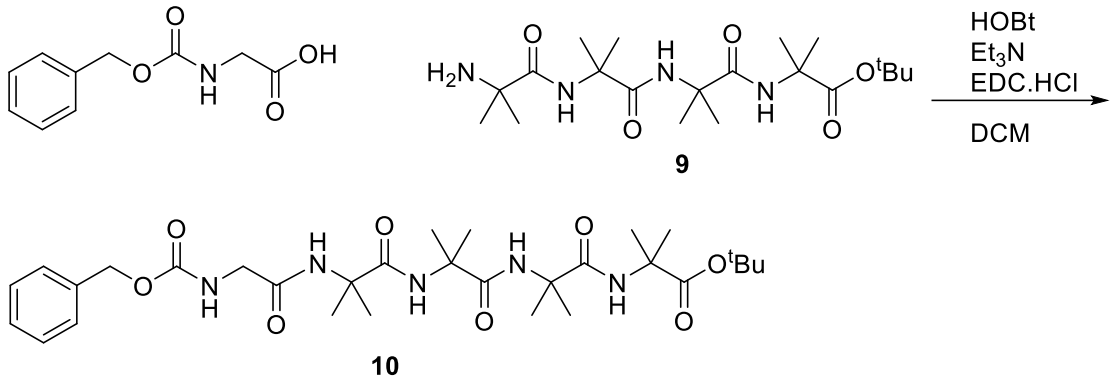

Scheme 8. Synthesis of Cbz-gly-Aib$_4$ with the same coupling reagents as Aib oligomer elongation.

The introduction of a chiral controller to Aib foldamer is different from an achiral amino acid, but it has been reported by Clayden's group. Carboxybenzyl protected L-αMeVal is an efficient chiral controller which can induce a preference for a right-handed screw sense, so we want to see the effect on our catalysts. Acyl fluoride was used to conduct the coupling between valine and tetramer followed the reported method.[24] In the reaction, cyanuric fluoride reacted with L-αMeVal first to afford the acyl fluoride and then amine-terminal tetramer was added for 3 days reaction with organic base (Scheme 9). The reaction gave a low yield of 20% which is much lower than reported.[12] The yield strongly depends on the cyanuric fluoride, as water in the air can result in hydrolysis of the cyanuric fluoride which shows a moisture. Besides TLC, the reaction process can also be easily monitored by ^{1}H NMR spectroscopy where methyl groups in valine and methylene in carboxybenzyl group can also function as an AB system reporter.

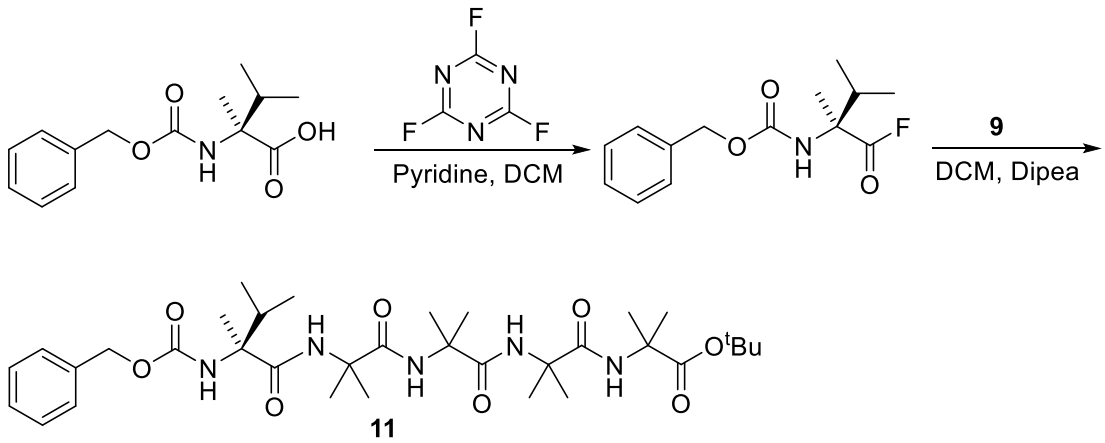

Scheme 9. Synthesis of Cbz-L-α-MeVal-Aib$_4$ with the same coupling reagents as Aib oligomer elongation.

3.1.3 Synthesis of *N*-substituted imidazolium dibromate salts

There are two major synthetic pathways to N-substituted imidazole compounds; Ullmann reaction or cyclization. Ullmann type reaction uses a Cu(I) catalyst to assist the coupling between imidazole and bromoaromatics. This reaction requires hard conditions like high temperature and strong base and the Cu waste is also harsh to remove. Diamine cyclization can be conducted at lower temperature and is relatively easier to work up. This reaction is always used to synthesize the NHCs with a bulky substitute.

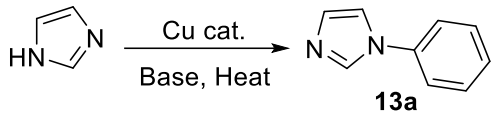

13a

Scheme 10. Synthesis of N-substituted imidazole by Ullmann-type reaction.

An Ullmann type reaction (Scheme 10) was conducted in two different conditions following two different reported methods.[52,53] The first trial was conducted with relatively milder conditions where the coupling reaction between imidazole and bromo aryls was conducted in DMF solvent with catalyst CuI and weak base stirring at 30 ^{o}C under nitrogen. Unfortunately, after workup, no product was collected from chromatography column (SiO_2), although a spot of assumed product was displayed on TLC.

Later, this reaction was performed following another reported set of conditions that requires high temperature and strong base. The reactants were same to the mild reaction, but temperature, catalyst, solvent and base were much stronger than before. Cu_2O and KOH were added into the reactants in DMSO solution, then stirred at 130 ^{o}C under nitrogen for 24 hours. This gave apparently good yield (54%) of N-substituted imidazole.[53]

Cyclization of diamines with formaldehyde (Scheme 11) is also a classic reaction to synthesize substituted imidazoles. For the purposes of studying a large steric substituent on the NHC, mesityl imidazole was selected to synthesized. The backbone of imidazole was built up by amine, 2,4,6-trimethylaniline, glyoxal formaldehyde and ammonium acetate in a corresponding acid solution with stirring under 70 ^{o}C overnight.[54] This reaction successfully produces the correct product after workup and fast chromatography purification with 70 % yield. Compared with the Ullmann type

reaction, the cyclization method is milder, purification is relatively easier and more suitable for laboratory synthesis on a large scale of simple imidazoles.

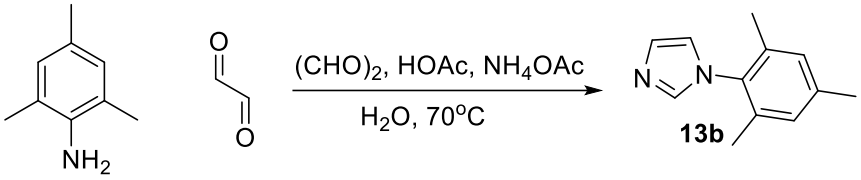

Scheme 11. Synthesis of N-substituted imidazole by cyclization.

Two different N-substituted aryl imidazoles **13a** and **13b** were synthesized by the method described above. In addition to methyl imidazole sold by Sigma-Aldrich, three imidazoles with different size N-substituents were obtained.

3.1.4 Synthesis of *N, N'*-substituted imidazolium dibromide salts

In order to connect the imidazole to the Aib foldamer, a linker is required as the nitrogen on imidazole cannot form a stable amide with the carboxylic acid on the Aib foldamer. This linker is needed a bridge to connect the two molecules and conduct chiral information from foldamer to imidazole. Aib tetramer was already synthesized by the well-established method, so *N, N*'-substituted imidazolium salts were synthesized, and then coupled with Aib tetramer.

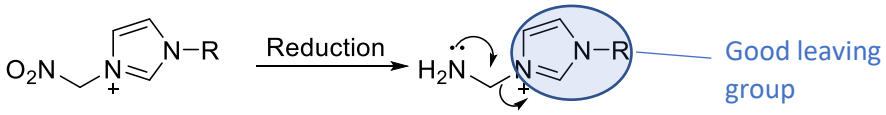

Figure 26. Decomposition of methylene bridge imidazolium salts.

A simple methylene bridge is unlikely to be stable, due to imidazole being a stable leaving group. A reduction reaction was tried with stable nitromethylene imidazole, as shown in Figure 26, but only *N*-substituted imidazole was obtained, as reported by ^{1}H NMR spectroscopy. Therefore, an ethylene linker was chosen. The reactants are all prepared from N-substituted imidazole and commercial bromoethylamine. The mechanism is proposed to be a S_n2 reaction. The imidazolium salts were prepared in quantitative yields following published procedures by alkylation of the N-substituted imidazole with the alkyl bromide in acetonitrile at room temperature.[54] Three imidazolium salts precursors (Scheme 12) were prepared.

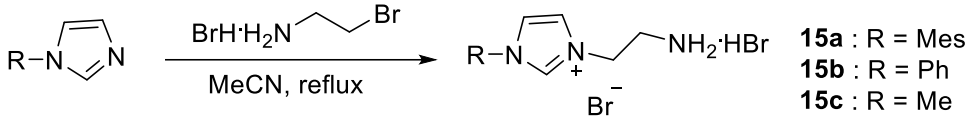

Scheme 12. Synthesis of imidazolium salts with different aryl groups.

Imidazolium salts **15a** and **15b** are solids that precipitate from the reaction mixture. However, in the case of **15c**, the same procedure leads to a pale yellow oil from its reaction mixture, although it becomes solid after purification. After simple decantation and filtration, each separated crude product is characterised by ^{1}H NMR spectroscopy. The proton spectra illustrated the main impurities are reactants; for **15a and 15b** this was the bromoethylamine and **15c** it was methyl imidazole. The purification is difficult for these crude products, as the products and impurities have similar chemical properties. Recrystallization is the reported method[54] to purify the product and was tried three times, but proton spectra illustrated there was no obvious changes in the impurity peaks after each trial. Column chromatography wouldn't work either, as both impurity and products are salts. RP-HPLC (reversed-phase high performance liquid chromatography) should be efficient in separating such polar molecules. The imidazole molecules can be detected and separated well, but 2-bromoethylamine may not be detected by UV or IR monitor of HPLC. HPLC in our lab is not suitable in purifying gram-scale reaction. Consequently, a method of crystallization was found by accident, where a white solid forms overnight from a solution of ethanol and acetonitrile. In the second trial, a solution (acetonitrile : ethanol (95:5)) was used to recrystallize and obtain the product (77% for **15a** and 66 % for **15b**). The recrystallization of **15c** is a bit different from the previous method, because the main impurity in this case is the reactant imidazole. After recrystallization, the solid required a cold diethyl ether wash (three times) to give the product (57 %).

All the salts **15a-c** are soluble in polar solvents, water, methanol or DMSO and were fully characterized by IR spectroscopy, NMR spectroscopy and electrospray ionization mass spectrometry (ESI-MS). This kind of imidazolium salts was observed typical NMR resonances. The most significant chemical shifts and coupling constants in the ^{1}H NMR spectra of the **15a-c** compounds are presented in Table 1.

In the ^{1}H NMR spectra, the acidic protons NC*H*N of the imidazole fragment were found in the range 9.14 – 9.98 ppm as a doublet with a coupling constant $J_{H,H}$ = 1.7

Hz; the resonances of the imidazole backbone protons were observed in the aromatic region of the spectra for all of the salts, as two triplets in the spectra of **15a-c** with coupling constant 1.8 or 1.9 Hz. The ethylene bridge were observed in the range 3.5 – 4.69 ppm (DMSO-d_6) and 4.00 – 4.63 (MeOD-d_4) as two triplets in the spectra with a coupling constant $J_{H,H}$ = 6.1, 5.8, 6.2 Hz for **15a, 15b, 15c** respectively. This is an important proof of the success of the reaction.

Compounds	NC**H**N	C**H**$_{im}$	NC**H**$_2$C**H**$_2$
	δ (ppm)	δ (ppm)	δ (ppm)
15a DMSO-d6	9.51	8.18	4.69
	d, $J_{H,H}$ =1.7 Hz	7.99	3.52
		t, $J_{H,H}$ =1.8 Hz	t, $J_{H,H}$ = 6.1 Hz
15b DMSO-d6	9.98	8.39	4.59
	d, $J_{H,H}$ =1.7 Hz	8.08	3.50
		t, $J_{H,H}$ =1.8 Hz	t, $J_{H,H}$ = 5.8 Hz
15c MeOD-d4	9.14	7.77	4.63
	d, $J_{H,H}$ =1.7 Hz	7.68	4.00
		t, $J_{H,H}$ =1.9 Hz	t, $J_{H,H}$ = 6.2 Hz

Table 1. Chemical shifts and coupling constants of the **15a-c** in ^{1}H NMR spectra.

3.1.5 Coupling imidazolium dibromide salts with Aib foldamers

The coupling of imidazolium dibromide salts with the Aib foldamer is inspired by the method for elongation of the Aib foldamer. Dr. W. Cullen used EDC·HCl as the coupling reagent to conduct this reaction. C-terminus acid tetramer firstly reacted with EDC to form an active O-acylisourea intermediate that is easily displaced by nucleophilic attack from N-terminal primary amino groups on the substituted imidazolium (Scheme 13). This method can be applied to both azido and L-α-MeVal capped Aib tetramer, which afforded similar yield.

Purification of the Aib-imidazolium conjugates through column chromatography (SiO_2, eluent DCM : MeOH 95 : 5) was monitored by PMA stain. The tetramer **8** is extremely hard because it is a UV/Vis invisible molecule and also hard to observe with PMA stain. Iodine vapor is an extra common TLC stain reagent, but in this case, it can be used to stain the TLC.[56] Triethylamine salts are not removed after chromatography

purification on silica gel, as its salt shares similar R_f values with the product. Therefore, further column chromatography is required with basic Al_2O_3 to remove triethylamine salt.

All the salts **16a-c and 17a-b** are soluble in chlorinated solvents and were fully characterized by IR spectroscopy, NMR spectroscopy and electrospray ionization mass spectrometry (ESI-MS). In comparison, the most significant chemical shifts and coupling constant in ^{1}H NMR spectra of the **16a-c and 17a-b** compounds are presented in Table 2.

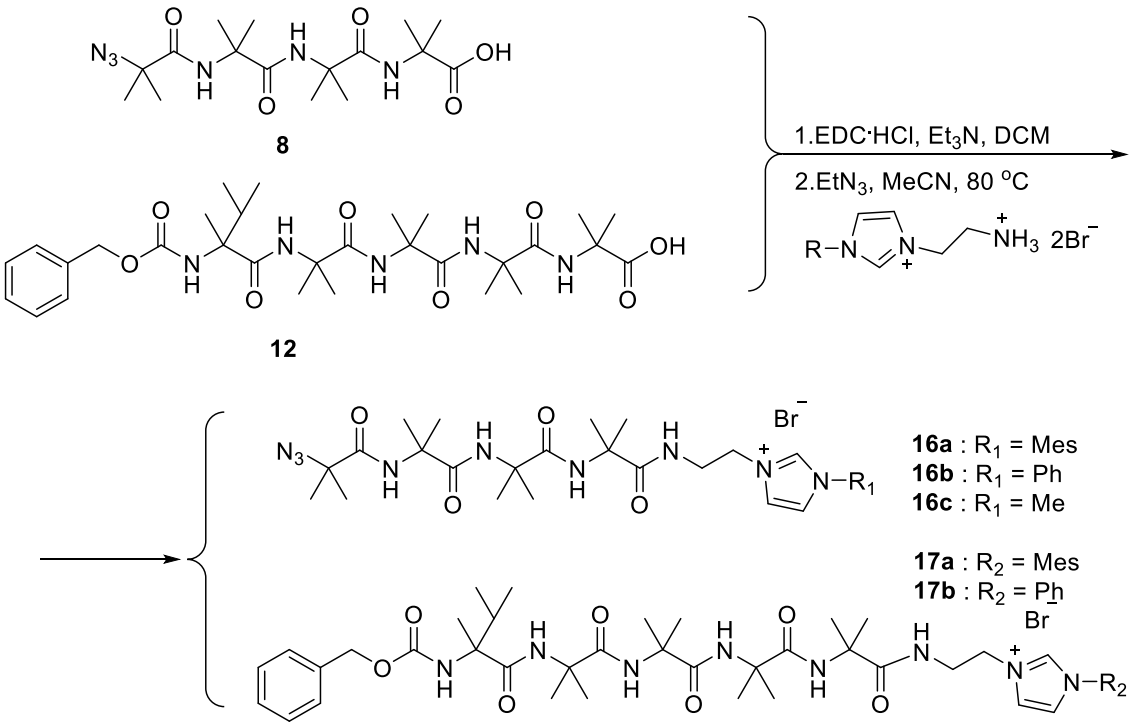

Scheme 13. Synthesis of Aib-imidazolium salts.

In the ^{1}H NMR spectra, the acidic protons NC*H*N of the imidazole fragment were found in the range 9.25 – 9.92 ppm; the imidazole backbone protons were observed in the aromatic region of the spectra for all of the salts, as two triplets in the spectra of **16a-c** and **17a-b** with a coupling constant range 1.7-1.9 Hz. The ethylene bridge protons were observed in the range 3.30 – 4.77 ppm. Those protons at relative high field, about 4.5 ppm, are the CH_2 closed to imidazole ring and another CH_2 at approximately 3.7 ppm is close to amide of Aib foldamer. Besides, there is an obvious difference between **16a-c** and **17a-b**. These methylene resonances tend to be simple triplets or doublets of triplets, if the foldamer is achiral. However, they become diastereotopic if an αMeVal is present, giving complex splitting patterns.

3.2.1 Installing rhodium onto NHC ligands

There are two methods to synthesize the rhodium complexes. The method used depends on the N-terminal functional group of the Aib foldamer. The azido ligands **16a-c** were deprotonated by inorganic base K_2CO_3 and then coordinated to the rhodium complexes (Scheme 14).[57] However, K_2CO_3 is too strong for Cbz-L-(αMeVal) ligands, and cyclization of Cbz-L-(αMeVal) and the first Aib residue was to form hydantoin. Therefore, a reported method was applied that used silver oxide to deprotonate and to form NHC silver when αMeVal is used as the chiral controller at N-terminus. Then rhodium complex was synthesized by transmetalation from the Ag(I)-NHC complexes in dry dichloromethane (Scheme 14).[58] Complexes **18a-c** and **19** were isolated as yellow microcrystalline solids after purification by column chromatography on silica gel and preparative TLC in high yields (70–95%).

Compounds	NC**H**N δ (ppm)	C**H**$_{im}$ δ (ppm)	NC**H**$_2$C**H**$_2$ δ (ppm)
16a	9.54 dd, $J_{H,H}$ = 3.6, 1.7 Hz	8.18 dd, $J_{H,H}$ = 3.6, 1.7 Hz 7.07 dd, $J_{H,H}$ = 3.6, 1.7 Hz	4.73 2H t, $J_{H,H}$ = 6.0 Hz 3.68 2H t, $J_{H,H}$ = 6.0 Hz
16b	9.92 m	8.01 m 7.66 s	4.68 2H dd, $J_{H,H}$ = 6.2, 3.3 Hz 3.85 – 3.69 2H m
16c	9.25 s	7.67 d, $J_{H,H}$ = 1.9 Hz 7.57 s	4.58 – 4.42 2H m 3.64 2H m
17a	9.52 d, $J_{H,H}$ = 1.7 Hz	8.18 dd, $J_{H,H}$ = 1.8 Hz 7.00 dd, $J_{H,H}$ = 1.8 Hz	4.85 – 4.73 1H m 4.71 – 4.57 1H m 3.97 1H m 3.30 1H m
17b	9.82 d, $J_{H,H}$ = 1.8 Hz	8.12 t, $J_{H,H}$ = 1.9 Hz 7.54 – 7.50 m	4.77 1H m 4.57 1H m 3.99 1H m 3.55 1H m

Table 2. Data of chemical shifts and coupling constants in ^{1}H NMR spectra of **16a**-c and **17a-b**.

Complexes **18a-c** are air stable in the solid state and in solution confirmed by continuous monitoring of the NMR samples in $CDCl_3$. Unlike these, the structurally similar but ancillary ligand NBD complex **20a** are relatively unstable. Both **20a** and **19b** were provided by Dr. Tilly was observed to degrade over three months. Another NBD complex **20b** was synthesized using the same conditions as **18c**. However, fractions from **20b** reaction mixture were observed to change colour changes during evaporation of the solvent after chromatography. Furthermore, no NMR spectra indicated that **20b** was present in one of those fractions. It was possible that the Aib-rhodium complexes with NBD ligand are relatively unstable in comparison with there with a COD ligand.

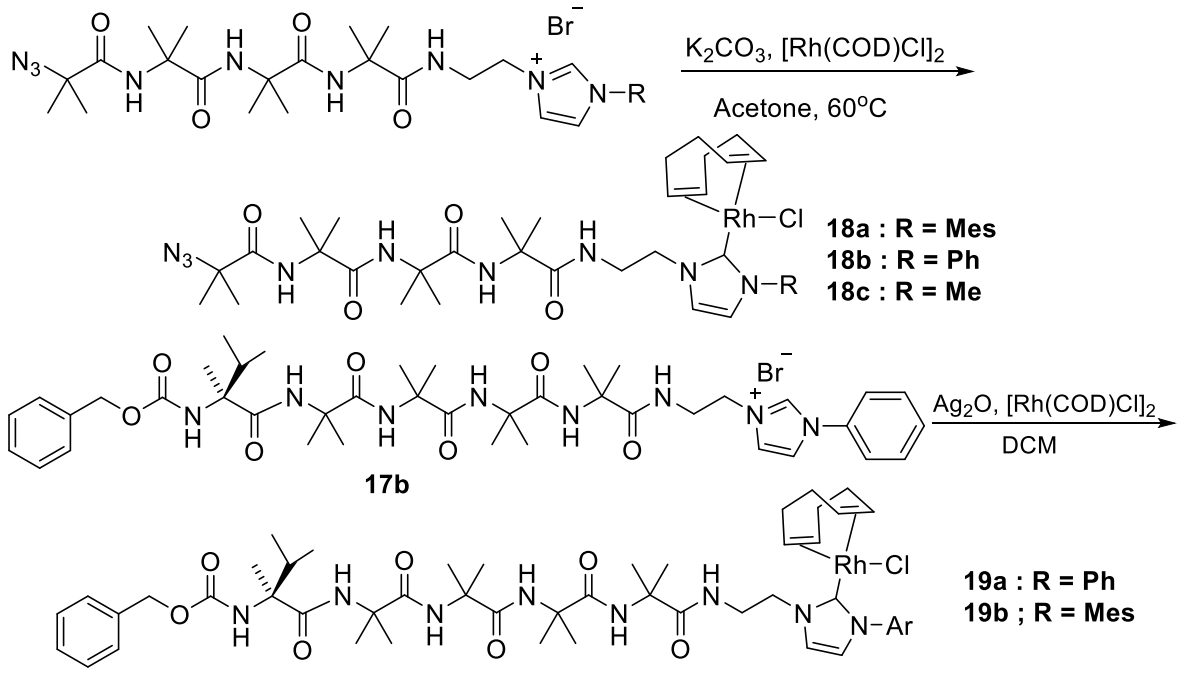

Scheme 14. Synthesis of rhodium(I) complexes with base K_2CO_3.

Complexes **18a-c and 19a** were completely soluble in chlorinated solvents (DCM) for column chromatography and monitoring of the NMR samples ($CDCl_3$). Complexes **18a-c and 19a** have been fully characterized by IR, ESI-MS mass spectrometry, and ^1H NMR and ^{13}C NMR using COSY, HSQC, and HMBC experiments for full resonance assignments. The most significant chemical shifts and coupling constants in ^1H spectra of the complexes **18a-c and 19a** are presented in Table 3.

The general trend which can be observed for all of the compounds, from precursors to complexes, is the increasing complexity of their ^{1}H NMR spectra (acquired at room temperature) with the increasing bulkiness of the N-substituents on the NHC.

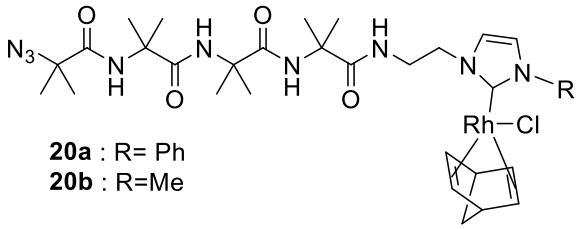

20a : R= Ph
20b : R=Me

Figure 27. Structure of **20a** and **20b** with ancillary ligand NBD (norbornadiene).

As expected, the acidic protons NC*H*N of the imidazole fragment were removed but, the resonances of the imidazole backbone protons were observed in the aromatic region of the spectra for all of the complexes, as two doublets in the spectra of azido complexes with a coupling constant range 1.9-2.0 Hz. Compound **19a** exhibits doublet with a coupling constant 2.0 Hz and also splits of peak due to αMeVal Compound **19a** is the mixture of diastereoisomers, which will be explained later.

The ethylene bridge protons were observed in the range 3.60 – 5.50 ppm. Those ethylene protons are at lower field compared to those in the precursor imidazolium salts due to the electron withdrawing of the rhodium. For azido complexes **18a, 18b** and **18c**, the multiplets are common for the ethylene protons with enantiotopic CH_2 signals, which originate from slow rotation around the NHC-metal bond producing a chiral axis. Nonetheless there is no overall screw sense preference as the mixture is racemic.

The NHC metal bond provides an axis of chirality due to the lack of an (average) symmetry plane. Depending on direction that the COD faces, two alternative chemical environments are created. Four signals were obtained for the diastereotopic CH_2 in the ethylene linker. With greater steric hindrance around the NHC, the splitting of these methylene protons on the ethylene linker increases. ^{1}H NMR spectra show that **18a** with a mesityl substituent has the largest differences in CH_2 chemical shift, $\Delta\delta$ are 1 and 1.24 ppm for the CH_2 next to the NHC and Aib respectively. This is followed by compound **18b** ($\Delta\delta$ of 0.35 and 0.32 ppm) with the less hindered phenyl substituent, and **18c** with a methyl exhibits close, even overlapping CH_2 signals for the methylene groups. If the rotation of the NHC metal bond was fast, the average chemical

environment would be identical for protons in the methylenes. The fact that we see the splitting mean that NHC-metal bond rotation is not fast at 25 °C. If we increase temperature so the rotation of NHC-metal bond is faster, then the ethylene bridge signals may coalesce. However, for complex **19a**, the helix screw sense is influenced by a chiral controller and makes diastereomeric pairs. This means the ethylene bridge CH_2 will always be diastereotopic even with fast rotation around the NHC-metal bond because of the controlled screw sense of the helix.

The olefinic and methylene protons of the cyclopentadiene ligand are different in the case of **18a-c**. Cyclopentadiene is a symmetric molecule with two sets of protons, olefinic and methylene in ^{1}H NMR spectrum. In the case of **18c**, each group of protons was observed to split. This is due to the chlorine dipole moment in the plane of chlorine, rhodium and carbon atoms. If the protons aligned to Cl, their signals are located at high field. The rest of the protons are not affected by Cl with signals at relatively low field. In addition, in the case of **18a 18b** and **19a**, there is a further split of protons. The split resulted from aryl ring magnetic cone anisotropy. Those protons spatially under the aryl ring are more shielded than other protons, thus results in different chemical shifts (Figure 28).

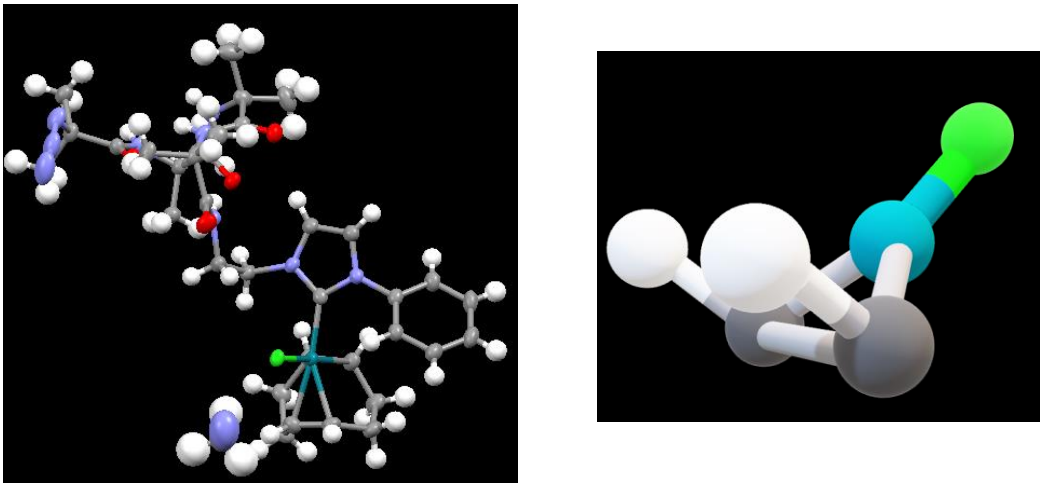

Figure 28. 3D structure of **18b** and the plane of Cl, Rh (left) and two methylene of COD ligand (right).

Compounds	C**H**=C**H**$_{im}$	NC**H**$_2$C**H**$_2$	Ancillary ligand
	δ (ppm)	δ (ppm)	cyclooctadiene (COD)
18a	7.40	5.42 (dt, J = 14.3, 4.4 Hz, 1H,	4.90 (dt, J = 7.5 Hz, 1H, 2 x CH_{COD})
	d, J = 1.9 Hz	CH_2N_{Imid})	4.79 (td, J = 7.5, 3.7 Hz, 1H, 2 x
	6.63	4.42 (ddd, J = 13.8, 9.5, 4.1 Hz,	CH_{COD})
	d, J = 1.9 Hz	1H, CH_2N_{Imid})	3.81 – 3.73 (m, 1H, CH_{COD})
		4.09 (dddd, J = 13.7, 9.4, 7.2, 4.1	3.08 (dd, J = 8.6, 5.2 Hz, 1H, CH_{COD})
		Hz, 1H, CH_2NH)	2.12 (ddt, J = 17.6, 9.5, 4.5 Hz, 1H,
		3.73 – 3.60 (m, 1H, CH_2NH)	CH_{2cod})
			2.06 – 1.90 (m, 1H, CH_{2cod})
			1.76 (m, 1H, CH_{2cod})
			1.70 – 1.57 (m, 1H, CH_{2cod})
18b	7.06	5.11 – 5.05 (m, 1H, C**H**$_2N_{imid}$)	5.02 (m, 1H, C**H**$_{COD}$)
	d, J = 2.0 Hz	4.79 – 4.67 (m, 1H, C**H**$_2N_{imid}$)	4.87 (m, 1H, C**H**$_{COD}$)
	7.46	4.02 (m, 1H, C**H**$_2$NH)	3.31 (m, 1H, C**H**$_{COD}$)
	d, J = 2.0 Hz	3.70 (m, 1H, C**H**$_2$NH)	2.52 (m, 1H, C**H**$_{COD}$)
			2.42 – 2.30 (m, 1H, CH_2CH_{COD})
			2.24 (m, 1H, CH_2CH_{COD})
			2.08 (m, 2H, $CH_2CH_{COD,}$ $CH_{2\ COD}$)
			1.76 (m, 3H, $CH_{2\ COD}$)
			1.44 (m, 1H, CH_2CH_{COD})
18c	7.17	4.69 – 4.55 (m, 2H, CH_2N_{imid})	5.09 – 4.98 (m, 2H, 2 x CH_{COD})
	d, J = 1.9Hz	3.95 – 3.83 (m, 1H, CH_2NH)	3.40 – 3.32 (m, 2H, 2 x CH_{2COD})
	6.74	3.83 – 3.71 (m, 1H, CH_2NH)	2.44 – 2.26 (m, 4H, 2 x CH_{2COD})
	d, J = 1.9 Hz		1.96 – 1.78 (m, 4H, 2 x CH_{2COD})
19a	7.64	5.39 (dd, J = 5.9, 3.3 Hz, 0.25H,	5.04 – 5.01 (m, 1H, CH=CH_{COD}),
	d, J = 12.4	CH_2-Imid)	4.96 – 4.86 (m, 1H, CH=CH_{COD})
	Hz	5.36 (dd, J = 5.9, 3.3 Hz, 0.25H,	3.44 – 3.38 (m, 1H, CH=CH_{COD}),
	7.06	CH_2-Imid)	2.58 – 2.53 (m, 1H, CH=CH_{COD}),
	dd, J = 12.4,	5.21 – 5.14 (m, 0.25H, CH_2-	2.44 – 2.34 (m, 1H, CH_2CH_{COD}),
	2.0 Hz	Imid, 0.25H, CH_2-Imid)	2.35 – 2.21 (m, 1H, CH_2CH_{COD}),
		4.65 (ddd, J = 14.3, 8.8, 3.2 Hz,	2.15 – 2.06 (m, 1H, CH_2CH_{COD}),
		0.5H, CH_2-Imid),	1.87 – 1.80 (m, 1H, CH_2CH_{COD}),
		4.56 (ddd, J = 13.7, 8.2, 5.3 Hz,	1.79 – 1.72 (m, 2H, CH_2CH_{COD}),
		0.5H, CH_2-Imid)	
		4.16 – 4.08 (m, 0.5H, CH_2NH)	
		4.08 – 4.00 (m, 0.5H, CH_2NH)	
		3.80 – 3.72 (m, 0.5H, CH_2NH)	
		3.61 – 3.56 (m, 0.5H, CH_2NH)	

Table 3. Significant chemical shifts and coupling constants in the ^{1}H spectra of the complexes **18a-c and 19a**.

The Aib-NHC rhodium complexes are mixture of diastereoisomers of Aib helical screw sense and axial chirality of NHC-metal bond. The ratio of diastereoisomers is calculated by the integration of peaks of ethylene and COD ligand in ^{1}H NMR spectra. However, there is no preference of one isomer was found in azido complex and L-αMeVal which are 1 : 1 ratio of diastereoisomers.

^{13}C NMR spectra display similar results as ^{1}H NMR spectra (Table 4). The carbon coordinated to rhodium was observed above 180 ppm with coupling constant of the range 50-51.5 Hz. **19a** were diasteroisomers and the isomers show different chemical shift. NHC backbone signals are located at the range of 120-124 ppm. One ethylene carbon closed to Aib foldamer exhibits signal at 40.7 ppm. The chemical shift of the other ethylene carbon at about 50 ppm was easily affected by the substituent on the other nitrogen of NHC. **19a** and **18b** shares similar chemical shifts of NHC and ethylene group due to same phenyl substituent on NHC. Chemical shifts of COD also display similar four methylene signals as their protons in ^{1}H NMR spectra due to different chemical environment (see Experimental Section).

Compounds	N**C**N δ (ppm)	**C**H$_{im}$ δ (ppm)	N**C**H$_2$**C**H$_2$ δ (ppm)
18a	180.9 J_{Rh-C} = 50.7 Hz	123.4, 122.8	51.4 (**C**N$_{im}$), 40.8 (**C**NH)
18b	182.2 J_{Rh-C} = 51.0 Hz	123.3, 121.1	50.6 (**C**N$_{im}$), 40.7 (**C**NH)
18c	181.47 J_{Rh-C} = 50.1 Hz	122.63, 121.84	49.7 (**C**N$_{im}$), 40.7 (**C**NH)
19a	182.4 J_{Rh-C} = 51.4 Hz 181.8 J_{Rh-C} = 50.9 Hz	123.8, 123.6, 121.0, 120.8	50.9 (**C**N$_{im}$), 50.8 (**C**N$_{im}$), 41.3 (**C**NH), 40.7 (**C**NH)

Table 4. Significant chemical shifts and coupling constants in the ^{13}C NMR spectra of the complexes **18a-c and 19a**.

3.2.2 VT NMR experiments

Rh-NHC complexes are reported to display slow rotation around the metal–carbene bond and yielding conformational enantiomers. The rotation rate can be determined by means of variable-temperature NMR spectroscopy; M. C. Cassani et al. reported a

pathway of rotation (or enantiomerization) of NHC-rhodium complexes with norbornadiene moiety.[59] In the case of our rhodium complexes, the rotation is expected to have different effects between azido and chiral controller complexes and be differently affected by steric hindrance from aryl groups.

As mentioned before, at 25 °C our rhodium complexes are assumed to be diastereoisomers with ^{1}H NMR signals of ethylene protons are split heavily. If the rotation of the NHC metal bond was really fast, a coalescence of the ethylene bridge will be observed giving triplets or triplets of triplets.

To try and measure the rotation rate around the NHC-Rh bond, the ^{1}H NMR spectra of the complexes **18b** were recorded at a series of temperatures ranging from -40 to 50 °C in $CDCl_3$ (boiling point 60.9 ° C) and are shown in Figure 21. COD and NBD are both common ancillary ligand in synthesis of rhodium complexes, but NBD is less hindered due to its bicyclic ring. The multiplets at 3.70 and 4.03 ppm observed at room temperature, deriving from the CH_2 of ethylene geminal protons broadens on decreasing the temperature, but no coalescence was observed upon heating to 50 °C. Therefore, the data is different from the reported results for NBD[46] in that there is no coalescence at 50 °C.

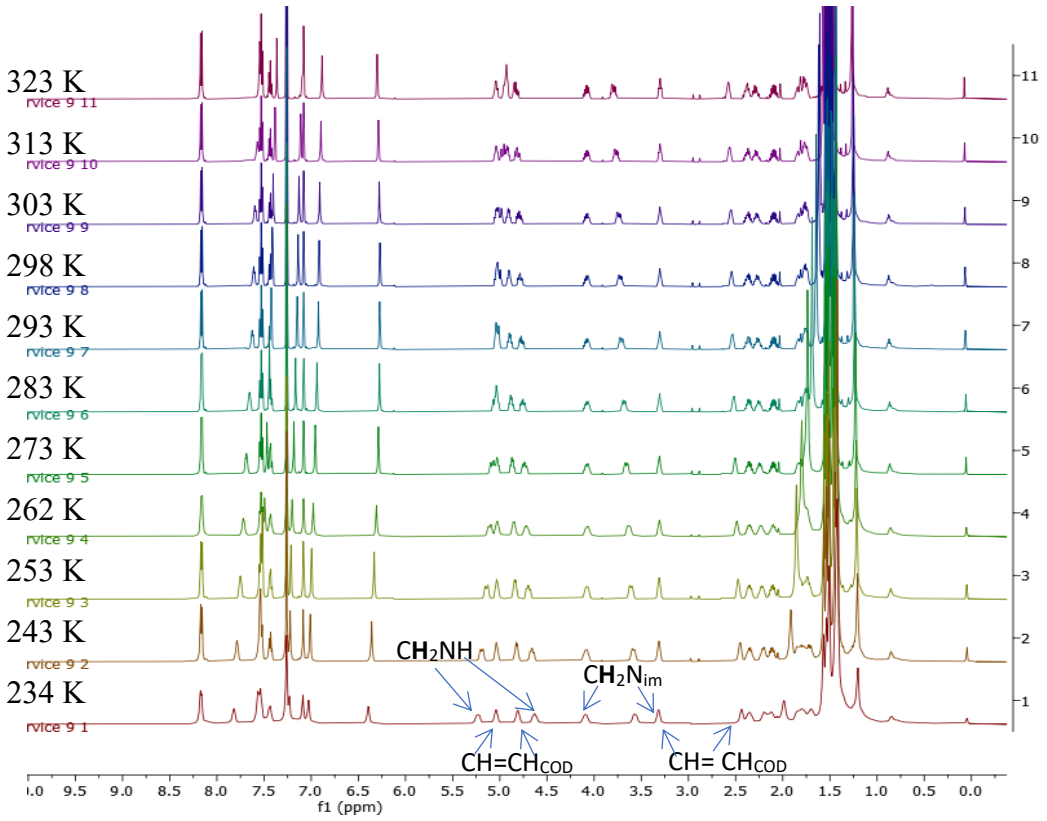

Figure 29. VT ^{1}H NMR spectra of **18b** from -40 °C to +50 °C (10 °C increment) in $CDCl_3$.

3.3 Catalysis by Aib foldamer-Rh complexes

With rhodium complexes in hand, we focused on the enantioselective hydrosilylation of ketones and alkynes. The principal aim to compare their behavior with what was found in the case of Aib-functionalized complexes described in the introduction in order to evaluate the influence of remote terminal chiral controller, the steric hindrance and of the functionalization on the reaction time and selectivity.

3.3.1 Hydrosilylation of carvone

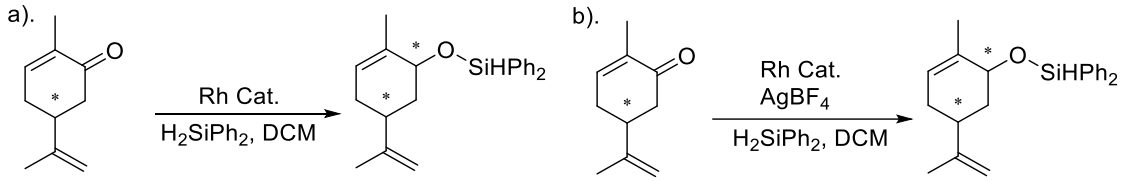

Following conditions reported for hydrosilylation of carvone by diphenylsilane[75] the catalytic hydrosilylation of carvone were carried out in sealed NMR tubes at room temperature in CD_2Cl_2 using two equivalent silane. All the hydrosilylation reactions were directly monitored by ^1H NMR spectroscopy (Scheme 15). The effect of adding silver(I), to remove the chloride from the catalyst, was also assessed.

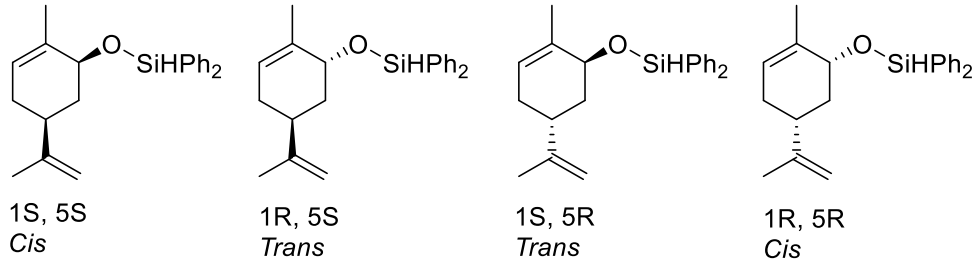

Figure 30. Products of hydrosilylation of carvone: diastereoisomers of silane protected

Carvone is a natural molecule with two commercially available mirror image enantiomers: R-(–)-carvone and S-(+)-carvone. The availability of both enantiomers means that the stereoselectivity of the catalyst can be measured using just one enantiomer of the catalyst. Hydrosilylation of carvone with the rhodium catalyst results in formation of silyl protected carveol with secondary stereocenter on the ketone. There are four distereoisomers of carveol shown in (Figure 30), which can be

classified as two groups of enantiomers, cis- and trans-carveol. Cis- and trans-carveol are shown by NMR spectroscopy to have different chemical shift, of which the proton on the α carbon appears as a triplet at 4.27 and 4.60 ppm in the ^{1}H NMR spectrum of cis and trans isomer respectively. There are no overlapping peaks, thus the ratio of integration can be applied as a measure of catalytic selectivity. In addition, the reaction process can be monitored by proton NMR (Figure 31), with peaks of the reactant decreasing, which can also be applied to calculate the conversion for each catalytic reaction.

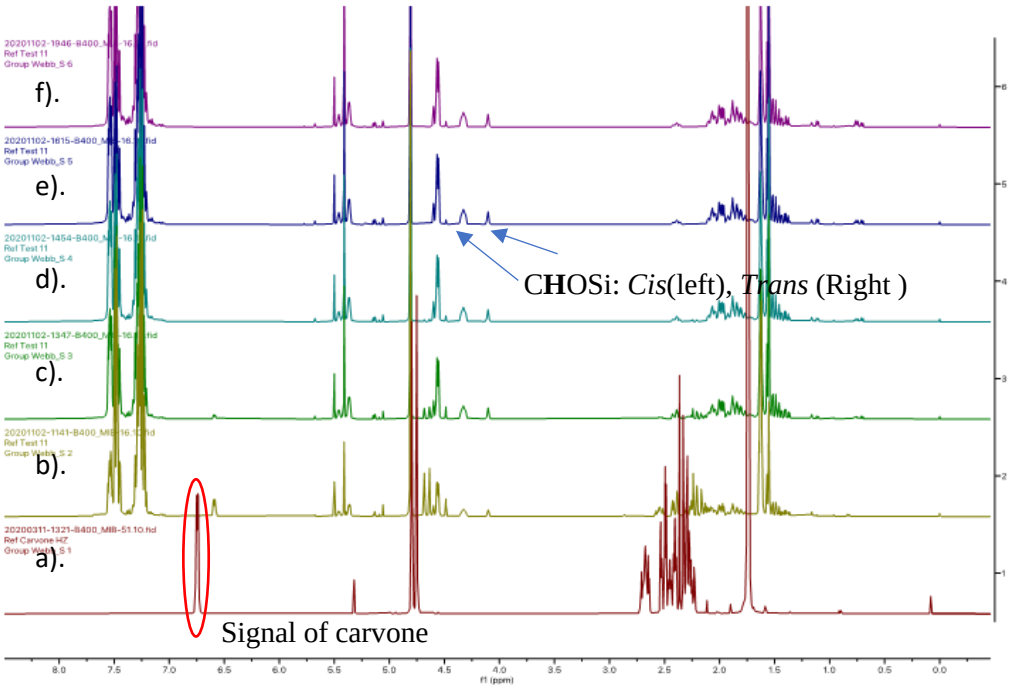

Figure 31. ^{1}H NMR (400 MHZ, $CDCl_3$, 298K) spectra of hydrosilylation of carvone; a). spectrum of reactant, carvone in CD_2Cl_2, b) spectra of catalytic hydrosilylation of carvone in 30 min, c) hydrosilylation process of 2h d) hydrosilylation process of 3h e) hydrosilylation process of 5h f) hydrosilylation process of 8h.

First of all, the nature of the silane used gave marked differences in reactivity. Diphenylsilane produced a high selectivity for trans carveol in 2 hours, while no reaction was observed with dimethylphenylsilane. The dimethylphenylsilane reaction was left overnight, even heated, but still no reaction occurred. The diphenylsilane reaction finished and exhibited peaks for cis and trans-carveol. Interestingly, there is observation of gas pressure was in the diphenylsilane reaction, with bubbling presumably due to hydrogen,[60] while dimethylphenylsilane displays no gas pressure. An interesting outcome also was recorded that in entry 14 (Table 5), as the produced hydrogen broke its glasses container (NMR tube), and finally the reaction stopped at

80% conversion. Entry 14 (Table 5) was completed by adding more silane, while the selectivity stayed the same to the end. Therefore, the diphenylsilane is better to perform hydrosilylation accompanied by production of hydrogen.

As regards the selectivity of the reactions, the silane protected cis carveol was the major product and there is no change in the ratio of trans to cis as the reactant disappears. The selectivity of reactions with different catalysts is presented in Table 5. The selectivity is reflected by ratio of integration of CHOSi in each diastereoisomer, of which the chemical shift of the cis is greater than the chemical shift of the trans.[61] One aim of this project is to find whether the N-terminal chiral controller can switch selectivity of catalytic reaction. However, there is no significant selectivity difference between rhodium catalysts with N-terminal azido or chiral controller. When the reaction completes, the ratio of product isomers is always about 0.75 : 0.25 (+/- about 10%) for cis and trans respectively, no matter which carvone and catalyst were used. In our studies, the highest diastereoselectivity was obtained with Cbz-L(αMeVal)Aib$_4$EtNHCMs Rh(COD)Cl, which provided the corresponding chiral cis-carveol in 50% ee. It was reported that two α-methylvaline at the terminus can afford highest screw sense preference. In Entry 16 (compound **22** provided by Dr. Tilly, Figure 32) was used to perform the hydrosilylation, but it gave a similar ratio to the single chiral controller. Hindrance effect around the NHC was investigated with methyl and phenyl groups in entry 1 and 2, but no obvious difference in selectivity was observed. The mesityl group shows a bit higher selectivity for cis isomer, but still similar to methyl and phenyl groups. In reaction entry 4 and 14, ancillary ligand NBD displays 100 % conversion, but almost the same diastereoselectivity as COD. Therefore, this illustrated that there is no chiral information transmission through the Aib foldamer and ethylene linker to the catalytic centre. More to the point, the catalytic reaction selectivity of this series of catalysts is intrinsic due to the hindrance of Aib foldamer.

In a previous study of hydrosilylation, it was reported that hydrosilylation frequently occurs from a square planar cationic rhodium species.[62] Therefore, the effect of adding silver tetrafluoroborate additive was investigated to perhaps form a cationic Rh(I) species. The addition of $AgBF_4$ was expected to increase by 10% the diastereoselectivity in hydrosilylation reactions.[63] However, the reactions with $AgBF_4$ often did not complete especially for azido foldamers. The expected small increase in diastereoselectivity was observed in azido complexes although the reactions did not

get to completion. On contrary, a small decrease in selectivity for cis was observed for the αMeVal capped foldamer catalysts (entry 13 and 19, Table 5) repeat reactions. Nonetheless these changes are small.

Entry	Catalyst	Carvone	Carvone concentration (M)	Additive	Ratio
					cis : trans[a]
1	**18c**	S	0.665	-	0.78 : 0.22
2	**18b**	S	0.333	-	0.79 : 0.21
3	**18b**	S	0.333	$AgBF_4$	0.80 : 0.20 not to completion
4	**20**	S	0.665	-	0.78 : 0.22
5	**18c**	S	0.333	-	0.75 : 0.25
6	**18c**	S	0.333	$AgBF_4$	0.81 : 0.19
7	**18b**	R	0.665	-	0.71 : 0.29
8	**18b**	R	0.333	-	0.74 : 0.26
9	**18b**	R	0.333	$AgBF_4$	0.82 : 0.18 Not to completion
10	**18c**	R	0.333	-	0.75 : 0.25
11	**18c**	R	0.333	$AgBF_4$	no reaction (possibly experimental error)
12	**19a**	S	0.333	-	0.76 : 0.24
13	**19a**	S	0.333	$AgBF_4$	0.78 : 0.22 0.70 : 0.30[b]
14	**19b**	S	0.665	-	0.75 : 0.25
15	**19b**	S	0.333	-	0.84 : 0.16
16	**22**	S	0.333	-	0.79 : 0.21 0.80 : 0.20[b]
17	**19a**	R	0.333	-	0.75 : 0.25
18	**19b**	R	0.333	-	0.79 : 0.21
19	**19b**	R	0.333	$AgBF_4$	0.76 : 0.24 0.69 : 0.31[b]
20	**22**	R	0.333	-	0.77 : 0.23

Table 5. Hydrosilylation of carvone with Aib-functionalized NHC Rhodium(I) Complexes performed with diphenylsilane in CD_2Cl_2 in sealed NMR tubes at room temperature. [a]The sum of cis and trans proportions are 1 and data were obtained from integration of cis and trans C**H**OSiHPh_2 in ^{1}H NMR spectra; [b] repeat hydrosilylation of carvone carveol in same reaction conditions. Catalysts **19b** and **22** were provided by Dr. D. Tilly.[81]

As mentioned earlier, Aib tetramer is the shortest peptide that can fold into a 3_{10} helix. It was thought that that cationic Rh(I) species could interact with the Aib tetramer and remove a hydrogen bond resulting in damage of the helical property. Complex **21** (Figure 32), pentamer was synthesized to potentially overcome this problem, as it adds another H-bond to stabilize the helix. In the case of **21**, the addition of $AgBF_4$ gave a selectivity increase of almost 10% for both S- and R- carvone, which reached ratio 0.81 : 0.19. This increase was a bit higher than the other cases, but is still small.

The catalysts used for hydrosilylation are 1 : 1 mixtures of diastereoisomers. Swamy *et al*. reported a rhodium catalyst that exhibits selectivity during the hydrosilylation of *R*-carvone with d.r. 3.75 : 1 whereas its mirror isomer displays 99% d.r..[63] This inspires us to separate the diastereoisomers in our catalysts in order to test their individual diastereoselectivity. A problem for the separating is rhodium rotation around NHC-rhodium bond. It is observed that proton peaks from different isomers coalesce by reducing bulkiness from mesityl to methyl group (Table 3). Free rotation by further reducing bulkiness could remove one chiral centre of metal resulting in our catalysts becoming enantiomers which is hardly separated by chromatography. Iodide should increase bulkiness as ligand, which should decrease the rotation rate around the NHC-metal bond.[64] It is possible to convert chloride to iodide by mixing with NaI. This might allow the separation of the isomers by chromatography.

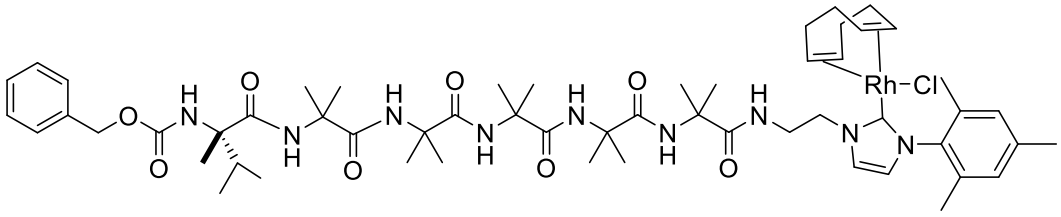

21

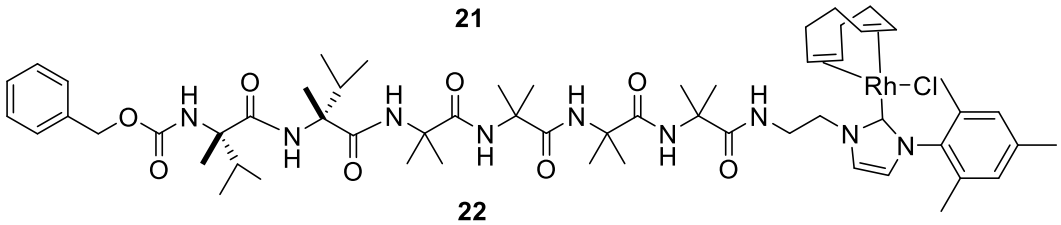

22

Figure 32. Structure of complex **21** and **22**.

An interesting phenomenon was observed with the phenyl terminated catalysts (entry 2, 12 and 13, with compound **18b** and **19a**). The signals of *cis* and *trans* carveol both decreased over time and a new peak form between cis and trans carveol (Figure 33). The rate of decrease was different between cis and trans carveol, as their ratio changed

in time. The phenomenon was not observed when suing the methyl and mesityl catalysts. The new formed compound was not separated from the reaction mixture due to the time issue. It was possible that the silyl group ($SiPh_3$) was hydrolysis over time. In summary, although there is no diastereoselectivity changes when azido is changed to a chiral controller at N-terminus of Aib foldamer, this work has shown that these complexes are still catalytically competent.

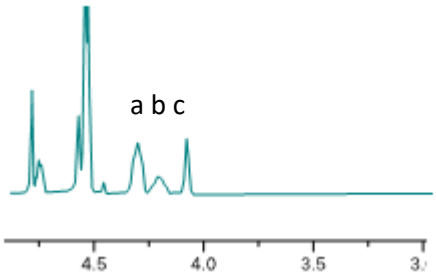

Figure 33. Spectrum of reaction mixture of hydrosilylation with phenyl after 48 hours. From left to right a: *cis* carveol, b: new peak, c: *trans* carveol.

3.3.2 Hydrosilylation of terminal alkynes

Transition-metal catalyzed hydrosilylation of alkynes is one of the most straightforward and effective ways for the synthesis of alkenyl-functionalized silanes. Vinylsilanes are highly attractive due to their versatility, low cost, lack of toxicity, wide functionality, and high chemical stability. Vinylsilanes are considered as an important class of organosilicon building blocks for the synthesis of molecules, polymers, and natural products. Although hydrosilylation of alkenes and alkynes with silanes or siloxanes has been widely studied, new strategies, which can increase the process effectiveness, decrease its costs and make it more environmentally friendly are continuously searched for. Although no chirality is introduced in these types of reactions, we were interested in applying these Aib foldamer-Rh complexes to the hydrosilylation of alkynes.

At the first step of the study, the catalytic hydrosilylation of 1-hexyne (77 μmol, 1 eq.) and phenylacetylene (77 μmol 1 eq.) were tested following the reported conditions, which is at room temperature with 1 mol % catalyst loading and a slight excess of silane $HSiMe_2Ph$ (85 μmol, 1.1 eq.) in $CDCl_3$ in sealed NMR tube.[69] The post-reaction mixtures were analyzed by ^1H NMR spectroscopy and the selectivity of vinylsilanes

was determined[69] (summarized in Table 6). Integration of the relevant resonances provided the proportions of each product.

Entry	Alkyne	Catalyst	Time / h	Conv. %	Cis %	Trans %	Gem %	2-ene %
1	1-hexyne	**18b**	227	49	50	31	23	0
2	1-hexyne	**19a**	126	100	18	41	12	30
3	1-hexyne	**18a**	42.5	64	81	10	7	2
4	1-hexyne	**21**	20	100	66	20	8	6
5	phenylacetylene	**18b**	194.5	71	38	44	18	-
6	phenylacetylene	**19a**	126	96	59	28	13	-
7	phenylacetylene	**18a**	44.5	74	83	14	3	-
8	phenylacetylene	**21**	45.5	91	78	17	5	-
9	phenylacetylene	**23**	216	100	0	88	12	-

Table 6. Hydrosilylation of terminal alkynes with Aib-functionalized NHC rhodium(I) complexes. With reactant alkynes 77 μmol, 1 eq.; Me_2PhSiH 85 μmol, 1.1 eq.; Rh cat. 1 mol % in solvent $CDCl_3$ 0.4 mL.

Catalytic hydrosilylation of 1-hexyne with **18b** and **19a** was found afford to four isomeric alkene silanes as products (Scheme 16). The peaks of the alkene protons were characterised by ^{1}H NMR spectroscopy. There are two kinds of double triplet with different coupling constant: δ (ppm)= 6.23 (dt, J = 14.4, 7.4 Hz) and 5.92 (dt, J = 18.5, 6.2 Hz) for cis and trans respectively. The other two isomers are minor compounds. The geminal alkene is with silane attached to the α-carbon has two peaks, each for one proton at 5.19 and 5.48 ppm. The 2-ene isomer is also a reported product with multiplet

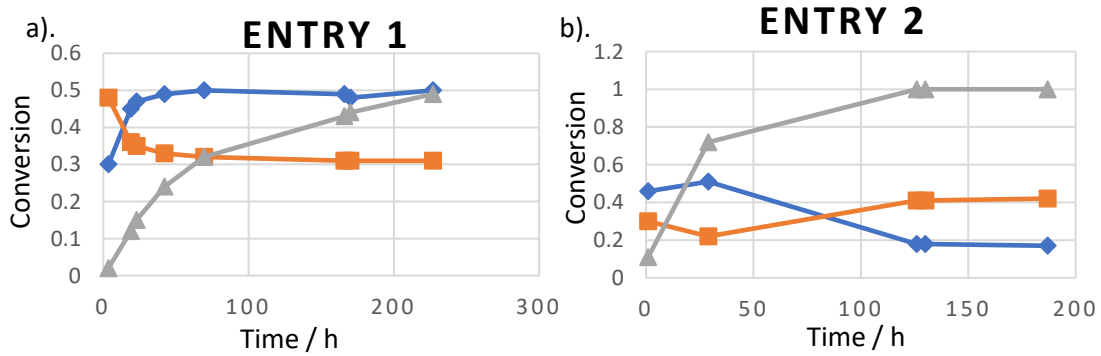

Figure 34. Reaction profile of conversion and selectivity vs. time for the hydrosilylation of 1-hexyne with a). **18b** and b). **19a**; catalyst loading 1%. Gray line (triangle): conversion; Blue line (diamond): percentage of cis isomer in product; Orange line (square): percentage of trans isomer in product.

at the range 5.0 to 5.3, but the isomer is hard to distinguish in our catalytic reactions.[65,66]

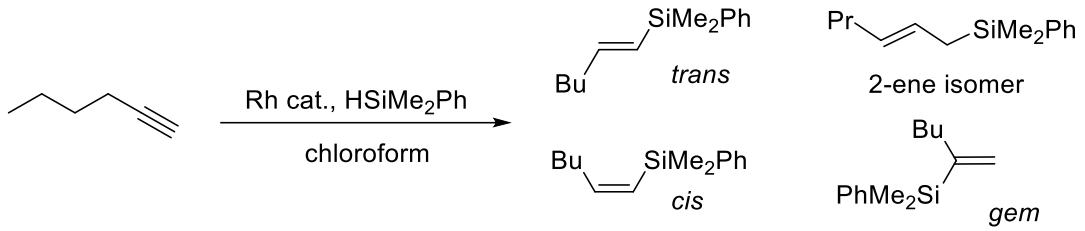

Scheme 16. Products of hydrosilylation of 1-hexyne.

The catalysts with different N-terminal functional groups displays different results. αMeVal capped catalyst **19a** display 100 % conversion, but azido capped catalyst **18b** did not go to competition during the same time. The steric hindrance around the nitrogen of NHC also gives different cis and trans selectivity. A mesityl substituent affords more cis isomer than the phenyl analogue. The azido complex exhibited higher selectivity for cis isomer than the αMeVal capped foldamer (Table 6 entry 1-4).

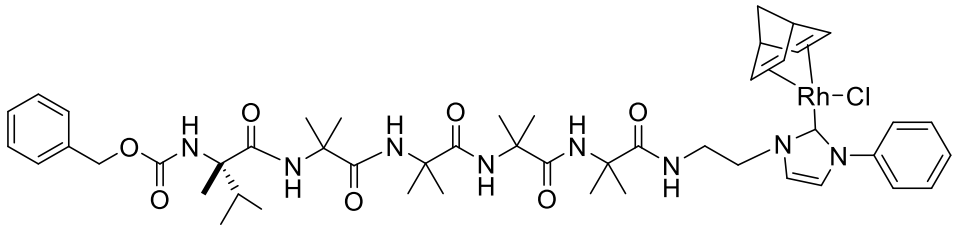

23

Figure 35. Structure of complex **23**.

Unlike 1-hexyne, there is no isomerisation possible with phenylacetylene substituent (Figure 36). There are three products of hydrosilylated phenylacetylene, which are trans, cis and geminal alkene isomers. In the ^{1}H NMR spectra, *trans* alkene is at 6.73 and 6.42 ppm with coupling constant J = 19.1 Hz; the *cis* and *geminal* alkene are overlapping in the range 5.86-5.78 ppm. The geminal alkene also displays a doublet at 5.48 ppm without overlapping.

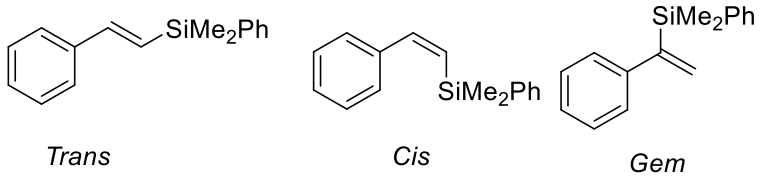

Figure 36. Products of hydrosilylated phenylacetylene.

The results from catalytic hydrosilylation with **18a, 18b, 19a, 21** and **23** are similar to the hydrosilylation of 1-hexyne, with αMeVal capped catalysts showing higher activity than the azido analogues during the same reaction time. Mesityl substituent on the NHCs shows higher preference for cis isomer than phenyl on the NHC. Azido catalysts with mesityl NHCs displayed the highest cis and trans ratio 0.83 : 0.14 (Table 5 entry 5-8).

For both 1-hexyne and phenylacetylene, once the conversion is complete, the cis vinylsilane isomerizes into trans vinylsilane. This behaviour is in line with what was previously reported by Crabtree et al. in the hydrosilylation of 1-hexyne with $HSiMePh_2$ catalyzed by $[RhCl(PPh_3)_3]$.[67] Total isomerization of cis vinylsilane to the trans was observed in the hydrosilylation of phenylacetylene with catalyst **23** (Cbz-L-αMeValAib$_4$EtNHCPh Rh(NBD)Cl) over 216 hours (Table 6 entry 9).

The reactions of azido capped catalyst do not go to completion. It is possible that the catalysts are poisoned due to a click reaction between the azide group and the alkynes.[68] Aib pentamer **21** showed the fastest reaction rate, with 90 % conversion in 50 hours. The hydrosilylation of 1-hexyne with catalysts afforded total conversion in 20 hours. The bulky NHC substituent on the NHC, mesityl, exhibited higher selectivity for cis compound in the hydrosilylation of 1-hexyne and phenylacetylene compare phenyl, although there is competing isomerization.

3.3.3 Hydrosilylation of Z (±)-1-phenyl-2-propyn-1-ol

It was reported that ruthenium catalytic hydrosilylation produces an α-hydrosilylated product instead of the β-hydrosilylated product when performed on tertiary propargylic alcohols. A variety of alkyne substrates gave regioselectivities in favour of the α-vinylsilane, an example of which is shown in Scheme 17. [69]

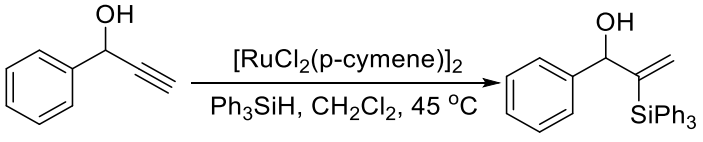

Scheme 17. Ruthenium catalytic α- hydrosilylation reaction with 98:2 selectivity for a-isomer, 60 % isolated yield).

Complex **18a** was tested for the catalytic hydrosilylation of the tertiary propargylic alcohol, racemic 1-phenyl-2-propyn-1-ol at 45 ^{o}C (water bath), using a slight excess of three different silanes in CD_2Cl_2 with 1 mol % catalyst loading.[69] All the reactions were routinely monitored in situ by ^{1}H NMR spectroscopy.

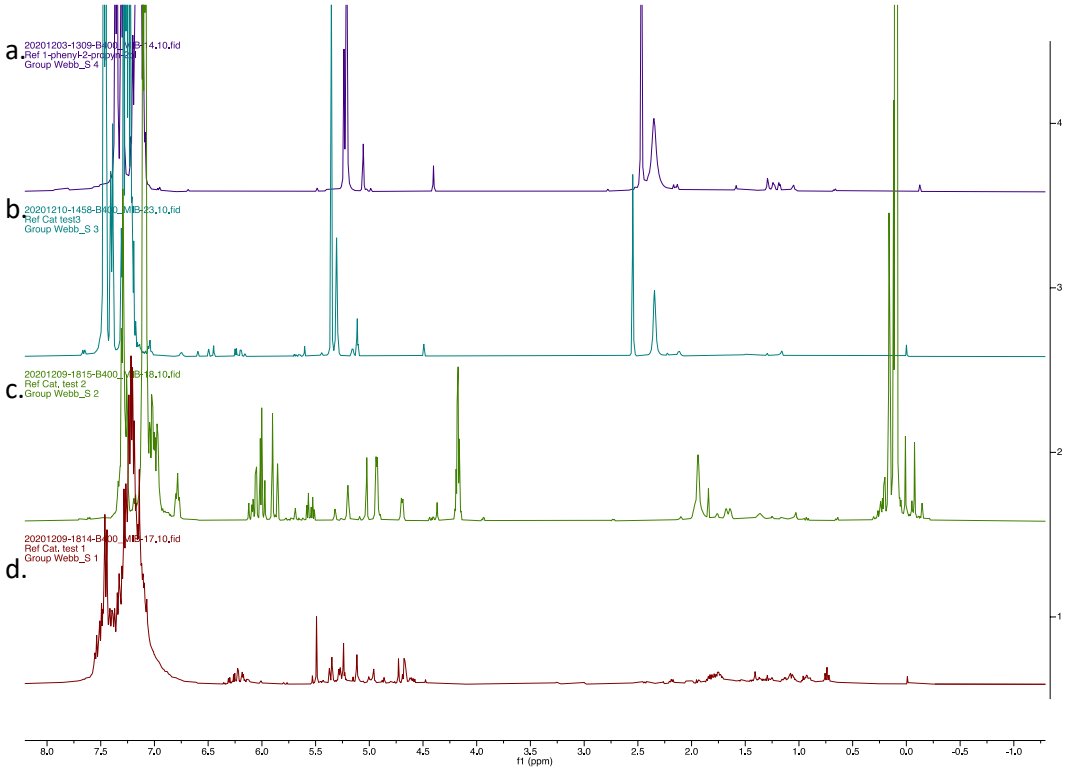

Figure 37. Results of 3 days hydrosilylation of **(**±)-1-phenyl-2-propyn-1-ol at room temperature. a). ^{1}H NMR (400 MHZ, CD_2Cl_2, 298K) spectrum of **(**±)-1-phenyl-2-propyn-1-ol; b). spectrum of hydrosilylation with triphenylsilane c). spectrum after hydrosilylation with dimethylphenylsilane; d). spectrum after hydrosilylation with diphenylsilane.

Different silanes were tested for this reaction. Triphenylsilane was used as it gave 87% selectivity for the α-hydrosilylated product with a rhodium(I) catalyst (Figure 37).[69,70] Phenyldimethylsilane and diphenylsilane were also tested. All the hydrosilylations were set up at room temperature, but no reaction was observed after 1 hour during monitoring by ^{1}H NMR spectroscopy. Then all three silane tests were put in a 45 ^{o}C water bath for 2 hours, as reported in the literature.[70] The phenyldimethylsilane then became as an efficient coupling partner with alkene signals formed in the ^{1}H NMR spectra. Triphenylsilane was presumably too hindered as no reaction was observed by

^{1}H NMR spectroscopy after three days and a little conversion was observed after a week (Figure 37 b). Diphenylsilane can couple with two equivalents of alkyne to afford divinyl silanes.[68] However the diphenylsilane reaction gave unidentified products overtime (Figure. 37d) with NMR signals are hard to integrate for peaks overlapping.

Products formed from reaction with dimethylphenylsilane gave resonances in the range of 4.5-7.0 ppm (Figure 37c) in the ^{1}H NMR spectra and reactant peaks decreasing over three days reaction time. The products are isomers and similar to those from hydrosilylated phenylacetylene (Figure 38).[70,71] In this case, the *cis* isomer is the major product and geminal isomer was in higher percentage in the products than hydrosilylation of phenylacetylene (Table 6. entry 7) with geminal alkene 19.9 %, *trans* 28.4% and *cis* 51.7%.

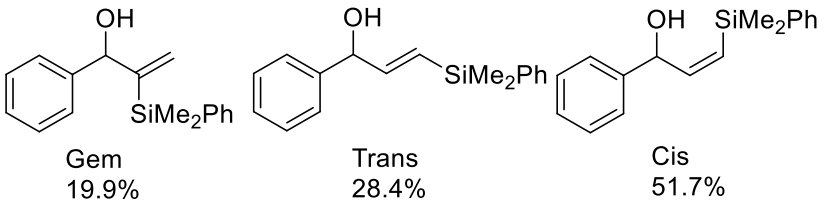

Figure 38. Products of hydrosilylated 1-phenyl-2-propyn-1-ol.

4 Synthesis of NHC ligand attached to Aib foldamer at an acute angle

The catalytic hydrosilylation of carvone by L-αMeVal capped Aib foldamer-Rh showed, but the diastereoselectivity is irrespective of the screw sense of the Aib foldamer. To improve the relay of chirality from the foldamers, NHCs were designed with a different angle so that the Aib foldamer directly interacts with metal center (Scheme 26). The new angle is based on imidazo[1, 5-a]pyridinium salts **26**, where the Aib foldamer can form amide bond with the amine substituent.

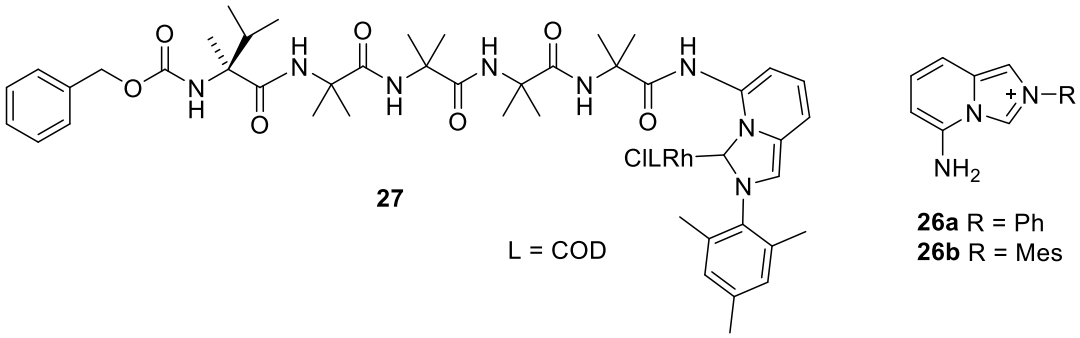

Scheme 18. Structure of proposed rhodium complex **27** and imidazo[1, 5-a]pyridinium salts **26**.

The proposed synthesis of the new NHC is shown in Scheme 18. Each imine intermediate was synthesized with 6-bromo-2-pyridinecarboxaldehyde and an acyl amine, followed by treatment with formaldehyde and TMS to afford imidazopyridinium salts **24**. The synthesis route to amine **26** was firstly designed by using reduction of azide. The azido molecule **25** was prepared by substitution of **24b** with sodium azide with the yield 11 %. The azide **25** was fully characterized by ESI-MS mass spectrometry, and ^{1}H and ^{13}C NMR using COSY, HSQC, and HMBC.

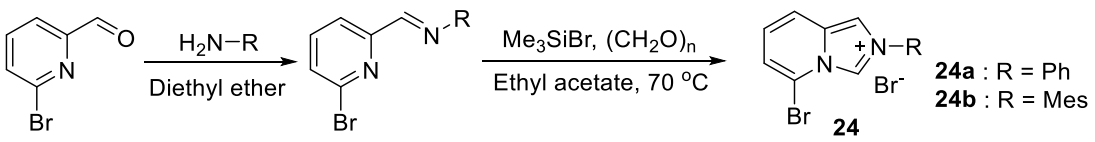

Scheme 19. Synthesis of imidazo[1, 5-a]pyridinium salts **24a-b** from aldehyde precursor.

Hydrogenation of azide **25** was performed using the same conditions used to synthesize N-terminal amine Aib foldamers; palladium on carbon in ethanol under hydrogen atmosphere. However, almost no product obtained. One fraction analysed by ESI-MS mass spectrometry showed the mass of product amine **26b**, 252.2 without Br anion. However, the mass spectrum also showed fractions with 241.4 and 773.8 molecular mass with 100% abundance. It was possible that the hydrogenation was over reducing the **26b** at unexpected positions and induces the formation of unknown trimer molecules.

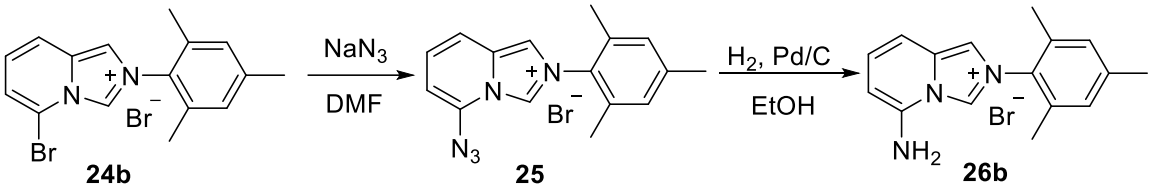

Scheme 20. Synthesis of imidazo[1, 5-a]pyridinium salts **26b** by hydrogenation.

Due to the failed hydrogenation of azide **25**, an alternative method was tried to produce amine compound **26b**. The method to be used was the well-established Staudinger reaction (Scheme 21), where bromine was first substituted by azide and then produces an iminophosphorane, which was reported as a stable compound.[63] In aqueous media, iminophosphorane should be hydrolysed to produce amine **26a**, according to standard the reaction and workup conditions.[72,73]

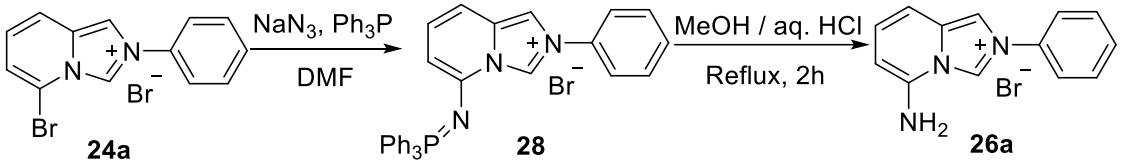

Scheme 21. Synthesis of imidazo[1, 5-a]pyridinium salts **26a** by Staudinger reaction.

The iminophosphorane **28** was synthesized by addition of sodium azide and triphenylphosphine, then the iminophosphorane was added to a solution of methanol and hydrochloride for 2h reflux.[76,77] After that, triphosphine oxide (TPPO) was obtained after neutralization by sodium hydroxide found by ^{1}H NMR spectrum. However, there is no product was obtained after workup and chromatography on silica gel. It is possible that the amine compound is sensitive to air or it degraded in the basic conditions. Therefore, the **26a** should be separated in acidic conditions for the next time.

5 Conclusion

A series of NHC rhodium complexes bearing both an Aib foldamer and increasingly bulky aryl substituents were synthesised, and their conformations studied in solution using NMR spectroscopy. The rhodium complexes were found to catalyze the hydrosilylation of a ketone, carvone, and three terminal alkynes 1-hexyne, phenylacetylene and 1-phenyl-2-propyn-1-ol. Good to excellent conversions were observed with mixtures of isomers formed.

Diastereoselectivity was observed in the catalytic hydrosilylation of carvone with H_2SiPh_2, and catalysis by neutral azido rhodium(I) complexes **18a-c** was compared with that of the N-terminal chiral L-αMeVal functionalized rhodium catalysts **19a**, **19b**, **21**, **22**. A preference for the *cis* isomer with Aib foldamers as the catalyst was observed no matter if the Aib foldamer had a screw sense preference. The ratio of *cis*:*trans* isomers was not significantly different between these catalysts. However, different reactivity was observed during hydrosilylation of terminal 1-hexyne, phenylacetylene and phenyl-2-propyn-1-ol with $HSiPhMe_2$, where Aib catalysts bearing an N-terminal chiral controller exhibited faster reaction rates. For example, the hydrosilylation of 1-hexyne was finished in 20 hours when using Aib pentamer catalyst **21**.

Different substituents on the NHC produce different effects on both the rotation around the Rh-NHC bond and the catalytic properties of the foldamers. The bulky mesityl group impedes the rotation of rhodium catalysts, while this effect is reduced with methyl group. For the hydrosilylation of carvone, there was no obvious difference in stereoselectivity between foldamer catalysis bearing different substituents on the NHC. However, for the hydrosilylation of terminal alkynes, the mesityl group shows higher reactivity and selectivity than the phenyl group.

Although no different diastereoselectivity was observed during catalysis by chirally controlled foldamers, a few avenues for future work are clear. The diastereoisomers of the Aib NHC complexes might be separable after replacing chloride with iodide, which can increase bulkiness and further decrease the rotation of the NHC-metal bond; perhaps the isomers can be isolated by chromatography. Alternatively, the Aib foldamer can also be set at a more acute angle to the NHC, allowing screw sense to exert a greater influence on the selectivity of catalytic reactions.

6 Experimental

General Information

Nuclear Magnetic Resonance (NMR)

Nuclear Magnetic Resonance (NMR) spectra (^{1}H NMR and ^{13}C NMR) were recorded on Bruker DPX 400 (400 MHz) or a Bruker AVIII HD 500 spectrometer equipped with a prodigy BBO 5 mm probe (500 MHz). All NMR characterisation experiments were performed at 25 °C and 1 atm unless otherwise stated. Chemical shifts (δ) are quoted in parts per million (ppm) downfield of trimethylsilane. Spectra were calibrated using the residual solvent peaks for $CDCl_3$ (δH: 7.26 ppm; δC: 77.16 ppm), CD_2Cl_2 (δH: 5.32 ppm; δC: 53.84 ppm) and $(CD_3)2SO$ (δH: 2.50 ppm; δC: 39.52 ppm) as appropriate. Coupling constants (J) are quoted in Hz and are rounded to the nearest 0.1 Hz. Splitting patterns are abbreviated to : singlet (s), doublet (d), triplet (t), quartet (q), multiplet (m), broad (b) or some combination thereof.

Mass Spectroscopy

High resolution mass spectra (HRMS) were recorded by staff at the University of Manchester on a Thermo Finnigan MAT95XP and are accurate to ±0.001 Da.

Infrared Spectroscopy

Infrared spectra were recorded on a Perkin Elmer (Spectrum One) FT-IR spectrometer with samples applied as films. Absorption maxima (ν_{max}) of interest are quoted in wavenumbers (cm^{-1}).

Melting points

Melting points were measured on a Stuart SMP10 melting point apparatus and are uncorrected.

Circular Dichroism

Optical rotation ($[\alpha]_D^T$) measurements were taken on a AA-100 polarimeter at 20°C.

HPLC

HPLC analyses were performed using the HPLC facilities of the Manchester Institute of Biotechnology on an Agilent 1100 Series instrument equipped with a Chiralpak®AS column.

Chromatography

Column chromatography was performed using silica gel and basic Al_2O_3.

Thin-layer chromatography (TLC)

Thin-layer chromatography (TLC) was performed using pre-coated plates (Macherey-Nagel Polygram SIL G/UV254). Visualisation was achieved by way of UV light (at 254 nm), and staining with either potassium permanganate, phosphomolybdic acid (in ethanol), or ninhydrin (in ethanol) as stains. Stained TLC plates were heated for visualization. Preparative column (flash) chromatography was carried out using commercially available normal phase silica gel or basic alumina when stated.

Solvents and Reagents

Reagents used were obtained from Sigma Aldrich or Bachem and were used as received.

Reaction Conditions

All reactions were carried out in oven-dried glassware, with magnetic stirring and under an atmosphere of nitrogen unless otherwise stated.

6.2 Synthetic Procedures

Synthesis of N_3AibO^{t}Bu

Sodium azide (11.7 g, 180 mmol) was added to a stirred solution of commercially available 2-bromo-2-methylpropionic acid (18 g, 108 mmol) in dry DMF (80 mL) under N_2, and the mixture was stirred at rt for 3 days. Then, the mixture was diluted with H_2O (45 mL), acidified with 1 M HCl to pH 2. The aqueous phase was extracted with MTBE (2 × 50 mL). The combined organic phase was washed with 1 M HCl (4 × 25 mL), dried over $MgSO_4$ and concentrated under reduced pressure to give N_3AibOH as a colorless oil (81%).

^{1}H NMR (400 MHz, $CDCl_3$): δ 1.49 (s, 9H, CH_3), 1.41 (s, 6H, CH_3) ppm. ^{13}C NMR (400 MHz, $CDCl_3$): δ 172.0 (CO), 82.6 (C), 63.5 ($(CH_3)_2$**C**), 28.0 (CH_3), 24.5 (CH_3) ppm. Data is consistent with that reported in the literature.[13]

Synthesis of N_3AibOH

Sodium azide (8.8 g, 135 mmol) was added to a stirred solution of commercially available tert-butyl a-bromoisobutyrate (16.9 mL, 90.6 mmol) in dry DMF (80 mL) under N_2, and the mixture was stirred at rt for 3 days. Then, the mixture was diluted with H_2O (45 mL), acidified with 1 M HCl to pH 2. The aqueous phase was extracted with MTBE (2 × 100 mL). The combined organic phase was washed with 1 M HCl (4 × 25 mL), dried over $MgSO_4$ and concentrated under reduced pressure to give N_3AibOH as a colorless oil (13.5 g, 80.5 %).[13]

^{1}H NMR (400 MHz, $CDCl_3$): δ 1.20 (6H, s, CH_3) ppm. **^{13}C NMR** (400 MHz: $CDCl_3$): δ 177.9 (CO), 62.9 ($(CH_3)_2$**C**), 24.3 (CH_3) ppm. Data is consistent with that reported in the literature. [13]

Synthesis of H_2NAibO^{t}Bu

N_3AibOtBu (13.5 g, 73 mmol) was dissolved in EtOH (65 mL). Pd/C (150 mg, 10%) was slowly added and the reaction mixture was vigorously stirred under H_2 atmosphere until NMR indicated consumption of the starting material. The mixture was then washed through a pad of Celite® with EtOAc and the filtrate was concentrated under reduced pressure to give the title compound as a colorless oil (5.7 g, 49 %) which was used without further purification.

^{1}H NMR (400 MHz, $CDCl_3$): δ 1.67 (bs, 2H, NH_2), 1.44 (s, 9H, CH_3), 1.28 (s, 6H, CH_3) ppm. **^{13}C NMR** (400 MHz, $CDCl_3$): δ 177.5 (CO), 80.7 (C), 55.1 ($(CH_3)_2$C), 28.0 (CH_3), 27.8 (CH_3) ppm. Data is consistent with that reported in the literature.[13]

General procedure I of adding monomer to N_3AibOH to foldamer chain (N_3Aib_nOH).

A solution of N_3AibOH (2 eq.) in CH_2Cl_2 and EDC•HCl (4 eq.) was stirred for 10 min. Then, HOBt (0.2 eq.) was added and the mixture was cooled at 0 ^{o}C and further stirred for 10 min. Et_3N (4 eq.) was then added dropwise and, after 5 min, $NH_2Aib_nO^tBu$ (1 eq., n=1,2,3,4) was finally added. The mixture was left to warm to rt and stirred for 27 h. The, the mixture was washed with 1 M HCl, saturated $NaHCO_3$ and brine. The organic layer was dried over $MgSO_4$, filtered and concentrated under reduced pressure. The crude product was the purified by flash chromatography (SiO_2, EtOAc/petroleum ether) to afford pure $N_3Aib_{n+1}O^tBu$.

Synthesis of $N_3Aib_2O^tBu$

Following general procedure I with NH_2AibO^tBu (2 g, 12.6 mmol) afforded the compound as an white solid (2.55 g, 75 %).

^{1}H NMR (400 MHz, $CDCl_3$): δ 7.09 (bs, 1H, NH), 1.51 (s, 6H, CH_3), 1.50 (s, 6H, CH_3), 1.45 (s, 9H, CH_3) ppm. **^{13}C NMR** (400 MHz, $CDCl_3$): δ 173.6 (CO), 171.2 (CO), 81.8 (C), 64.4 ((CH_3)$_2$**C**), 56.8 ((CH_3)$_2$**C**), 27.9 (CH_3), 24.5 (CH_3), 24.4 (CH_3) ppm. Data is consistent with that reported in the literature.[13]

Synthesis of $H_2NAib_2O^tBu$

$N_3Aib_2O^tBu$ (2.55 g, 9.5 mmol) was dissolved in EtOH (25 mL). Pd/C (100 mg, 10%) was slowly added and the reaction mixture was vigorously stirred under H_2 atmosphere until ^{1}H NMR spectroscopy indicated consumption of the starting material. The mixture was then washed through a pad of Celite® with EtOAc and the filtrate was concentrated under reduced pressure to give the title compound as a colorless oil (2.23 g, 97%) which was used without further purification.

^{1}H NMR (400 MHz, $CDCl_3$): δ 8.07 (bs, 1H, NH), 1.49 (s, 6H, CH_3), 1.44 (s, 9H, CH_3), 1.32 (s, 6H, CH_3) ppm. **^{13}C NMR** (400 MHz, $CDCl_3$): δ 176.6 (CO), 174.1 (CO), 81.2 (C), 56.3 ((CH_3)$_2$**C**), 54.9 ((CH_3)$_2$**C**), 29.2 (CH_3), 28.0 (CH_3), 24.7 (CH_3) ppm. Data is consistent with that reported in the literature.

Synthesis of $N_3Aib_3O^tBu$

Following general procedure I with $NH_2Aib_2O^tBu$ (2.23 g, 9.2 mmol) afforded the compound as an white solid (1.45 g, 48%).

^{1}H NMR (400 MHz, $CDCl_3$): δ 7.19 (bs, 1H, NH), 6.97 (bs, 1H, NH), 1.55 (s, 6H, CH_3), 1.52 (s, 6H, CH_3), 1.51 (s, 6H, CH_3), 1.45 (s, 9H, CH_3) ppm. **^{13}C NMR** (400 MHz, $CDCl_3$): δ 174.2 (CO), 173.0 (CO), 171.9 (CO), 81.9 (C), 64.5 ((CH_3)$_2$**C**), 57.3 ((CH_3)$_2$**C**), 57.1 ((CH_3)$_2$**C**), 27.9 (CH_3), 25.0 (CH_3), 24.5 (CH_3), 24.1 (CH_3) ppm. Data is consistent with that reported in the literature. [13]

Synthesis of $H_2NAib_3O^tBu$

$N_3Aib_3O^tBu$ (1.45 g, 4.4 mmol) was dissolved in EtOH (25 mL). Pd/C (100 mg, 10%) was slowly added and the reaction mixture was vigorously stirred under H_2 atmosphere until ^{1}H NMR spectroscopy indicated consumption of the starting material. The mixture was then washed through a pad of Celite® with EtOAc and the filtrate

was concentrated under reduced pressure to give the title compound as a white solid which was used without further purification.

^{1}H NMR (400 MHz, $CDCl_3$): δ 8.16 (bs, 1H, NH), 7.46 (bs, 1H, NH), 1.52 (s, 6H, CH_3), 1.49 (s, 6H, CH_3), 1.43 (s, 9H, CH_3), 1.34 (s, 6H, CH_3) ppm. **^{13}C NMR** (400 MHz, $CDCl_3$): δ 177.8 (CO), 174.2 (CO), 173.6 (CO), 81.4 ((CH$_3$)$_2$**C**), 57.1 ((CH$_3$)$_2$**C**), 56.8 ((CH$_3$)$_2$**C**), 55.1 ((CH$_3$)$_2$**C**), 29.1 (CH_3), 28.0 (CH_3), 25.3 (CH_3), 24.4 (CH_3) ppm. Data is consistent with that reported in the literature. [13]

Synthesis of N$_3$Aib$_4$O^{t}Bu

Following general procedure I with H_2NAib$_3$O^{t}Bu (1.45 g, 4.4 mmol) afforded the compound as an white solid (1.43g, 75%).

^{1}H NMR (400 MHz, $CDCl_3$): δ 7.00 (bs, 1H, NH), 6.96 (bs, 1H, NH), 6.50 (bs, 1H, NH), 1.52 (s, 6H, CH_3), 1.51 (s, 6H, CH_3), 1.50 (s, 6H, CH_3), 1.47 (s, 6H, CH_3), 1.43 (s, 9H, CH_3) ppm. **^{13}C NMR** (400 MHz, $CDCl_3$): δ 173.9 (CO), 173.1 (CO), 172.5 (CO), 172.4 (CO), 81.0 ((CH$_3$)$_2$**C**), 64.3 ((CH$_3$)$_2$**C**), 57.2 ((CH$_3$)$_2$**C**), 57.0 ((CH$_3$)$_2$C), 56.7 ((CH$_3$)$_2$**C**), 28.0 (CH_3), 25.3 (CH_3), 25.1 (CH_3), 24.53 (CH_3), 24.46 (CH_3) ppm. Data is consistent with that reported in the literature.[13]

Synthesis of H$_2$NAib$_4$O^{t}Bu

N$_3$Aib$_4$O^{t}Bu (1 g, 2.27 mmol) was dissolved in EtOH (100 mL) and Pd/C (200 mg) was added. The flask was sealed, vacated then vigorously stirred under H_2 at room temperature for 3 days. The reaction was monitored by TLC (2:1, PE: EtOAc). The mixture was washed through a pad of Celite® with EtOAc. The organic layer was dried with $MgSO_4$, filtered then evaporated under reduced pressure to give H_2NAib$_4$OtBu as a white solid (973 mg, 99 %).

^{1}H NMR (400 MHz, $CDCl_3$): δ 8.13 (bs, 1H, NH), 7.27 (bs, 1H, NH), 6.59 (bs, 1H, NH), 1.47 (s, 6H, CH_3), 1.46 (s, 12H, CH_3), 1.41 (s, 9H, CH_3), 1.35 (s, 6H, CH_3) ppm. **^{13}C NMR** (400 MHz, $CDCl_3$): δ 178.2 (CO), 174.0 (CO), 173.1 (CO), 173.0 (CO), 80.6 (C), 56.8 ((CH$_3$)$_2$**C**), 56.7 ((CH$_3$)$_2$**C**), 56.5 ((CH$_3$)$_2$**C**), 55.0 ((CH$_3$)$_2$**C**), 29.0 (CH_3), 28.0 (CH_3), 25.5 (CH_3), 25.2 (CH_3), 25.0 (CH_3) ppm. Data is consistent with that reported in the literature.[13]

Synthesis of N$_3$AiB$_4$OH

TFA (0.6 mL) was added to a solution of $N_3Aib_4CO_2tBu$ (628 mg, 1.59 mmol) in CH_2Cl_2 (4 mL) and stirred for 5h. After completion of the reaction, the reaction mixture was concentrated under reduced pressure to yield $N_3Aib_4CO_2H$ as a white solid (557 mg, quantitative). Analytical data are in accordance with previously reported data.

^{1}H NMR (400 MHz, DMSO-d_6) δ 7.85 (s, 1H, N*H*), 7.46 (s, 1H, N*H*), 7.26 (s, 1H, N*H*), 1.45 (s, 6H, (CH_3)$_2$C), 1.35 (s, 6H, (CH_3)$_2$C), 1.34 (s, 6H, (CH_3)$_2$C), 1.29 (s, 6H, (CH_3)$_2$C). **^{13}C NMR** (101 MHz, DMSO-d_6) δ 175.6 (*C*=O), 173.3 (*C*=O), 172.6 (*C*=O), 171.9 (*C*=O), 63.6 (*C*(CH$_3$)$_2$), 56.4 (*C*(CH$_3$)$_2$), 55.6 (*C*(CH$_3$)$_2$), 54.8 (*C*(CH$_3$)$_2$), 24.7 (2C, (*C*H$_3$)$_2$C), 24.5 (2C, (*C*H$_3$)$_2$C), 24.4 (2C, (*C*H$_3$)$_2$C), 23.9 (2C, (*C*H$_3$)$_2$C). Data is consistent with that reported in the literature.[13]

Synthesis of $H_2NAib_5O^tBu$

N_3Aib_5OtBu (300 mg, 0.68 mmol) was dissolved in EtOH (50 mL) and Pd/C (30 mg) was added. The flask was sealed, vacated then vigorously stirred under H_2 at room temperature for 3 days. The reaction was monitored by TLC (2:1, PE: EtOAc). The mixture was washed through a pad of Celite® with EtOAc. The organic layer was dried with $MgSO_4$, filtered then evaporated under reduced pressure to give H_2NAib_5OtBu (282 mg, 0.68 mmol).

^{1}H NMR (400 MHz, Acetone-d_6) δ 8.96 (s, 3H, NH_3^+), 8.61 (s, 1H, N*H*), 7.97 (s, 1H, N*H*), 7.67 (s, 1H, N*H*), 7.58 (s, 1H, N*H*), 1.78 (s, 6H, 2 x (CH_3)C), 1.50 (s, 6H, 2 x (CH_3)C), 1.48 (s, 6H, 2 x (CH_3)C), 1.46 – 1.43 (bs, 9H, 3 x (CH_3)C), 1.43 – 1.40 (bs, 9H, 3 x (CH_3)C). **^{13}C NMR** (101 MHz, Acetone) δ 175.3 (*C*=O), 175.3 (*C*=O), 175.2 (*C*=O), 175.0 (*C*=O), 172.7 (*C*=O), 81.4 (*C*(CH$_3$)$_3$), 58.7 (*C*(CH$_3$)$_2$), 58.2 (*C*(CH$_3$)$_2$), 57.6 (*C*(CH$_3$)$_2$), 57.3 (*C*(CH$_3$)$_2$), 56.9 (*C*(CH$_3$)$_2$), 28.0 (3C, (*C*H$_3$)$_3$C), 25.5 (2C, (*C*H$_3$)$_2$C), 25.3 (2C, (*C*H$_3$)$_2$C), 25.2 (2C, (*C*H$_3$)$_2$C), 24.9 (2C, (*C*H$_3$)$_2$C), 24.3 (2C, (*C*H$_3$)$_2$C). Data is consistent with that reported in the literature.[13]

Synthesis of Cbz-(L-αMeVal)Aib$_4$OtBu

Cyanuric fluoride (416 mg, 3.08 mmol) and pyridine (487 mg, 6.61 mmol) were added to a solution of Z-L-(aMeVal) (583.2 mg, 2.2 mmol) in dry DCM (10 mL) at 0 ^{o}C. The reaction mixture was stirred at 0 ^{o}C for 1 h and 20 ^{o}C for 2 h to afford Z-L-(aMeVal)F.

To a stirred solution of $H_2NAib_4O^tBu$ (353 mg, 1.1 mmol) and DIPEA (0.8 mL, 4.4 mmol) in dry dichloromethane (20 mL) was added a solution of Z-L-(αMeVal)F (186 mg, 1.15 mmol) in dry dichloromethane (5 mL) and the reaction stirred at 20 °C under nitrogen for 3 days. The mixture was concentrated, then ethyl acetate (50 mL) was added and the organic phase was washed with aqueous 5 % $KHSO_4$ (3 x 30 mL), water (3 x 30 mL), then aqueous saturated $KHCO_3$ (3 x 30 mL). The organic phase was dried ($MgSO_4$), concentrated under reduced pressure. The white solid was triturated in diethylether then filtered on filter paper. The solid on the filter paper was dissolved in methanol, then concentrated under reduced pressure provided the product as a white solid (106 mg, 0.51 mmol, 17 %).

^{1}H NMR (400 MHz, $CDCl_3$) δ 7.38 – 7.15 (m, 9H, 3N*H*, 5 x CH_{Ar}), 6.21 (s, 1H, NH_{Cbz}), 5.39 (s, 1H, NH), 5.08 (d, *J* = 12.2 Hz, 1H, CH_2Ph), 4.93 (d, *J* = 12.2 Hz, 1H, CH_2Ph), 1.88 – 1.79 (m, 1H, C*H*$(CH_3)_2$), 1.44 (s, 3H, CH_3), 1.39 (s, 3H, CH_3), 1.37 (s, 3H, CH_3), 1.36 (s, 3H, CH_3), 1.35 (s, 6H, 2 x CH_3), 1.31 (d, *J* = 3.0 Hz, 15H, 2 x CH_3, $(CH_3)_3$C), 1.11 (s, 3H, CH_3), 0.87 (d, *J* = 6.7 Hz, 3H, $(CH_3)_2$CH)), 0.83 (d, *J* = 6.8 Hz, 3H, $(CH_3)_2$CH)). **^{13}C NMR** (101 MHz, $CDCl_3$) δ 174.2 (*C*=O), 174.1 (*C*=O), 173.9 (*C*=O), 173.8 (*C*=O), 172.6 (*C*=O), 156.2 (*C*=O_{Cbz}), 136.2 (*C*), 128.8 (2C, 2 x *C*H_{Ph}), 128.7 (*C*H_{Ph}), 128.4 (2C, 2 x *C*H_{Ph}), 79.8 (*C*$(CH_3)_3$), 67.5 (*C*H_2Ph), 63.1 (C_{Val}), 57.0 (C_{Aib}), 56.8 (C_{Aib}), 56.8 (C_{Aib}), 56.1 (C_{Aib}), 35.6 (*C*H$(CH_3)_2$), 28.0 (3C, $(CH_3)_3$C), 27.3 (*C*H_{3AiB}), 27.0 (*C*H_{3AiB}), 26.9 (*C*H_{3Aib}), 25.7 (*C*H_{3Aib}), 24.2 (*C*H_{3Aib}), 23.9 (*C*H_{3Aib}), 23.6 (*C*H_{3Aib}), 23.5 (*C*H_{3Aib}), 17.7 (*C*$H_{3\ Val}$), 17.4 ($(CH_3)_2CH_{Val}$), 17.3 ($(CH_3)_2CH_{Val}$). **FTIR (neat)** ν_{max} = 3421, 3341, 3307, 3232, 2980, 2940, 2237, 1729, 1697, 1683, 1667, 1638, 1537, 1501, 1456, 1384, 1363, 1308, 1269, 1224, 1213, 1147, 1071, 1038 cm^{-1}. **MP** 215-216 °C. Data is consistent with that reported in the literature.[13]

Synthesis of Cbz-(L-αMeVal)Aib$_4$OH

To a stirred solution of Cbz-(L-αMeVal)Aib$_4$OtBu (280 mg, 0.5 mmol) in dry dichloromethane was added trifluoroacetic acid (0.25 mL, 3.2 mmol) and the mixture was stirred at 20 °C for 5 hours (completion of the reaction was monitored by thin layer chromatography). After concentration under reduced pressure the residue was triturated several times with diethylether and concentrated to provide the product as a white solid (250 mg, 0.5 mmol, quantitative).

^{1}H NMR (400 MHz, $CDCl_3$) δ 7.73 (s, 1H, N*H*), 7.53 (s, 1H, N*H*), 7.46 (s, 1H, N*H*), 7.36 – 7.24 (m, 5H, 5 x C*H*$_{Ph}$), 6.33 (s, 1H, N*H*), 5.28 (s, 1H,N*H*), 5.11 (d, *J* = 12.2 Hz, 1H, C*H*$_2$Ph), 4.97 (d, *J* = 12.2 Hz, 1H, C*H*$_2$Ph), 1.87 (p, *J* = 6.8 Hz, 1H, C*H*$(CH_3)_2$), 1.53 (s, 3H, (C*H*$_3$)C), 1.50 (s, 3H, (C*H*$_3$)C), 1.44 (s, 3H, (C*H*$_3$)C), 1.41 (s, 3H, (C*H*$_3$)C), 1.36 (s, 3H, (C*H*$_3$)C), 1.35 (s, 3H, (C*H*$_3$)C), 1.34 (s, 3H, (C*H*$_3$)C), 1.33 (s, 3H, (C*H*$_3$)C), 1.13 (s, 3H, (C*H*$_3$)C), 0.91 (d, *J* = 6.8 Hz, 3H, (C*H*$_3$)CH), 0.87 (d, *J* = 6.8 Hz, 3H, (C*H*$_3$)CH). **^{13}C NMR** (101 MHz, $CDCl_3$) δ 188.8 (*C*O_2H), 176.4 (*C*=O), 175.7 (*C*=O), 174.0 (*C*=O), 173.0 (*C*=O), 156.1 (*C*=O$_{Cbz}$), 136.0 (*C*$_{Ph}$), 128.8 (2C, 2 x *C*H$_{Ph}$), 128.7 (*C*H$_{Ph}$), 128.1 (2C, 2 x *C*H$_{Ph}$), 67.5 (*C*(CH_3)(*i*Pr)), 63.0 (*C*H_2Ph), 57.7 (*C*$(CH_3)_2$), 57.0 (*C*$(CH_3)_2$), 56.9 (*C*$(CH_3)_2$), 56.6 (*C*$(CH_3)_2$), 35.5 (*C*H$(CH_3)_2$), 26.6 (2 x *C*H$_3$), 26.5 (*C*H$_3$), 25.6 (*C*H$_3$), 24.6 (*C*H$_3$), 23.9 (*C*H$_3$), 23.5 (*C*H$_3$), 23.2 (*C*H$_3$), 17.4 (*C*H$_3$), 17.3 (*C*H$_3$), 17.1 (*C*H$_3$). Data is consistent with that reported in the literature.[13]

Synthesis of Cbz-(L-αMeVal)Aib$_5$O^{t}Bu

Cyanuric fluoride (0.15 mL, 1.76 mmol) and pyridine (0.28 mL, 3.5 mmol) were added to a solution of Z-L-(αMeVal) (200 mg, 1.26 mmol) in dry DCM (4 mL) at 0 ^{o}C. The reaction mixture was stirred at 0 ^{o}C for 1 h and 20 ^{o}C for 2 h to afford Z-L-(αMeVal)F.

To a stirred solution of H_2NAib$_5$OtBu (261 mg, 0.63 mmol) and DIPEA (0.18 mL, 1.26 mmol) in dry dichloromethane (10 mL) was added a solution of Z-L-(αMeVal)F (345 mg) in dry dichloromethane (5 mL) and the reaction stirred at 20 °C under nitrogen for 3 days. The mixture was concentrated, then ethyl acetate (50 mL) was added and the organic phase was washed with aqueous 5 % $KHSO_4$ (3 × 30 mL), water (3 × 30 mL), then aqueous saturated $KHCO_3$ (3 × 30 mL). The organic phase was dried ($MgSO_4$), concentrated under reduced pressure. The white solid was triturated in diethylether then filtered on a filter paper. The solid on the filter paper was dissolved in methanol, concentration of methanol under reduced pressure provided the product the product (140 mg, 0.252 mmol, 40 %).

^{1}H NMR (400 MHz, CDCl3) δ 7.57 (s, 1H, NH), 7.46 (s, 1H, NH), 7.37 (s, 6H, NH, 5 × CHPh), 7.27 (s, 1H, NH), 6.28 (s, 1H, NHCbz), 5.28 (s, 1H, NH), 5.18 (d, J = 12.2 Hz, 1H, CH2Ph), 5.03 (d, J = 12.2 Hz, 1H, CH2Ph), 1.93 (m, 1H, CH$(CH_3)_2$), 1.52 – 1.45 (m, 18H, 6 x CH_3 Aib), 1.43 (m, 21 H, 7 x CH3), 1.20 (s, 3H, CH_3), 0.98 (d, J = 6.8 Hz, 3H, $(CH_3)_2$CH), 0.95 (d, J = 6.8 Hz, 3H, $(CH3)_2$CH). **^{13}C NMR** (101 MHz, $CDCl_3$) δ 175.0 (C=O), 174.3 (C=O), 174.2 (C=O), 174.1 (C=O), 173.7 (C=O), 172.7

(C=O), 156.2 (C=OCbz), 136.0 (C), 128.9 (2C, 2 × CHPh), 128.8 (CHPh), 128.4 (2C, 2 × CHPh), 79.8 ($C(CH_3)_3$), 67.7 (CH_2Ph), 63.2 (CMeVal), 57.0 (C_{Aib}), 56.9 (C_{Aib}), 56.8 (2C, 2 × C_{Aib}), 56.1 (C_{Aib}), 35.8 ($CH(CH_3)_2$), 28.0 (3C, (CH_3)), 27.4 (CH_{3Aib}), 27.0 (CH_{3Aib}), 26.9 (CH_{3Aib}), 26.8 (CH_{3Aib}), 25.6 (CH_{3Aib}), 24.3 (CH_{3Aib}), 23.9 (CH_{3Aib}), 23.7 (CH_{3Aib}), 23.5 (2C, 2 × CH_{3Aib}), 17.8 (CH_3 Val), 17.4 (($CH_3)_2$CHVal), 17.3 (($CH_3)_2$CHVal). FTIR (neat) ν_{max} = 3310, 2981, 2935, 1656, 1519, 1451, 1374, 1262, 1145, 591 cm^{-1}. HR – MS (ESI, positive ion mode) – m/z for $[C_{38}H_{62}N_6O_9Na]^+$ 769.4470, found 769.4436. MP 212-214 °C. Data is consistent with that reported in the literature.[13]

Synthesis of Cbz-(L-αMeVal)Aib$_5$OH

TFA (0.6 mL) was added to a solution of Z-(L-αMeVal)Aib$_5$O*t*Bu (120 mg, 0.16 mmol mmol) in CH_2Cl_2 (4 mL) and stirred for 5h. After completion of the reaction, the reaction mixture was concentrated under reduced pressure to yield Z-(L)-αMeValAib$_5$OH as a white solid (93 mg, 0.135 mmol, 84 %).

^{1}H NMR (400 MHz, $CDCl_3$) δ 7.76 (s, 1H, N*H*), 7.72 (s, 1H, N*H*), 7.62 (s, 1H, N*H*), 7.52 (s, 1H, N*H*), 7.41 – 7.30 (m, 5H, 5 x CH_{Ph}), 6.54 (s, 1H, N*H*), 5.51 (s, 1H, N*H*), 5.18 (d, *J* = 12.3 Hz, 1H, CH_2Ph), 5.04 (d, *J* = 12.2 Hz, 1H, CH_2Ph), 1.97 (p, *J* = 6.9 Hz, 2H, C*H*$(CH_3)_2$), 1.61 (s, 3H, (CH_3)C), 1.58 (s, 3H, (CH_3)C), 1.52 – 1.46 (m, 9H, (C$H_3)_3$C), 1.44 (s, 3H, (CH_3)C), 1.43 (s, 3H, (CH_3)C), 1.42 (s, 3H, (CH_3)C), 1.40 (s, 3H, (CH_3)C), 1.39 (s, 3H, (CH_3)C), 1.21 (s, 3H, (CH_3)C), 0.99 (d, *J* = 6.7 Hz, 3H, (CH_3)CH), 0.94 (d, *J* = 6.8 Hz, 3H, (CH_3)CH). **^{13}C NMR** (101 MHz, $CDCl_3$) δ 176.8 (*C*=O), 176.75 (*C*=O), 175.9 (*C*=O), 175.8 (*C*=O), 175.1 (*C*=O), 174.3 (*C*=O), 156.5 (*C*=O_{Cbz}), 136.9 (*C*), 128.7 (2C, 2 x *C*H), 128.2 (*C*H), 127.8 (2C, 2 x *C*H), 67.0 (*C*(CH_3)(*i*Pr)), 63.0 (*C*H_2Ph), 57.4 (*C*$(CH_3)_2$), 56.9 (*C*$(CH_3)_2$), 56.8 (*C*$(CH_3)_2$), 56.7 (2C, 2 x *C*$(CH_3)_2$), 34.8 (*C*H$(CH_3)_2$), 26.5 (4C, 3 x *C*H_3), 26.1 (*C*H_3), 24.5 (*C*H_3), 23.7 (*C*H_3), 23.4 (*C*H_3), 23.2 (2C, 2 x *C*H_3), 17.5 (*C*H_3), 17.3 (*C*H_3), 16.7 (*C*H_3). **FTIR (neat)** ν_{max} = 3289, 2985, 2939, 1652, 1521, 1451, 1375, 1220, 1162, 663 cm^{-1}. **HR – MS** (ESI, positive ion mode) – *m/z* for $[C_{34}H_{54}N_6O_9Na]^+$ 713.3844, found 713.3816. **MP** 219-221 °C. Data is consistent with that reported in the literature.[13]

Synthesis of 1-Phenyl-1H-Imidazole (DMSO)

Bromobenzene (0.7065 g, 5.4mmol), imidazole (0.387 g, 4.5 mmol) was added in DMSO (10 mL), then the mixture was heated to 130 °C for 24 hours in the presence

of Cu_2O (0.0655 g, 0.45 mmol) as a catalyst and KOH (9 mmol, 0.5275 g) as base under N_2 atmosphere. The cooled mixture was partitioned between ethyl acetate (10 mL) and water (3 mL). The organic layer was washed with ethyl acetate (3 x 5 mL). The combined organic layers was washed with brine (5 mL), dried over sodium sulphate and concentrated to give crude product. The crude product was purified by column chromatography on silica gel (eluent: ethyl acetate : petroleum ether 2:1, R_f = 0.2). The yield was 0.2954 g, 46%.

^{1}H NMR (400 MHz, $CDCl_3$) δ 7.88 (s, 1H, C*H*$_{Imid}$), 7.51 (d, *J* = 7.1 Hz, 2H, 2 x C*H*$_{Ph}$), 7.46 – 7.35 (m, 3H, 3 x C*H*$_{Ph}$), 7.31 (s, 1H, C*H*$_{Imid}$), 7.23 (s, 1H, C*H*$_{Imid}$). Data is consistent with that reported in the literature.[74]

Synthesis of 1-(2,4,6-Trimethylphenyl)-1H-imidazole

A mixture of glacial acetic acid (10 mL), 37% aqueous formaldehyde (3 mL) and 37% aqueous glyoxal (4.6 mL) was heated to 70 °C. A solution of 2,4,6-trimethylaniline (5.39 g, 40.0 mmol), ammonium acetate (3.08 g, 40.0 mmol) in water 2 mL and glacial acetic acid (10 mL) was added dropwise after which the reaction mixture was heated at 70 °C for 18 hours. After cooling to room temperature the resulting brown solution was added very slowly to a stirred solution of $NaHCO_3$ 29.4 g in water 300 mL. A brownish solid was precipitated and filtered. Evaporation of the water under reduced pressure gave crude product which was purified by column chromatography on silica gel (eluent: 10% MeOH in DCM, R_f = 0.6) to yield product, 3.565 g 47.9%.[75]

^{1}H NMR (400 MHz, $CDCl_3$) *δ* 7.43 (d, *J* = 1.1 Hz, 1H, C*H*$_{Imid}$), 7.23 (d, *J* = 1.1 Hz, 1H, C*H*$_{Imid}$), 6.96 (s, 2H, 2 x C*H*$_{Ph}$), 6.89 (d, *J* = 1.1 Hz, 1H, C*H*$_{Imid}$), 2.33 (s, 3H, C*H*$_3$), 1.98 (s, 6H, 2 x C*H*$_3$). Data is consistent with that reported in the literature.[75]

Synthesis of 1-(2-Aminoethyl)-3-(2,4,6-methylphenyl)-1H-imidazol-3-ium dibromide

A solution of 1-(2,4,6-methylphenyl)-1H-imidazole (705 mg, 3.75 mmol) in MeCN (8 mL) was heated to reflux. 2-Bromoethylamine hydrobromide (767 mg, 1.5 mmol) was added and the reaction mixture was heated to reflux overnight. The reaction mixture was cooled to RT, yielding a brown liquid containing a white precipitate. The white precipitate was filtered. The filtrate was recrystalized in a solution (acetonitrile : ethanol (95:5)) (3 mL) to afford white solid as product 826 mg, 56 %.

^{1}H NMR (400 MHz, DMSO) δ 9.51 (t, J = 1.6 Hz, 1H, CH_{Im}), 8.31 – 8.19 (m, 2H, NH_2), 8.18 (t, J = 1.8 Hz, 1H, CH_{Im}), 7.99 (t, J = 1.8 Hz, 1H, CH_{Im}), 7.15 (s, 2H, 2 x CH), 4.60 (t, J = 6.1 Hz, 2H, CH_2), 3.52 (t, J = 6.1 Hz, 2H, CH_2), 2.34 (s, 3H, CH_3), 2.08 (s, 6H, 2 x CH_3). **^{13}C NMR** (101 MHz, DMSO) δ 140.2 (CH$_{im}$), 138.0 (C), 134.4 (2C, 2 x CMe), 131.1 (C), 129.3 (2C, 2 x CH), 124.1 (CH$_{im}$), 123.3 (CH$_{im}$), 46.8 (CH$_2$), 37.9 (CH$_2$), 20.6 (CH$_3$), 17.2 (2C, 2 x CH$_3$). **FTIR (neat)** ν_{max} = 3290, 2929, 1628, 1263, 1017, 799 cm^{-1} **HR – MS** (ESI, positive ion mode) – *m/z* for $[C_{14}H_{20}N_3]^+$ 230.1657, found 230.1652.

Synthesis of 1-(2-Aminoethyl)-3-phenyl-1H-imidazol-3-ium dibromide

A solution of 1-(phenyl)-1H-imidazole (389 mg, 2.6 mmol) in MeCN (8 mL) was heated to reflux. 2-Bromoethylamine hydrobromide (532 mg, 2.6 mmol) was added and the reaction mixture was refluxed overnight. The reaction mixture was cooled to RT, yielding a pale yellow liquid containing a white precipitate. The filtrate was recrystalized in a solution (acetonitrile : ethanol (95:5)) (3 mL) to afford yellow solid as product 380 mg, 42 %.

^{1}H NMR (400 MHz, DMSO) δ 9.98 (d, J = 1.7 Hz, 1H, CH_{im}), 8.39 (t, J = 1.9 Hz, 1H, CH_{im}), 8.35 – 8.10 (m, 3H, NH_3^+), 8.08 (t, J = 1.8 Hz, 1H, CH_{im}), 7.82 (dd, J = 7.9, 1.7 Hz, 2H, 2 x CH_{Ph}), 7.69 (dd, J = 8.6, 7.0 Hz, 2H, 2 x CH_{Ph}), 7.61 (dd, J = 8.6, 1.7 Hz, 1H, CH_{Ph}), 4.59 (t, J = 5.8 Hz, 2H, CH_2), 3.50 (t, J = 5.8 Hz, 2H, CH_2). **^{13}C NMR** (101 MHz, DMSO) δ 136.3 (C_{Ph}), 134.7 (CH$_{Imid}$), 130.2 (2C, 2 x CH$_{Ph}$), 129.9 (CH$_{Ph}$), 123.6 (CH$_{Imid}$), 121.8 (2C, 2 x CH$_{Ph}$), 121.2 (CH$_{Im}$), 46.8 (CH$_{2\ imid}$), 38.3 (CH$_2$NH$_2$). **FTIR (neat)** ν_{max} = 3355, 2921, 1628, 1511, 1263, 1201, 1049, 1017 cm^{-1} **HR – MS** (ESI, positive ion mode) – *m/z* for $[C_{11}H_{14}N_3]^+$ 188.1182, found 188.1189.

Synthesis of 1-(2-Aminoethyl)-3-methyl-1H-imidazol-3-ium dibromide

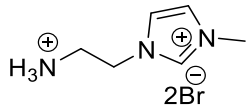

A solution of 1-methyl-imidazole (2.0525 g, 25 mmol) in MeCN (25 mL) was heated to reflux. 2-Bromoethylamine hydrobromide (2.5612 g, 12.5 mmol) was added and the reaction mixture was refluxed overnight. The reaction mixture was cooled to RT, yielding a yellow oil. The mixture was decanted and the oil was dried under the

vacuum to give the crude product. The crude product was recrystalized by the solvent 5% ethanol in acetonitrile to yield the product as yellow solid 0.18g, 6 %.

^{1}H NMR (400 MHz, CD_3OD) δ 9.14 (d, J = 1.9 Hz, 1H, NC*H*N_{Imid}), 7.77 (q, J = 1.8 Hz, 1H, C*H*$_{imid}$), 7.68 (t, J = 1.8 Hz, 1H, C*H*$_{imid}$), 4.63 (t, J = 6.2 Hz, 2H, C*H*$_2$), 4.00 (s, 3H, C*H*$_3$), 3.58 (t, J = 6.2 Hz, 2H, C*H*$_2$).

General procedure II

To a solution of N_3AiB_4OH or Cbz-L-MeVal-AiB_4OH (1 e.q.) in dry dichloromethane was added *N*-(3-dimethylaminopropyl)-*N′*-ethylcarbodiimide EDC·HCl (2 e.q.). The mixture was then cooled to 0°C, triethylamine (2 e.q.) was added and the mixture was stirred for 3 hours at 20 °C. The resulting mixture was concentrated, dissolved in acetonitrile. The arylimidazolium ethylammonium dibromide salt (1.1 e.q.) was added, followed with triethylamine (1.18 e.q.) and the suspension was heated at 80 °C for 3 days (the suspension solubilised upon heating). The mixture was concentrated undervacuum; the residue was purified by chromatography on silica (eluent CH_2Cl_2 / MeOH 95:5). The fractions containing the product with antriethylammonium salt as an impurity were purified again by column chromatography (basic Al_2O_3, DCM/MeOH 95:5) to yield the imidazolium bromide salt.

Synthesis of $N_3Aib_4Et(NHC\text{-}Me)^+$ Br^-

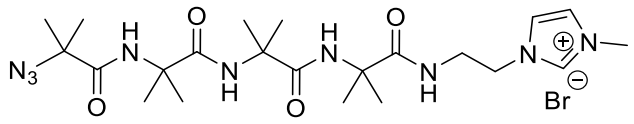

Following general procedure II with methylimidazolium salt (244 mg, 0.85 mmol) afforded the compound as a white solid (163 mg, 0.29 mmol, 57 %).

^{1}H NMR (400 MHz, CD_3OD) δ 8.84 (s, 1H, CH_{im})7.65 (d, J = 2.0 Hz, 1H, CH_{im}), 7.54 (d, J = 2.0 Hz, 1H, CH_{im}), 4.39 (dd, J = 6.4, 4.1 Hz, 2H, CH_2), 3.95 (s, 3H, Me), 3.67 – 3.60 (m, 2H, CH_2), 1.52 (s, 6H, 2 × CH_3), 1.46 (s, 6H, 2 × CH_3), 1.44 (s, 6H, 2 × CH_3), 1.38 (s, 6H, 2 × CH_3).

^{13}C NMR (101 MHz, MeOD) δ 177.01 (C=O), 175.65 (C=O), 175.05 (C=O), 173.49 (C=O), 137.41(CH_{im}), 123.37 (CH_{im}), 122.49 (CH_{im}),63.36 (CMe_2), 56.87 (CMe_2), 56.55(2C, CMe_2), 39.40 (NH-CH_2), 39.29 (N-CH_2), 35.30 (N-CH_3), 24.46 (2C, $(CH_3)_2C$), 24.00 (2C, $(CH_3)_2C$), 23.53 (2C, $(CH_3)_2C$), 23.24 (2C, $(CH_3)_2C$).**FTIR (neat)** νmax = 3313, 2112, 1654, 1455, 1384, 1363, 1168 cm^{-1}; **HR – MS** (ESI,

positive ion mode) – *m/z* for $[C_{30}H_{46}N_9O_4]^+$ 492.3029, observed 492.3041; M.P. no melting point 240 °C Charcoal.

Synthesis of N_3Aib_4Et (NHC-Ms)$^+Br^-$

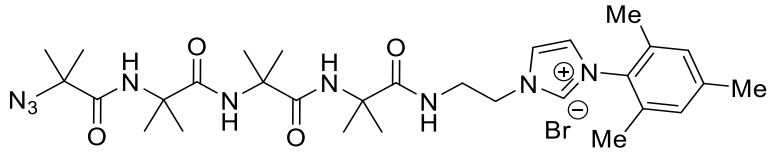

Following general procedure II with 1-(2-aminoethyl)-3-(2,4,6-methylphenyl)-1H-imidazol-3-ium bromide, hydrobromide salt (430 mg, 1.1 mmol) afforded the compound as a yellow oil (262 mg, 0.44 mmol, 44 %).

^{1}H NMR (400 MHz, $CDCl_3$) δ 9.54 (dd, *J* = 3.6, 1.7 Hz, 1H, C*H*$_{im}$), 8.18 (dd, *J* = 3.6, 1.7 Hz, 2H, C*H*$_{im}$, N*H*), 7.80 (t, *J* = 6.1 Hz, 1H, N*H*CH_2), 7.56 (s, 1H, N*H*), 7.07 (dd, *J* = 3.6, 1.7 Hz, 1H, C*H*$_{im}$), 7.02 (s, 1H, N*H*), 6.95 (s, 2H, 2 x C*H*$_{Ms}$), 4.73 (t, *J* = 6.0 Hz, 2H, C*H*$_{2\ Imid}$), 3.68 (t, *J* = 6.0 Hz, 2H, C*H*$_2$NH), 2.30 (s, 3H, C*H*$_{3Ms}$), 2.05 (s, 6H, 2 x C*H*$_{3Ms}$), 1.54 (s, 6H, 2 x C*H*$_3$), 1.47 (s, 6H, 2 x C*H*$_3$), 1.40 (s, 6H, 2 x C*H*$_3$), 1.26 (s, 6H, 2 x C*H*$_3$). **^{13}C NMR** (101 MHz, $CDCl_3$) δ 176.3 (*C*=O), 175.8 (*C*=O), 175.0 (*C*=O), 173.5 (*C*=O), 141.1 (*C*H$_{Im}$), 137.5 (*C*$_{Ms}$), 134.5 (2C, 2 x *C*H$_{Ms}$), 131.0 (*C*$_{Ms}$), 129.7 (2C, 2 x *C*$_{Ms}$), 125.0 (*C*H$_{Im}$), 122.6 (*C*H$_{Im}$), 63.8 (*C*Me$_2$), 57.1 (*C*Me$_2$), 56.9 (2C, 2 x *C*Me$_2$), 50.8 (*C*H$_2$), 40.5 (*C*H$_2$), 25.3 (2C, (*C*H$_3$)$_2$C), 24.8 (2C, (*C*H$_3$)$_2$C), 24.7 (2C, (*C*H$_3$)$_2$C), 24.3 (2C, (*C*H$_3$)$_2$C), 21.1 (*C*H$_{3Ms}$), 17.6 (2C, 2 x *C*H$_{3Ms}$). **FTIR (neat)** ν_{max} = 3318, 2982, 2113, 1654, 1521, 1363, 1211, 1027 cm^{-1} **HR – MS** (ESI, positive ion mode) – *m/z* for $[C_{30}H_{46}N_9O_4]^+$ 596.3667, found 596.3681.

Synthesis of N_3Aib_4Et(NHC-Ph)$^+Br^-$

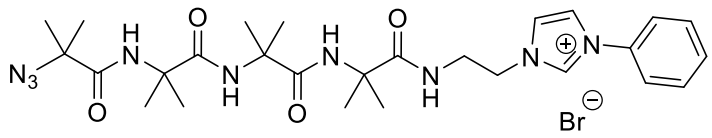

Following general procedure II with 1-(2-aminoethyl)-3-(phenyl)-1H-imidazol-3-ium bromide, hydrobromide salt (384 mg, 1.1 mmol) afforded the compound as yellow foam (270 mg, 0.49 mmol, 49 %).

^{1}H NMR (400 MHz, $CDCl_3$) δ 9.92 (m, 1H, C*H*$_{im}$), 8.37 (s, 1H, N*H*), 8.01 (m, 1H, C*H*$_{im}$), 7.86 (t, *J* = 6.1 Hz, 1H, N*H*CH_2), 7.75 – 7.68 (m, 2H, 2 x C*H*$_{Ph}$), 7.66 (s, 1H, C*H*$_{im}$), 7.61 – 7.48 (m, 4H, N*H*, 3 x C*H*$_{Ph}$), 7.08 (s, 1H, N*H*), 4.68 (dd, *J* = 6.2, 3.3 Hz,

2H, CH_2), 3.85 – 3.69 (m, 2H, CH_2NH), 1.58 (s, 6H, 2 x CH_3), 1.51 (s, 6H, 2 x CH_3), 1.44 (s, 6H, 2 x CH_3), 1.35 (s, 6H, 2 x CH_3). **^{13}C NMR** (101 MHz, $CDCl_3$) δ 176.4 (*C*=O), 175.9 (*C*=O), 175.0 (*C*=O), 173.5 (*C*=O), 135.8 (*C*H $_{Imid}$), 134.8 (*C*), 130.4 (2C, 2 x *C*H$_{Ph}$), 130.3 (*C*H$_{Ph}$), 124.7 (*C*H$_{Im}$), 122.3 (2C, 2 x *C*H$_{Ph}$), 120.6 (*C*H$_{Im}$), 63.8 (*C*Me$_2$), 57.1 (*C*Me$_2$), 56.9 (*C*Me$_2$), 56.9 (*C*Me$_2$), 50.5 (*C*H$_2$), 39.8 (*C*H$_2$), 25.3 (2C, (*C*H$_3$)$_2$C), 24.9 (2C, (*C*H$_3$)$_2$C), 24.7 (2C, (*C*H$_3$)$_2$C), 24.2 (2C, (*C*H$_3$)$_2$C). **FTIR (neat)** νmax = 3323, 2987, 2936, 2114, 1659, 1538, 1224 cm^{-1}. **HR – MS** (ESI, positive ion mode) – *m/z* for $[C_{27}H_{40}N_9O_4]^+$ 554.3198, found 554.3184.

General procedure III for installing rhodium on azido AiB NHC foldamers

To a 0.03M solution of [N_3AiB$_4$Et(NHCR)$^+$,Br$^-$] (1 eq.) in dry acetone was added potassium carbonate K_2CO_3 (3 equiv.) and *bis*(1,5-cyclooctadiene)dirhodium(I) dichloride $[Rh(COD)Cl]_2$ (0.5 eq.). The mixture was heated at 60 °C for 5 h. The resulting mixture was concentrated, the residue was purified using chromatography on silica (eluent CH_2Cl_2 100 % then applying a slow gradient to CH_2Cl_2 /MeOH 90 : 10) to afford the product as a yellow solid.

Synthesis of N$_3$Aib$_4$Et(NHC-Ph) RhCl(COD)

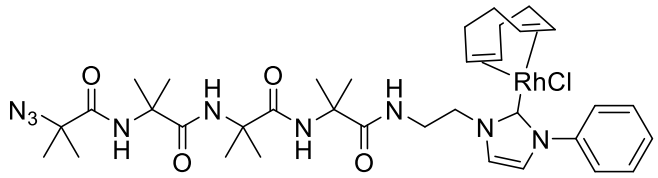

Following general procedure III with [N_3AiB$_4$NH(CH$_2$)$_2$(NHCPh)$^+$Br$^-$] (94 mg, 0.148 mmol), dry acetone (4.5 mL), potassium carbonate K_2CO_3 (22 mg, 0.22 mmol), *bis*(1,5-cyclooctadiene)dirhodium(I) dichloride $[Rh(COD)Cl]_2$ (37 mg, 0.074 mmol) afforded the product (as a mixture of two diastereoisomers in a 1 : 1 ratio) as a yellow solid (73 mg, 0.096 mmol, 65 %).

^{1}H NMR (400 MHz, $CDCl_3$) *δ* 8.15 (d, *J* = 7.7 Hz, 2H, 2 x C*H*$_{Ph}$), 7.67 (dd, *J* = 6.8, 4.5 Hz, 1H, N*H*CH$_2$), 7.51 (m, 2 Hz, 2H, 2 x C*H*$_{Ph}$), 7.46 (d, *J* = 2.0 Hz, 1H, C*H*$_{Im}$), 7.41 (t, *J* = 7.4 Hz, 1H, C*H*$_{Ph}$), 7.15 (s, 1H, N*H*), 7.06 (d, *J* = 2.0 Hz, 1H, C*H*$_{Im}$), 7.03 (s, 1H, N*H*), 6.50 (s, 1H, N*H*), 5.11 – 5.05 (m, 1H, C*H*$_2$N$_{imid\ dia1}$), 5.02 (m, 1H, C*H*$_{COD\ dia1}$), 4.87 (m, 1H, C*H*$_{COD\ dia2}$), 4.79 – 4.67 (m, 1H, C*H*$_2$N$_{imid\ dia2}$), 4.02 (m, 1H, C*H*$_2$NH $_{dia1}$), 3.70 (m, 1H, C*H*$_2$NH $_{dia2}$), 3.31 (m, 1H, C*H*$_{COD\ dia1}$), 2.52 (m, 1H, C*H*$_{COD\ dia2}$), 2.42 – 2.30 (m, 1H, C*H*$_2$CH$_{dia1\ cod}$), 2.24 (m, 1H, C*H*$_2$CH$_{dia2\ cod}$), 2.08 (m, 2H,

C*H*$_2$CH$_{dia1\ cod,}$ C*H*$_{2\ COD}$), 1.76 (m, 3H, C*H*$_{2\ COD\ dia1\ dia2}$), 1.50 (q, *J* = 10.3, 8.2 Hz, 12H, 2 x (CH$_3$)$_2$C), 1.46 – 1.36 (m, 12H, 2 x (CH$_3$)$_2$C), 1.44 (m, 1H, C*H*$_2$CH $_{COD\ dia2}$).

^{13}C NMR (101 MHz, $CDCl_3$) δ 182.2 (d, $J_{Rh\text{-}C}$ = 51.0 Hz, N*C*N$_{imid}$) , 175.8 (*C*=O), 173.7 (*C*=O), 173.4 (*C*=O), 173.0 (*C*=O), 140.5 (*C*$_{Ph}$), 128.9 (2C, 2 x *C*H$_{Ph}$), 127.8 (*C*H$_{Ph}$), 124.6 (2C, 2 x *C*H$_{Ph}$), 123.3 (*C*H$_{imid}$), 121.0 (*C*H$_{imid}$), 97.6 (d, $J_{Rh\text{-}C}$ = 7.0 Hz, *C*H$_{COD\ dia}$), 97.4 (d, $J_{Rh\text{-}C}$ = 7.0 Hz, *C*H$_{COD\ dia}$), 69.08 (d, $J_{Rh\text{-}C}$ = 14.5 Hz, *C*H$_{COD\ dia}$), 68.56 (d, $J_{Rh\text{-}C}$ = 14.5 Hz, *C*H$_{COD\ dia}$), 64.0 (*C*(CH$_3$)$_2$N$_3$), 57.4 (*C*(CH$_3$)$_2$), 57.0 (*C*(CH$_3$)$_2$), 57.0 (*C*(CH$_3$)$_2$), 50.6 (*C*H$_2$N$_{imid}$), 40.7 (*C*H$_2$NH), 33.4 (*C*H$_{2\ COD}$), 31.8 (*C*H$_{2\ COD}$), 29.0 (*C*H$_{2\ COD}$), 28.5 (*C*H$_{2\ COD}$), 26.1 (1C, (*C*H$_3$)$_2$C $_{dia}$), 25.8 (1C, (*C*H$_3$)$_2$C $_{dia}$), 25.0 (1C, (*C*H$_3$)$_2$C $_{dia}$), 25.0 (1C, (*C*H$_3$)$_2$C $_{dia}$), 24.8 (1C, (*C*H$_3$)$_2$C $_{dia}$), 24.6 (1C, (*C*H$_3$)$_2$C $_{dia}$), 24.4 (2C, (*C*H$_3$)$_2$C $_{dia}$). **FTIR (neat)** νmax = 3305, 2984, 2936, 2878, 2834, 2111, 1651, 1519, 1383, 1222, 909, 730 cm^{-1}. **HR – MS** (ESI, positive ion mode) – *m/z* for [C$_{35}$H$_{51}$N$_9$O$_4$Rh]$^+$ 764.3114, found 764.3090. **MP** 143-145 °C

Synthesis of N$_3$Aib$_4$Et(NHC-Ms) RhCl(COD)

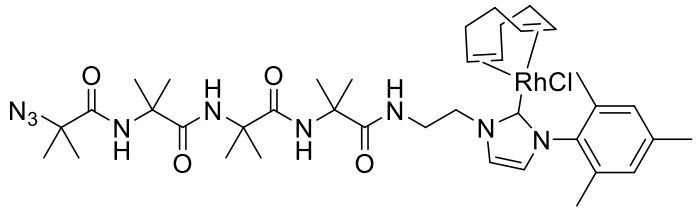

Following general procedure III with [N$_3$AiB$_4$NH(CH$_2$)$_2$(NHCMs)$^+$,Br$^-$] (120 mg, 0.18 mmol), dry acetone (5 mL), potassium carbonate K_2CO_3 (36 mg, 0.36 mmol), *bis*(1,5-cyclooctadiene)dirhodium(I) dichloride (43 mg, 0.09 mmol) afforded the product as a yellow solid (105 mg, 0.126 mmol, 70 %).

Mixture of 2 diastereoisomers ratio 1:1

^{1}H NMR (400 MHz, $CDCl_3$) δ 7.65 (dd, *J* = 7.1, 4.6 Hz, 1H, N*H*CH$_2$), 7.40 (d, *J* = 1.9 Hz, 1H, C*H*$_{Imid}$), 7.08 (s, 1H, N*H*$_{Aib}$), 7.03 (dd, *J* = 6.0, 1.9 Hz, 1H, C*H*$_{Ph\ dia}$), 6.98 (s, 1H, N*H*$_{AiB}$), 6.87 (dd, *J* = 6.0, 1.9 Hz, 1H, C*H*$_{Ph\ dia\ 2}$), 6.63 (d, *J* = 1.9 Hz, 1H, C*H*$_{Imid}$), 6.40 (s, 1H, N*H*$_{Aib}$), 5.42 (dt, *J* = 14.3, 4.4 Hz, 1H, C*H*$_{2Imid\ dia}$), 4.90 (dt, *J* = 7.5 Hz, 1H, 2 x C*H*$_{COD\ dia1}$), 4.79 (td, *J* = 7.5, 3.7 Hz, 1H, 2 x C*H*$_{COD\ dia2}$), 4.42 (ddd, *J* = 13.8, 9.5, 4.1 Hz, 1H, C*H*$_{2Imid\ dia}$), 4.09 (dddd, *J* = 13.7, 9.4, 7.2, 4.1 Hz, 1H, CH$_2$NH $_{dia1}$), 3.81 – 3.73 (m, 1H, C*H*$_{COD\ dia}$), 3.73 – 3.60 (m, 1H, CH$_2$NH $_{dia}$), 3.08 (dd, *J* = 8.6, 5.2 Hz, 1H, C*H*$_{COD\ dia}$), 2.39 (d, *J* = 8.9 Hz, 3H, 2 x C*H*$_{3Ph\ dia}$), 2.34 (s, 3H, 2 x C*H*$_{3Ph\ dia}$),

2.12 (ddt, J = 17.6, 9.5, 4.5 Hz, 1H, C$H_{2\text{cod dia1}}$), 2.06 – 1.90 (m, 1H, C$H_{2\text{cod dia2}}$), 1.82 (s, 3H, C$H_{3\text{Ph}}$), 1.76 (m, 1H, C$H_{2\text{cod dia1}}$), 1.70 – 1.57 (m, 1H, C$H_{2\text{cod dia2}}$), 1.52 (s, 3H, (CH_3)$_2$C $_{\text{dia1}}$), 1.51 (s, 6H, (CH_3)$_2$C), 1.49 (s, 3H, (CH_3)$_2$C $_{\text{dia2}}$), 1.46 (s, 6H, (CH$_3$)$_2$C), 1.41 (s, 6H, (CH$_3$)$_2$C). **^{13}C NMR** (101 MHz, $CDCl_3$) δ 180.9 (d, J = 50.7 Hz, NCN$_{\text{imid}}$), 175.5 (C=O), 173.6 (C=O), 173.3 (C=O), 173.1 (C=O), 138.4(C_{Ph}), 136.9 (C_{Ph}(CH$_3$)$_{\text{dia}}$), 136.4 (C_{Ph}(CH$_3$)$_{\text{dia}}$), 134.9 (C_{Ph}), 129.4 (CH$_{\text{Ph dia}}$), 128.2 (CH$_{\text{Ph dia}}$), 123.4 (CH$_{\text{imid}}$), 122.8 (CH$_{\text{imid}}$), 96.2 (d, $J_{\text{Rh-C}}$ = 7.2 Hz, CH$_{\text{COD}}$), 96.0 (d, $J_{\text{Rh-C}}$ = 6.6 Hz, CH$_{\text{COD}}$), 69.8 (d, $J_{\text{Rh-C}}$ = 14.3 Hz, CH$_{\text{COD}}$), 69.1 (d, $J_{\text{Rh-C}}$ = 14.5 Hz, CH$_{\text{COD}}$), 64.0 (C(CH$_3$)$_2$N$_3$), 57.5 (C(CH$_3$)$_2$), 57.0 (C(CH$_3$)$_2$), 57.0 (C(CH$_3$)$_2$), 51.4 (CH$_2$N$_{\text{imid}}$), 40.8 (CH$_2$NH), 33.9 (CH$_2$ $_{\text{COD}}$), 31.3 (CH$_2$ $_{\text{COD}}$), 29.5 (CH$_2$ $_{\text{COD}}$), 28.3 (CH$_2$ $_{\text{COD}}$), 25.8 (1C, (CH$_3$)$_2$C), 25.7 (1C, (CH$_3$)$_2$C), 25.5 (1C, (CH$_3$)$_2$C), 25.3 (1C, (CH$_3$)$_2$C), 25.0 (1C, (CH$_3$)$_2$C), 24.8 (1C, (CH$_3$)$_2$C), 24.4 (1C, (CH$_3$)$_2$C), 24.4 (1C, (CH$_3$)$_2$C), 21.1 (CH$_{3\text{Ph}}$ $_{\text{dia}}$), 20.5 (CH$_{3\text{Ph dia}}$), 17.9 (CH$_3$ $_{\text{Ph}}$). **FTIR (neat)** ν_{max} = 3328, 2929, 2114, 1662, 1522, 1261, 1019, 802 cm^{-1}. **HR – MS** (ESI, positive ion mode) – *m/z* for [C$_{38}$H$_{57}$N$_9$O$_4$Rh]$^+$ 806.3583, found 806.3572. **MP** 130-135 °C.

Synthesis of N$_3$Aib$_4$Et(NHC-Me) RhCl(COD)

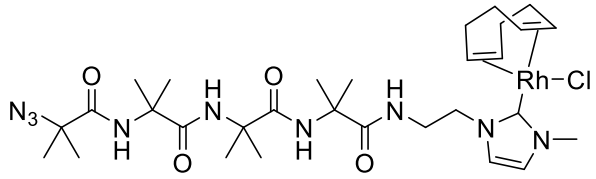

Following general procedure III with [N$_3$Aib$_4$NH(CH$_2$)$_2$(NHCMe)$^+$,Br$^-$] (28 mg, 0.05 mmol), dry acetone (5 mL), potassium carbonate K_2CO_3 (13.8 mg, 0.1 mmol), *bis*(1,5-cyclooctadiene)dirhodium(I) dichloride (12.4 mg, 0.025 mmol) afforded the product as a yellow solid (11 mg, 0.014 mmol, 30 %).

^{1}H NMR (500 MHz, $CDCl_3$) δ 7.48 (t, J = 5.7 Hz, 1H, NHCH$_2$), 7.17 (d, J = 1.9 Hz, 1, CH_{Imid} H), 7.13 (s, 1H, NH), 6.94 (s, 1H, NH), 6.74 (d, J = 1.9 Hz, 1H, CH_{Imid}), 6.32 (s, 1H, NH), 5.09 – 4.98 (m, 2H, 2 x CH_{COD}), 4.69 – 4.55 (m, 2H, CH_2imid), 4.00 (s, 3H, CH_3Imid), 3.95 – 3.83 (m, 1H, CH_2NH), 3.83 – 3.71 (m, 1H, CH_2NH), 3.40 – 3.32 (m, 2H, 2 x C$H_{2\text{COD}}$), 2.44 – 2.26 (m, 4H, 2 x C$H_{2\text{COD}}$), 1.96 – 1.78 (m, 4H, 2 x C$H_{2\text{COD}}$), 1.51 (s, 3H, C$H_{3\text{Aib}}$), 1.51 (s, 3H, C$H_{3\text{Aib}}$), 1.50 (s, 3H, C$H_{3\text{Aib}}$), 1.49 (s, 3H, C$H_{3\text{Aib}}$), 1.48 (s, 3H, C$H_{3\text{Aib}}$), 1.46 (s, 3H, C$H_{3\text{Aib}}$), 1.43 (s, 3H, C$H_{3\text{Aib}}$), 1.41 (s, 3H, C$H_{3\text{Aib}}$). **^{13}C NMR** (126 MHz, $CDCl_3$) δ 181.5 (d, J = 50.1 Hz, C=Rh), 175.7 (C=O$_{\text{AiB}}$), 173.3(C=O$_{\text{AiB}}$), 173.2 (C=O$_{\text{AiB}}$), 172.9 (C=O$_{\text{AiB}}$), 122.6 (CH$_{\text{imid}}$), 121.8 (CH$_{\text{imid}}$), 97.8

(d, $J_{Rh\text{-}C}$ = 6.8 Hz, *C*H=CH$_{cod\ dia}$), 97.7 (d, $J_{Rh\text{-}C}$ = 6.8 Hz, *C*H=CH$_{cod\ dia}$), 69.5 (d, $J_{Rh\text{-}C}$ = 14.6 Hz, *C*H=CH$_{cod\ dia}$), 68.9 (d, $J_{Rh\text{-}C}$ = 14.6 Hz, *C*H=CH$_{cod\ dia}$), 64.2 (*C*$_{Aib}$N$_3$), 57.3 (*C*$_{Aib}$), 57.0 (2C, 2 x C$_{Aib}$), 49.7 (*C*H$_2$-Imid), 40.7 (*C*H$_2$NH), 37.9 (*C*H$_3$-Imid), 33.2 (*C*H$_{2\ COD}$), 32.5 (*C*H$_{2\ COD}$), 29.8 (*C*H$_{2\ COD}$), 29.0 (*C*H$_{2\ COD}$), 25.8 (CH$_{3\ Aib}$), 25.6 (CH$_{3\ Aib}$), 25.3 (CH$_{3\ Aib}$), 25.2 (CH$_{3\ Aib}$), 25.1 (CH$_{3\ Aib}$), 25.0 (CH$_{3\ Aib}$), 24.5 (CH$_{3\ Aib}$), 24.5 (CH$_{3\ Aib}$). **FTIR (neat)** ν_{max} = 3320, 2929, 2112, 1662, 1525, 1244 cm^{-1}. **HR – MS** (ESI, positive ion mode) – *m/z* for [C$_{30}$H$_{49}$N$_9$O$_4$Rh]$^+$ 702.2963, found 702.2948.

Synthesis of Cbz-(*L*-αMeVal)AiB$_4$Et(NHC-Ph)$^+$, Br$^-$

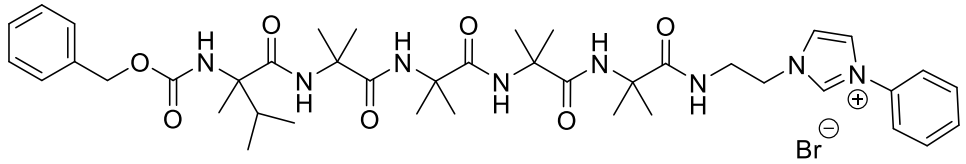

Following general procedure II Cbz-(*L*-αMeVal)AiB$_4$OH(100 mg, 0.165 mmol), EDC·HCl(32 mg, 0.165 mmol) and Et$_3$N (0.46 mL, 0.33 mmol)in DCM (10 mL), then in acetonitrile (8 mL) with phenylimidazolium salt (86 mg, 0.28mmol) and Et$_3$N (0.33 mL, 2.31 mmol) afforded the compound as an white solid (69 mg, 0.089 mmol, 54 %).

^{1}H NMR (400 MHz, CDCl$_3$) δ 9.82 (d, *J* = 1.8 Hz, 1H, C*H$_{imid}$*), 8.12 (t, *J* = 1.9 Hz, 1H, C*H$_{imid}$*), 7.90 (s, 1H, N*H*), 7.79 (s, 1H, N*H*), 7.73 – 7.68 (m, 1H, N*H*CH$_2$), 7.68 – 7.62 (m, 2H, 2 x C*H*$_{Ph}$), 7.54 – 7.50 (m, 1H, C*H$_{imid}$*), 7.50 – 7.44 (m, 3H, 3 x C*H*$_{Ph}$), 7.41 (d, *J* = 7.4 Hz, 2H, 2 x C*H*$_{Ph}$), 7.26 (t, *J* = 7.7 Hz, 2H, 2 x C*H*$_{Ph}$), 7.18 (d, *J* = 6.7 Hz, 2H, C*H*$_{Ph}$, N*H*), 7.12 (s, 1H, N*H*), 6.68 (s, 1H, N*H*$_{Cbz}$), 5.14 (d, *J* = 13.1 Hz, 1H, C*H*$_2$Ph), 4.94 (d, *J* = 13.1 Hz, 1H, C*H*$_2$Ph), 4.77 (m, 1H, C*H*$_2$N$_{imid}$), 4.57 (m, 1H, C*H*$_2$N$_{imid}$), 3.99 (m, 1H, C*H*$_2$NH), 3.35 (m, 1H, C*H*$_2$NH), 2.43 (m, 1H, C*H*(CH$_3$)$_2$), 1.43 (s, 3H, C*H*$_3$), 1.36 (m, 6H, 2 x C*H*$_3$), 1.32 (s, 3H, C*H*$_3$), 1.28 (m, 6H, 2 x C*H*$_3$), 1.23 (s, 3H, C*H*$_3$), 1.18 (s, 3H, C*H*$_3$), 1.10 (s, 3H, C*H*$_3$), 0.92 (d, *J* = 6.6 Hz, 3H, (C*H*$_3$)$_2$CH), 0.78 (d, *J* = 6.8 Hz, 3H, (C*H*$_3$)$_2$CH). **^{13}C NMR** (101 MHz, CDCl$_3$) δ 176.7 (*C*=O$_{AiB}$), 176.4 (*C*=O$_{Aib}$), 175.6 (*C*=O$_{val}$), 175.4 (*C*=O$_{Aib}$), 175.4 (*C*=O$_{Aib}$), 156.7 (*C*=O$_{Cbz}$), 137.4 (*C*$_{Ph}$), 135.6 (*C*H$_{imid}$), 134.9 (*C*$_{Ph}$), 130.3 (2C, 2 x CH$_{Ph}$), 130.1 (*C*H$_{Ph}$), 128.6 (2C, 2 x *C*H$_{Ph}$), 127.7 (*C*H$_{Ph}$), 127.0 (2C, 2 x *C*H$_{Ph}$), 125.0 (*C*H$_{imid}$), 122.4 (2C, 2 x C*H*$_{Ph}$), 120.5 (*C*H$_{imid}$), 66.5 (*C*H$_2$Ph), 63.0 (*C*), 57.0 (*C*), 56.7 (*C*), 56.6 (*C*), 56.2 (*C*), 50.5 (*C*H$_2$N$_{imid}$), 39.9 (*C*H$_2$NH), 34.1 (*C*H(CH$_3$)$_2$), 27.3 (*C*H$_3$), 26.7 (2C, 2 x *C*H$_3$), 26.3 (*C*H$_3$), 23.2 (*C*H$_3$), 22.9 (*C*H$_3$), 22.8 (*C*H$_3$), 22.7 (*C*H$_3$), 17.3 (1C, (*C*H$_3$)$_2$CH), 17.1 (1C, (*C*H$_3$)$_2$CH), 15.7 (*C*H$_{3\ aMeVal}$). **FTIR (neat)** ν_{max} = 3307, 2991, 2941, 1656,

1531, 1456, 1392, 1261, 1237 cm^{-1}. **HR – MS** (ESI, positive ion mode) – *m/z* for $[C_{41}H_{59}N_8O_7]^+$ 775.4501, found 775.4483.

General procedure IV for installing rhodium on azido AiB NHC foldamers

To a solution of [Cbz-L-α-MeValAiB$_n$Et(NHCR)$^+$,Br$^-$] (1 eq.) in dry DCM was added potassium carbonate Ag_2O (1 eq.) and *bis*(1,5-cyclooctadiene)dirhodium(I) dichloride $[Rh(COD)Cl]_2$ (0.5 eq.). The mixture was stirred in the dark at 20 °C for 5 h. The resulting mixture was concentrated, the residue was purified using chromatography on silica (eluent CH_2Cl_2 100 % then applying a slow gradient to CH_2Cl_2 /MeOH 90 : 10) to afford the product as a yellow solid.

Synthesis of Cbz-(*L*-σMeVal)AiB$_4$Et(NHC-Ph) (RhCl(COD))

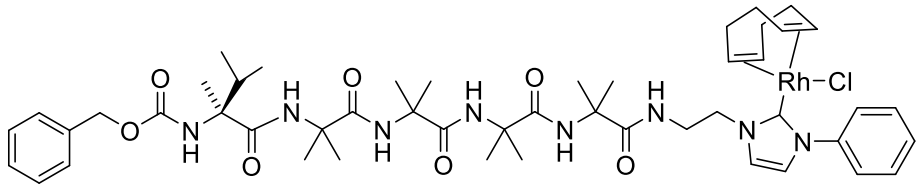

Following general procedure IV, to [Cbz-(*L*-alphaMeVal)AiB$_4$EtNHCPh$^+$, Br$^-$] (54 mg, 0.072 mmol) in dry CH_2Cl_2 (12 mL) was added silver oxide (17 mg, 0.072 mmol), *Bis*(1,5-cyclooctadiene)dirhodium(I) dichloride $[Rh(COD)Cl]_2$ (18 mg, 0.036 mmol). The product 1:1 mixture of diastereoisomers was obtained as a yellow solid (47 mg, 0.047 mmol, 65 %).

^{1}H NMR (500 MHz, $CDCl_3$) δ 8.23 – 8.14 (m, 2H, 2 × C*H*$_{\text{Ph ortho}}$), 7.90 (dd, *J* = 7.5, 3.9 Hz, 0.5H, N*H*CH$_{2\ \text{dia}}$), 7.83 (t, *J* = 5.9 Hz, 0.5H, N*H*CH$_{2\ \text{dia}}$), 7.68 (s, 0.5H, N*H*$_{\text{AiBdia}}$), 7.66 (s, 0.5H, N*H*$_{\text{AiBdia}}$), 7.64 (d, *J* = 12.40 Hz, 1H, C*H*$_{\text{imid}}$), 7.54 –7.50 (m, 2H, 2 × C*H*$_{\text{Ph meta}}$), 7.50 – 7.48 (m, 1H, N*H*), 7.44 – 7.40 (m, 1H, C*H*$_{\text{Ph para}}$), 7.39 – 7.33 (m, 5H, 5 x C*H*$_{\text{Bn}}$), 7.32 (m, 1H, N*H*$_{\text{AiB}}$), 7.06 (dd, *J* = 12.4, 2.0 Hz, 1H, C*H*$_{\text{imid}}$), 6.33 (s, 1H, N*H*$_{\text{AiB}}$), 5.39 (dd, *J* = 5.9, 3.3 Hz, 0.25H, C*H*$_2$-Imid $_{\text{dia}}$), 5.36 (dd, *J* = 5.9, 3.3 Hz, 0.25H, C*H*$_2$-Imid $_{\text{dia}}$), 5.29 (s, 0.5H, N*H*Cbz $_{\text{dia}}$), 5.28 (s, 0.5H, N*H*Cbz $_{\text{dia}}$), 5.21 – 5.14 (m, 0.25H, C*H*$_2$-Imid $_{\text{dia,}}$ 0.25H, C*H*$_2$-Imid $_{\text{dia,}}$ 1H, C*H*$_2$Ph $_{\text{dia}}$), 5.04 – 5.01 (m, 1H, C*H*$_2$Ph $_{\text{dia}}$, 1H, C*H*=CH$_{\text{COD dia}}$), 4.96 – 4.86 (m, 1H, C*H*=CH$_{\text{COD dia}}$), 4.65 (ddd, *J* = 14.3, 8.8, 3.2 Hz, 0.5H, C*H*$_2$-Imid $_{\text{dia}}$), 4.56 (ddd, *J* = 13.7, 8.2, 5.3 Hz, 0.5H, C*H*$_2$-Imid $_{\text{dia,}}$), 4.16 – 4.08 (m, 0.5H, C*H*$_2$NH $_{\text{dia}}$), 4.08 – 4.00 (m, 0.5H, C*H*$_2$NH $_{\text{dia}}$), 3.80 – 3.72 (m, 0.5H, C*H*$_2$NH $_{\text{dia}}$), 3.61 – 3.56 (m, 0.5H, C*H*$_2$NH $_{\text{dia}}$), 3.44 – 3.38 (m, 1H, C*H*=CH$_{\text{COD}}$), 2.58 – 2.53 (m, 1H, C*H*=CH$_{\text{COD}}$), 2.44 – 2.34 (m, 1H, C*H*$_2$CH$_{\text{COD}}$), 2.35

– 2.21 (m, 1H, CH_2CH$_{COD}$), 2.15 – 2.06 (m, 1H, CH_2CH$_{COD}$), 1.98 – 1.89 (m, 1H, CH(CH$_3$)$_2$), 1.87 – 1.80 (m, 1H, CH_2CH$_{COD}$), 1.79 – 1.72 (m, 2H, CH_2CH$_{COD}$), 1.63 (s, 1.5H, CH_3C$_{AiB\ dia}$), 1.61 (s, 1.5H, CH_3C$_{AiB\ dia}$), 1.51 (s, 3H, CH_3C$_{AiB}$), 1.49 – 1.45 (m, 8H, CH_2CH$_{COD}$, 2 × CH_3C$_{AiB}$), 1.45 – 1.38 (m, 2 × CH_3C$_{AiB}$, CH_3C$_{MeVal}$), 1.25 (s, 3H, CH_3C$_{AiB}$), 1.21 – 1.17 (m, 3H, CH_3C$_{AiB}$), 0.98 (dd, J = 6.8, 2.2 Hz, 3H, CH_3CH), 0.95 (d, J = 6.8 Hz, 3H, CH_3CH). **^{13}C NMR** (126 MHz, $CDCl_3$) δ 182.4 (d, J = 51.4 Hz, 0.5C, C=Rh $_{dia}$), 181.8 (d, J = 50.9 Hz, 0.5 C, C=Rh $_{dia}$), 176.2 (0.5C, C=O $_{Aib\ dia}$), 176.1 (0.5C, C=O $_{Aib\ dia}$), 175.5 (C=O $_{Aib}$), 174.9 (0.5C, C=O $_{Aib\ dia}$), 174.7 (0.5C, C=O $_{AiB\ dia}$), 174.0 (C=O $_{AiB}$), 172.9 (0.5C, C=O $_{MeVal\ dia}$), 172.8 (0.5C, C=O $_{MeVal\ dia}$), 156.2 (C=O $_{Cbz}$), 140.8 (0.5C, C_{Ph}), 140.8 (0.5C, C_{Ph}), 136.0 (0.5C, C_{Bn}), 136.0 (0.5C, C_{Bn}), 128.9 (2C, 2 x CH$_{Bn}$), 128.9 – 128.8 (3C, 3 x CH_{Bn}), 128.4 (2 x 0.5C$H_{Ph\ meta\ dia}$), 128.3 (2 x 0.5C$H_{Ph\ meta\ dia}$), 127.7 (0.5C$H_{Ph\ para\ dia}$), 127.6 (0.5C$H_{Ph\ para\ dia}$), 124.9 (2 × 0.5C$H_{Ph\ ortho\ dia}$), 124.8 (2 x 0.5C$H_{Ph\ ortho\ dia}$), 123.8 (0.5C, CH$_{imid\ dia}$), 123.6 (0.5C, CH$_{imid\ dia}$), 121.0 (0.5C, CH$_{imid\ dia}$), 120.8 (0.5C, CH$_{imid\ dia}$), 97.7 – 97.0 (2C, 2 x CH=CH$_{COD}$), 69.4 – 68.4 (2C, 2 x CH=CH$_{COD}$), 67.7 (CH$_2$Ph), 63.2 (0.5C, $C_{MeVal\ dia}$), 63.1 (0.5C, $C_{MeVal\ dia}$), 57.5 (0.5C, $C_{AiB\ dia}$), 57.4 (0.5C, $C_{AiB\ dia}$), 57.0 (1C, C_{AiB}), 56.9 (0.5C, $C_{AiB\ dia}$), 56.9 (0.5C, $C_{AiB\ dia}$), 56.8 (0.5C, $C_{AiB\ dia}$), 56.7 (0.5C, $C_{AiB\ dia}$), 50.9 (0.5C, CH$_2$-Imid $_{dia}$), 50.8 (0.5C, CH$_2$-Imid $_{dia}$), 41.3 (0.5C, CH$_2$NH $_{dia}$), 40.7 (0.5C, CH$_2$NH $_{dia}$), 35.8 (0.5C, CH(CH$_3$)$_{2\ dia}$), 35.6 (0.5C, CH(CH$_3$)$_{2\ dia}$), 33.5 (0.5C, CH$_{2\ COD\ dia}$), 33.3 (0.5C, CH$_{2\ COD\ dia}$), 31.9 (0.5C, CH$_{2\ COD\ dia}$), 31.9 (0.5C, CH$_{2\ COD\ dia}$), 29.8 (0.5C, CH$_{2\ COD\ dia}$), 29.8 (0.5C, CH$_{2\ COD\ dia}$), 29.1 (0.5C, CH$_{2\ COD\ dia}$), 29.0 (0.5C, CH$_{2\ COD\ dia}$), 27.4 – 26.4 (4 × CH$_3$C $_{AiB\ dia}$), 24.6-22.8 3 (4 × CH$_3$C $_{AiB\ dia}$), 17.7 (0.5C, CH$_3$C $_{MeVal\ dia}$), 17.6 (0.5C, CH$_3$C $_{MeVal\ dia}$), 17.4 (0.5C, CH$_3$CH $_{MeVal\ dia}$), 17.4 (0.5C, CH$_3$CH $_{MeVal\ dia}$), 17.3 (0.5C, CH$_3$CH $_{MeVal\ dia}$), 17.3 (0.5C, CH$_3$CH $_{MeVal\ dia}$). **FTIR (neat)** ν_{max} = 3311, 2991, 2937, 2878, 1662, 1531, 1460, 1392, 1266, 1233 cm^{-1} **HR – MS** (ESI, positive ion mode) – *m/z* for $[C_{49}H_{70}N_8O_7Rh]^+$ 985.4417, found 985.4386. **MP**: 145 °C.

Synthesis of Cbz-(L-αMeVal) (Aib)$_5$(Et)(NHC)Ms$^+$Br$^-$

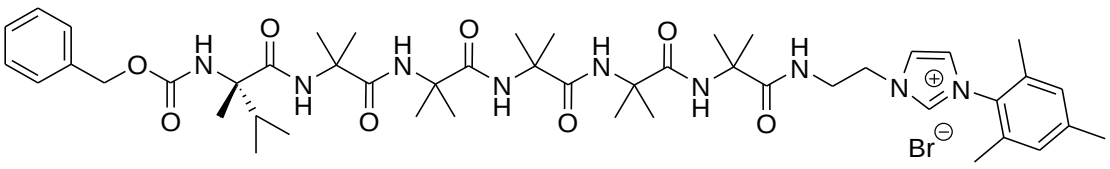

To a solution of Cbz-(L-αMeVal)Aib$_5$OH (79 mg, 0.114 mmol) in dry dichloromethane (6 mL) was added triethylamine (0.017 mL, 0.114 mmol) then *N*-(3-

dimethylaminopropyl)-*N′*-ethylcarbodiimide EDC.HCl (22 mg, 0.114 mmol). The mixture was stirred at 20 °C for 4 hours at 20 °C then was concentrated, and the residue was dissolved in dry acetonitrile (6 mL). 1-(2-Aminoethyl)-3-(mesityl)-1H-imidazol-3-ium bromide, hydrobromide salt (75 mg, 0.194 mmol, 1.7 equiv.) was added to the mixture, followed with triethylamine (0.018 mL, 0.114 mmol) and the suspension was heated at 80 °C for 3 days. The mixture was concentrated, the residue was purified by chromatography on silica (eluent CH_2Cl_2 / MeOH 90:10) to afford the compound as a white solid (60 mg, 0.061 mmol, 54 %).

^{1}H NMR (400 MHz, $CDCl_3$) δ 9.63 (s, 1H, CH_{imid}), 8.23 (d, J = 2.2 Hz, 1H, CH_{imid}), 7.84 (s, 1H, NH), 7.80 – 7.71 (m, 3H, 2 × NH_{Aib}, NHCH_2), 7.49 (d, J = 7.5 Hz, 2H, 2 × C$H_{Phortho}$), 7.36 (t, J = 7.5 Hz, 2H, 2 × CH_{Phmeta}), 7.31 – 7.25 (m, 3H, 2 × NH, CH_{Phpara}), 7.24 (s, 1H, NH), 7.10 (d, J = 2.2 Hz, 1H, CH_{imid}), 7.01 (s, 1H, CH_{Mes}), 7.00 (s, 1H, CH_{Mes}), 6.45 – 6.42 (m, 1H, NH_{CBz}), 5.22 (d, J = 12.8 Hz, 1H, CH_2Ph), 5.05 (d, J = 12.8 Hz, 1H, CH_2Ph), 4.90 (dd, J = 13.5, 5.3 Hz, 1H, CH_2N_{imid}), 4.74 (dd, J = 13.7, 8.6 Hz, 1H, CH_2N_{imid}), 4.09 – 4.02 (m, 1H, CH_2NH), 3.47 – 3.35 (m, 1H, CH_2NH), 2.48 – 2.40 (m, 1H, CH(CH_3)$_2$), 2.35 (s, 3H, CH_3Ph_{para}), 2.15 (s, 3H, CH_3Ph_{ortho}), 2.09 (s, 3H, CH_3Ph_{ortho}), 1.48 (s, 3H, CH_{3Aib}), 1.46 (s, 3H, CH_{3Aib}), 1.44 (s, 3H, CH_{3Aib}), 1.42 (s, 3H, CH_{3Aib}), 1.40 (s, 3H, CH_{3Aib}), 1.38 (s, 3H, CH_3C_{aMeVal}), 1.35 (s, 3H, CH_{3Aib}), 1.30 (s, 3H, CH_{3Aib}), 1.27 (s, 3H, CH_{3Aib}), 1.25 (s, 3H, CH_{3Aib}), 1.23 (s, 3H, CH_{3Aib}), 1.01 (d, J = 6.7 Hz, 3H, (CH_3)$_2$CH), 0.89 (d, J = 6.7 Hz, 3H, (CH_3)$_2$CH). **^{13}C NMR** (101 MHz, $CDCl_3$) δ 176.8 (C=O$_{AiB}$), 176.3 (C=O$_{AiB}$), 176.1 (C=O$_{AiB}$), 175.5 (C=O$_{AiB}$), 175.3 (C=O$_{AiB}$), 175.0 (C=O$_{val}$), 156.6 (C=O$_{Cbz}$), 140.9 (C_{Mes}), 137.6 (CH$_{imid}$), 137.1 (C_{Ph}), 134.8 (C_{Mes}), 134.3 (C_{Mes}), 131.1 (C_{Mes}), 129.8 (CH$_{Mes}$), 129.5 (CH$_{Mes}$), 128.6 (2C, 2 x CH$_{Phmeta}$), 127.9 (CH$_{Phpara}$), 127.4 (2C, 2 x CH$_{Phortho}$), 124.9 (CH$_{imid}$), 122.5 (CH$_{imid}$), 66.7 (CH$_2$Ph), 63.0 (C_{aMeVal}), 57.1 (C_{Aib}), 56.7 (C_{Aib}), 56.5 (C_{Aib}), 56.4 (C_{Aib}), 56.3 (C_{Aib}), 50.7 (CH$_2N_{imid}$), 40.4 (CH$_2$NH), 34.3 (CH(CH$_3$)$_2$), 27.7 – 26.0 (5C, 5 x CH$_3C_{Aib}$), 23.5 – 22.2 (5C, 5 x CH$_3C_{Aib}$), 21.1 (CH$_3C_{Mes}$), 17.6 (CH$_3C_{Meortho}$), 17.6 (CH$_3C_{Meortho}$), 17.3 (1C, (CH$_3$)$_2$CH), 17.2 (1C, (CH$_3$)$_2$CH), 16.0 (CH$_{3\ aMeVal}$). **FTIR (neat)** ν_{max} = 3294, 2981, 2935, 1653, 1526, 1453, 1383, 1361, 1260, 1225, 1212, 1166, 1071, 1026, 734, 697, 670 cm^{-1}. **HR – MS** (ESI, positive ion mode) – *m/z* for $[C_{48}H_{72}N_9O_8]^+$ 902.5498.

Synthesis of Cbz-L(αMeVal)Aib$_5$EtNHCMs Rh(COD)Cl

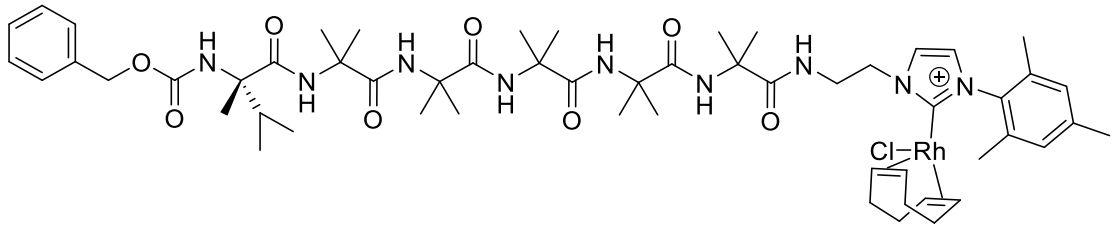

To a solution of [Cbz-(L-aMeVal)Aib$_5$NH(CH$_2$)$_2$(Imid)Ms$^+$, Br$^-$] (35 mg, 0.0354 mmol) in dry dichloromethane (12 mL) was added silver oxide (8 mg, 0.036 mmol) under inert atmosphere, the mixture was stirred for 2h in the dark then [Rh(COD)Cl]$_2$ (9 mg, 0.0177 mmol) was added and the reaction was stirred at room temperature for 21h, concentrated and purified by column chromatography (SiO$_2$, DCM/MeOH 9:1) to yield the compound as a yellow solid (32 mg, 0.0276, 78 %). Rf = 0.31

^{1}H NMR (500 MHz, CDCl$_3$) δ 7.84 (m, 1H, N*H*CH$_2$), 7.74 (s, 0.5H, N*H*$_{dia}$), 7.73 (s, 0.5H, N*H*$_{dia}$), 7.66 (s, 0.5H, N*H*$_{dia}$), 7.59 (s, 0.5H, N*H*$_{dia}$), 7.54 (s, 0.5H, 0.5 x C*H*$_{Imid\ dia1}$), 7.50 (bs, 1H, N*H*$_{dia}$), 7.40 (d, *J* = 1.8 Hz, 0.5H, 0.5 x C*H*$_{Imid\ dia2}$), 7.39 – 7.30 (m, 5H, 5 x C*H*$_{Ph}$), 7.29 (s, 0.5H, 0.5 x N*H*$_{dia}$), 7.27 (s, 0.5H, 0.5 x N*H*$_{dia}$), 7.03 (s, 1H, C*H*$_{Mes}$), 6.88 (s, 0.5H, 0.5 x C*H*$_{Mes}$), 6.86 (s, 0.5H, 0.5 x C*H*$_{Mes}$), 6.65 (s, 0.5H, N*H*), 6.64 (d, *J* = 1.8 Hz, 0.5H, 0.5 x C*H*$_{Imid\ dia1}$), 6.62 (s, 0.5H, N*H*), 6.59 (d, *J* = 1.8 Hz, 0.5H, 0.5 x C*H*$_{Imid\ dia2}$), 5.74 (s, 0.5H, 0.5 x N*H*Cbz) 5.71 (s, 0.5H, 0.5 x N*H*Cbz), 5.54 (ddd, *J* = 14.5, 7.4, 3.8 Hz, 1H, C*H*$_2$Imid $_{dia}$), 5.17 (dd, *J* = 12.4, 4.6 Hz, 1H, C*H*$_2$Ph), 5.03 (dd, *J* = 12.4, 5.4 Hz, 1H, C*H*$_2$Ph), 4.87 – 4.76 (m, 1H, CH=CH$_{COD}$), 4.70 (td, *J* = 7.9, 3.6 Hz, 1H, CH=CH$_{COD}$), 4.38 (td, *J* = 10.2, 5.0 Hz, 0.5H, C*H*$_2$Imid$_{dia}$), 4.24 (tdd, *J* = 14.5, 8.6, 3.3 Hz, 0.5H, C*H*$_2$Imid$_{dia}$), 4.30 – 4.16 (m, 1H, 0.5 x C*H*$_2$Imid$_{dia}$, 0.5 x C*H*$_2$NH), 4.15 – 4.05 (m, 0.5H, 0.5 x C*H*$_2$NH), 3.90 – 3.75 (m, 1.5H, 0.5 x C*H*$_2$NH, C*H*=CH$_{COD}$), 3.62 – 3.53 (m, 0.5H, 0.5 x C*H*$_2$NH), 3.02 (m, 1H, C*H*=CH$_{COD}$), 2.49 – 2.34 (m, 1 H, C*H*$_{2a}$CH$_{COD}$), 2.41 (s, 1.5H, 1.5 x C*H*$_{3Ms\ dia}$), 2.40 (s, 1.5H, 1.5 x C*H*$_{3Ms\ dia}$), 2.35 (s, 3H, C*H*$_{3Ms}$), 2.20 – 2.10 (m, 1H, C*H*$_{2d}$CH$_{COD}$), 2.05 – 1.91 (m, 2H, C*H*$_{2c}$CH$_{COD}$, C*H*(CH$_3$)$_2$), 1.93 – 1.80 (m, 1H, C*H*$_{2a}$CH$_{COD}$), 1.86 (s, 1.5H, 1.5 x C*H*$_{3Ms\ dia}$), 1.82 (s, 1.5H, 1.5 x C*H*$_{3Ms\ dia}$), 1.76 – 1.69 (m, 1 H, C*H*$_{2c}$CH$_{COD}$), 1.69 – 1.62 (m, 1 H, C*H*$_{2d}$CH$_{COD}$), 1.62 (s, 1.5H, 0.5 x C*H*$_3$C), 1.57 (s, 1.5H, 0.5 x C*H*$_3$C), 1.53 – 1.43 (m, 2H, C*H*$_{2b}$CH$_{COD}$), 1.52 (s, 1.5H, 0.5 x C*H*$_3$C), 1.50 – 1.39 (m, 27H, 9 x C*H*$_3$C), 1.39 (s, 1.5H, 0.5 x C*H*$_3$C), 0.97 (dd, *J* = 6.7 Hz, 3H, (C*H*$_3$)$_2$CH), 0.92 (dd, *J* = 6.9 Hz, 3H, (C*H*$_3$)$_2$CH). **^{13}C NMR** (101 MHz, CDCl$_3$) δ 181.2 (d, *J* = 50.4 Hz, 0.5C, *C*=Rh

$_{dia}$), 181.1 (d, J = 51.3 Hz, 0.5C, C=Rh $_{dia}$), 176.1 (0.5C, C=O$_{Aib\ dia}$), 176.1 (0.5C, C=O$_{Aib\ dia}$), 176.0 (0.5C, C=O$_{Aib\ dia}$), 175.9 (0.5C, C=O$_{Aib\ dia}$), 175.5 (0.5C, C=O$_{Aib\ dia}$), 175.4 (0.5C, C=O$_{Aib\ dia}$), 175.0 (0.5C, C=O$_{Aib\ dia}$), 174.9 (0.5C, C=O$_{Aib\ dia}$), 174.4 (1C, C=O$_{Aib}$), 173.4 (1C, C=O$_{aMeVal}$), 156.4 (0.5C, C=O $_{Cbz\ dia}$), 156.3 (0.5C, C=O $_{Cbz\ dia}$), 138.3 (0.5C, C_{Mes}), 138.2 (0.5C, C_{Mes}), 137.1 (0.5C, C_{Mes}), 137.1 (0.5C, C_{Mes}), 136.7 (0.5C, C_{Mes}), 136.7 (0.5C, C_{Mes}), 136.3 (0.5C, C_{Bn}), 136.3 (0.5C, C_{Bn}), 135.2 (0.5C, C_{Mes}), 135.0 (0.5C, C_{Mes}), 129.4 (0.5C, CH$_{Mes}$), 129.3 (0.5C, CH$_{Mes}$), 128.8 (2C, 2 x CH$_{Bn}$), 128.6 (1C, CH$_{Bn}$), 128.2 (0.5C, CH$_{Mes}$), 128.1 (0.5C, CH$_{Mes}$), 128.1 (1C, CH$_{Bn}$), 128.1 (1C, CH$_{Bn}$), 124.2 (0.5C, CH$_{imid\ dia}$), 124.1 (0.5C, CH$_{imid\ dia}$), 122.4 (0.5C, CH$_{imid\ dia}$), 122.2 (0.5C, CH$_{imid\ dia}$), 96.8 (d, $J_{Rh\text{-}C}$ = 6.1 Hz, 0.5C, CH=CH$_{cod\ dia}$), 96.6 (d, $J_{Rh\text{-}C}$ = 6.1 Hz, 0.5C, CH=CH$_{cod\ dia}$), 96.4 (d, $J_{Rh\text{-}C}$ = 6.7 Hz, 0.5C, CH=CH$_{cod\ dia}$), 96.2 (d, $J_{Rh\text{-}C}$ = 6.7 Hz, 0.5C, CH=CH$_{cod\ dia}$), 69.1 (d, $J_{Rh\text{-}C}$ = 13.4 Hz, 0.5C, CH=CH$_{cod\ dia}$), 69.0 (d, $J_{Rh\text{-}C}$ = 13.8 Hz, 0.5C, CH=CH$_{cod\ dia}$), 68.4 (d, $J_{Rh\text{-}C}$ = 14.6 Hz, 0.5C, CH=CH$_{cod\ dia}$), 68.2 (d, $J_{Rh\text{-}C}$ = 14.6 Hz, 0.5C, CH=CH$_{cod\ dia}$), 67.4 (CH$_2$Ph), 63.1 (0.5C, $C_{MeVal\ dia}$), 63.1 (0.5C, $C_{MeVal\ dia}$), 57.5 (0.5C, $C_{AiB\ dia}$), 57.4 (0.5C, $C_{AiB\ dia}$), 57.0 (0.5C, $C_{AiB\ dia}$), 56.9 (0.5C, $C_{AiB\ dia}$), 56.8 (0.5C, $C_{AiB\ dia}$), 56.7 (0.5C, $C_{AiB\ dia}$), 56.7 (1.5C, 1.5 x $C_{AiB\ dia}$), 56.6 (0.5C, $C_{AiB\ dia}$), 51.4 (0.5C, CH$_2$-Imid $_{dia}$), 51.3 (0.5C, CH$_2$-Imid $_{dia}$), 41.2 (0.5C, CH$_2$NH$_{dia}$), 41.1 (0.5C, CH$_2$NH$_{dia}$), 35.4 (0.5C, 0.5 x CH(CH$_3$)$_2$), 35.3 (0.5C, 0.5 x CH(CH$_3$)$_2$), 34.1 (0.5C, CH$_{2a\ COD\ dia}$), 33.9 (0.5C, CH$_{2a\ COD\ dia}$), 31.8 (0.5C, CH$_{2b\ COD\ dia}$), 31.7 (0.5C, CH$_{2b\ COD\ dia}$), 29.2 (0.5C, CH$_{2c\ COD\ dia}$), 29.2 (0.5C, CH$_{2c\ COD\ dia}$), 28.2 (0.5C, CH$_{2d\ COD\ dia}$), 28.2 (0.5C, CH$_{2d\ COD\ dia}$), 27.3 – 26.2 (m, 5 X CH$_3$C $_{AiB\ dia}$), 24.5 – 22.9 (m, 5 X CH$_3$C $_{AiB\ dia}$), 21.2 (CH$_3$Ph), 19.9 (0.5C, 0.5 x CH$_3$Ph$_{dia}$), 19.9 (0.5C, 0.5 x CH$_3$Ph$_{dia}$), 18.0 (0.5C, 0.5 x CH$_3$Ph$_{dia}$), 18.0 (0.5C, 0.5 x CH$_3$Ph$_{dia}$), 17.5 (0.5C, 0.5 x CH$_3$C$_{aMeVal\ dia}$), 17.5 (0.5C, 0.5 x CH$_3$CH $_{aMeVal\ dia}$), 17.4 (0.5C, 0.5 x CH$_3$CH $_{aMeVal\ dia}$), 17.3 (0.5C, 0.5 x CH$_3$C $_{aMeVal\ dia}$), 17.3 (0.5C, 0.5 x CH$_3$CH $_{aMeVal\ dia}$), 17.2 (0.5C, 0.5 x CH$_3$CH $_{aMeVal\ dia}$). **HR – MS** (ESI, positive ion mode) – *m/z* for $[C_{56}H_{83}O_8N_9Rh]^+$ 1112.5414, found 1112.5370. **MP** 138-142 °C.

Synthesis of (E)-2,4,6-Trimethyl-N-(6-bromopyridin-2-yl)methylenebenzamine

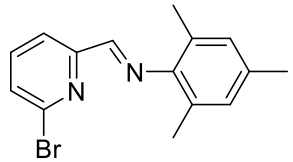

2,4,6-Trimethylaniline (0.80 g, 5.95 mmol, 1.1 eq.) was added to a solution of 6-Bromo-2-pyridinecarboxaldehyde (1 g, 5.4 mmol) and $MgSO_4$ in diethyl ether (20

mL), the mixture was stirred at room temperature overnight. The reaction mixture was concentrated under vacuum. The excess 2,4,6-Trimethylaniline was evaporated under high vacuum at 80 °C, leaving behind the product as a yellow solid (1.56 g, 96%).[76]

^{1}H NMR (400 MHz, $CDCl_3$): δ = 8.28 (s, 1H, CH=N), 8.26 (dd, J = 7.6, 1.2 Hz, 1H, CH), 7.69 (t, J = 7.6 Hz, 1H, CH), 7.59 (dd, J = 7.8, 1.2 Hz, 1H, CH), 6.90 (s, 2H, CH_{Mes}), 2.29 (s, 3H, CH_3), 2.13 (m, 6H, CH_3).

Synthesis of (*E*)-*N*-(6-bromopyridin-2-yl)methylenebenzamine

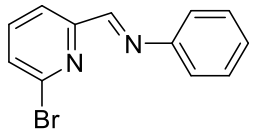

Aniline (0.55 g, 5.95 mmol, 1.1 eq.) was added to a solution of 6-Bromo-2-pyridinecarboxaldehyde (1 g, 5.4 mmol) and $MgSO_4$ in diethyl ether (20 mL), the mixture was stirred at room temperature overnight. The reaction mixture was concentrated under vacuum. The excess aniline was evaporated under high vacuum at 80 °C to afford yellow product (1.12 g, 80%).

^{1}H NMR (400 MHz, $CDCl_3$): δ 7.45-7.35 (m, 9H).

Synthesis of 5-Bromo-2-phenyl-imidazo[1,5-a]pyridinium Bromide

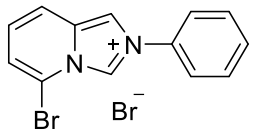

Bromotrimethylsilane (0.688 mL, 5.23 mmol) was added dropwise to a solution of (*E*)-*N*-(6-bromopyridin-2-yl)methylenebenzamine (1.46 g, 4.73 mmol) and paraformaldehyde (0.16 g, 5.23 mmol) in ethyl acetate (50 mL). The reaction mixture was stirred for 2 h at 70 °C, product was precipitated along the reaction course. After filtration, the white solid was washed twice with diethyl ether to yield the analytically pure product (1.57 g, 94%).[75]

^{1}H NMR (400 MHz, MeOD) δ 10.30 (d, *J* = 2.0 Hz, 1H, NCHN), 8.74 (d, *J* = 1.9 Hz, 1H, CH_{im}), 7.99 (d, *J* = 9.3 Hz, 1H, CH_{py}), 7.96 – 7.88 (m, 2H, CH_{ph}), 7.81 – 7.67 (m, 3H, CH_{ph}), 7.64 (dd, *J* = 7.2, 0.8 Hz, 1H, CH_{py}), 7.32 (dd, *J* = 9.3, 7.2 Hz, 1H, CH_{py}). ^{13}C NMR (101 MHz, MeOD) δ = 135.28(C_{ph}), 132.33(C_{im}), 130.85(**C**$_{ph}$), 130.21(2 x C_{ph}), 126.26(C_{im}), 125.69(C_{py}), 123.29(C_{ph}), 122.73(C_{py}), 117.56(C_{py}), 114.66(C_{im}), 112.31(C_{py}).

Data is consistent with that reported in the literature.[75]

Synthesis of 5-Bromo-2-mesityl-imidazo[1,5-a]pyridinium bromide

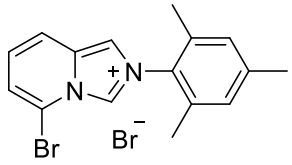

Bromotrimethylsilane (0.75 mL, 5.7 mmol) was added dropwise to a solution of (*E*)-2,4,6-trimethyl-*N*-(6-bromopyridin-2-yl)methylenebenzamine (1.58 g, 5.2 mmol) and paraformaldehyde (0.17 g, 5.7 mmol) in ethyl acetate (50 mL). The reaction mixture was stirred for 2 h at 70 °C, The product precipitated during the reaction course. After filtration, the white solid was washed twice with diethyl ether to yield the analytically pure product (1.57 g, 94%).[76]

^{1}H NMR (300 MHz, $CDCl_3$) δ 9.84 (dd, J = 1.8, 0.9 Hz, 1H, NCHN), 8.80 (d, J = 1.8 Hz, 1H, CH_{Im}), 8.53 (d, J = 9.3 Hz, 1H, CH_{Py}), 7.49 (dd, J = 7.5, 0.9 Hz, 1H, CH_{Py}), 7.28 (dd, J = 9.3, 7.2 Hz, 1H, CHPy), 7.04 (s, 2H, CH_{Mes}), 2.36 (s, 3H, CH_3), 2.07 (s, 6H, CH_3).

Data is consistent with that reported in the literature.[76]

Synthesis of 5-azido-2-mesityl-imidazo[1,5-a]pyridinium bromide

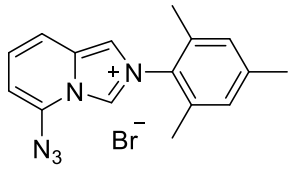

Sodium azide (300 mg, 4.62 mmol) was added to a stirred solution of 5-Bromo-2-mesityl-imidazo[1,5-a]pyridinium bromide (1.5 g, 4.2 mmol) in dry DMF (20 mL) under N_2, and the mixture was stirred at rt for 3 days. The reaction mixture was concentrated under vacuum and the residue was extracted by DCM 5 mL and washed with H_2O (2 x 5 mL). The DCM solution was dried by Na_2SO_4 followed by filtration and concentration. The residue was purified by flash chromatography (SiO_2, CH_2Cl_2/acetone: 7/3 to 1/2) to give the title compound.

^{1}H NMR (400 MHz, $CDCl_3$) δ 9.65 (d, J = 1.8 Hz, 1H, NCHN), 8.29 (d, J = 1.8 Hz, 1H, CH_{Im}), 8.00 (d, J = 9.3 Hz, 1H, CH_{Py}), 7.44-7.30 (m, 1H, CH_{Py}), 6.92 (s, 2H, CH_{Mes}), 2.25 (s, 3H, CH_3), 1.96 (s, 6H, CH_3). **^{13}C NMR** (101 MHz, $CDCl_3$) δ 141.45(C_{Mes}), 133.84(C_{Mes}), 132.58(**C**$_{py}N_3$), 131.60(**C**$_{py}$), 130.92 (2C, **C**H_{Mes}), 129.66 (2C, **C**H_{Mes}, 126.25(**C**$_{py}$H), 123.41(N**C**$_{im}$HN), 116.00(**C**$_{im}$H), 115.08(**C**$_{py}$H),

105.15(**C**$_{py}$H), 21.02(**C**H$_{3Mes}$), 17.41(2C, **C**H$_{3Mes}$). Data is consistent with that reported in the literature.[76]

Hydrosilylation of carvone[75]

a). Carvone (S or R, 40 μL, 0.265 mmol) was added to a solution of Aib-functionalized NHC rhodium(I) complexes (1 mol %) and diphenylsilane (90 μL, 0.48 mmol) in CD_2Cl_2 (0.4 mL) in sealed NMR tubes at room temperature. After 3days the solution became yellow from colourless.

b). Carvone (S or R, 20 μL, 0.1325 mmol) was added to a solution of Aib-functionalized NHC rhodium(I) complexes (1 mol %) and diphenylsilane (45 μL, 0.24mmol) in CD_2Cl_2 (0.4 mL) in sealed NMR tubes at room temperature. After 3days the solution became yellow from colourless.

c). Carvone (S or R, 20 μL, 0.1325 mmol) was added to a solution of Aib-functionalized NHC rhodium(I) complexes (1 mol %) and diphenylsilane (45 μL, 0.24mmol) in CD_2Cl_2 (0.4 mL) in NMR tube at room temperature. Then $AgBF_4$ (1 mol%) was added to the solution with formation of brown precipitate. After 3 days the solution was dark.

The peaks of C**H**OSiPh$_3$ were used to calculate cis and trans silyl protected carveol. For S-carvone the product peaks (C**H**OSiPh$_3$) are at 4.59, 4.36 ppm and R-cavone 4.54, 4.32 ppm.

Hydrosilylation of *S*-carvone

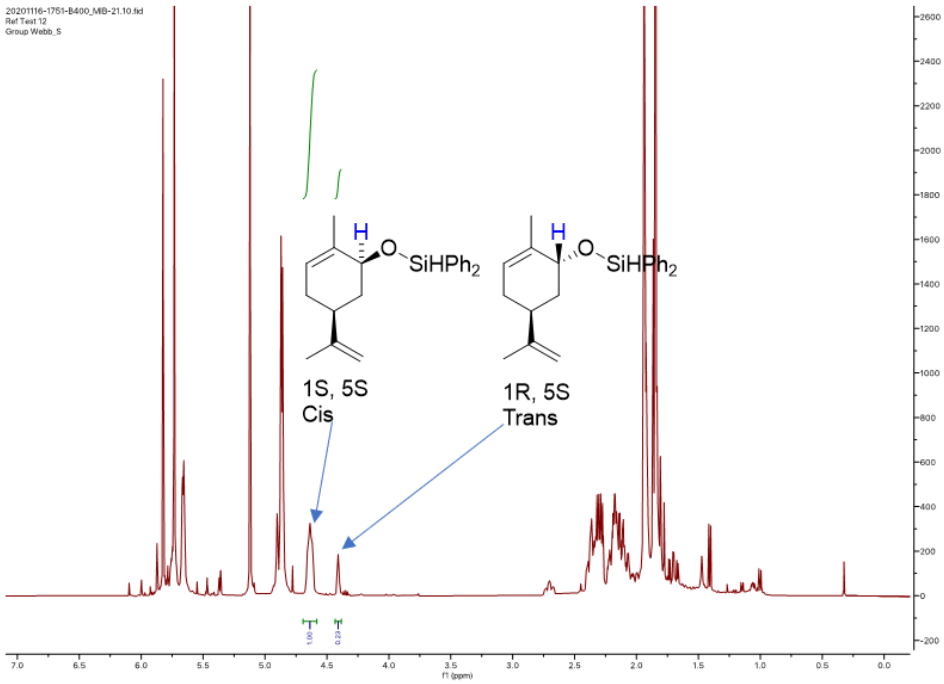

Hydrosilylation of *R*-carvone

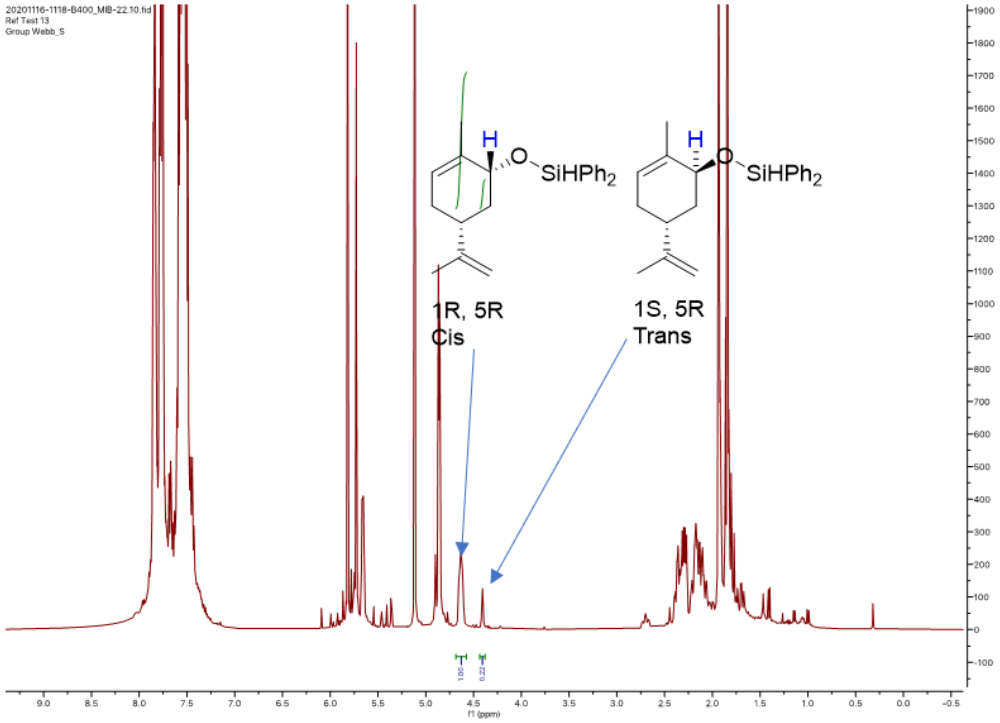

Hydrosilylation of terminal alkynes

The hydrosilylation of terminal alkynes was performed with reactant alkynes (77 μmol, 1 eq.), Me_2PhSiH (85 μmol, 1.1 eq.) and Rh catalyst (1 mol %) in solvent $CDCl_3$ 0.4 mL in sealed NMR tubes at room temperature.[69]

Hydrosilylation of 1-hexyne

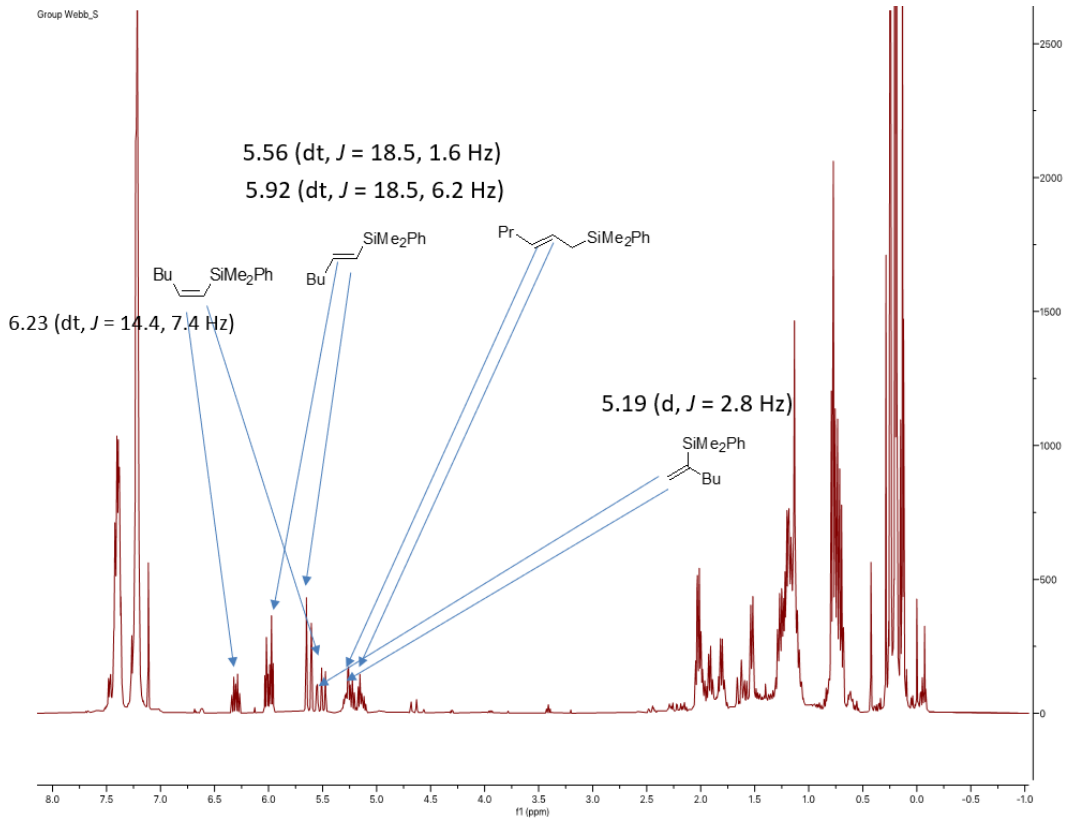

Hydrosilylation of phenylacetylene

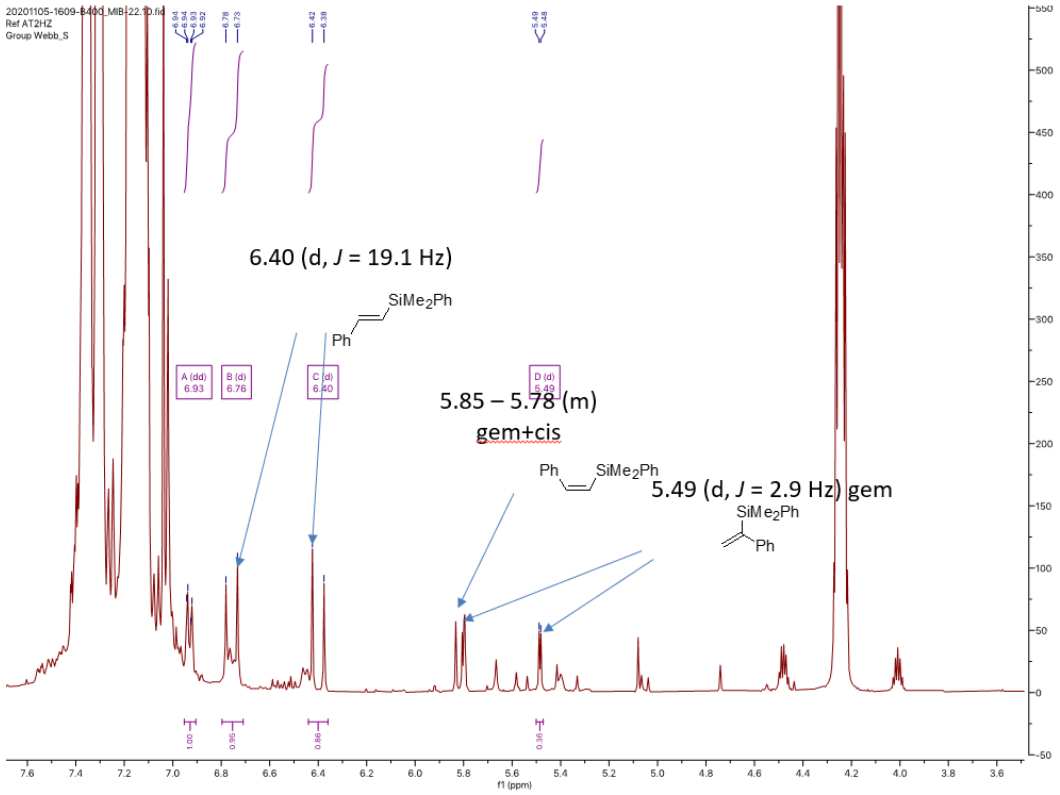

7 References

[1] (a) S. H. Gellman, *Acc. Chem. Res*., 1998, *31*, 173–180; (b) D. J. Hill, M. J. Mio, R. B. Prince, T. S. Hughes, J. S. Moore, *Chem. Rev.* 2001, *101*, 3893–4012; (c) G. Guichard, I. Huc *Chem. Commun*., 2011, *47*, 5933–5941; (d) C. M Goodman, S. Choi, S. Shandler, W. F. DeGrado *Nature Chem. Biol.* 2007, *3*, 252-262; (e) S. Hecht, I. Huc, Foldamers: structure, properties, and applications, Wiley-VCH, Weinheim, 2007.

[2] B. A. F. Le Bailly, J. Clayden *Chem. Commun.*, **2016**, *52*, 4852-4863.

[3] K. Maeda, E. Yashima, Dynamic Helical Structures: Detection and Amplification of Chirality. Topics in Current Chemistry, vol 265. Springer, Berlin, Heidelberg, 2006.

[4] S. J. George, Z. Tomovic, A. P. H. J. Schenning and E. W. Meijer, *Chem. Commun*., 2011, 47, 3451–3453.

[5] M. De Poli, M. De Zotti, J. Raftery, J. A. Aguilar, G. A. Morris and J. Clayden, *J. Org. Chem.* 2013, 78, 2248−2255.

[6] S. J. Pike, T. Boddaert, J. Raftery, S. J. Webb and J. Clayden, *New J. Chem.*, 2015, 39, 3288.

[7] C. Toniolo and E. Benedetti, *Trends in Biochemical Sciences*, 1991, 16, 350-353.

[8] (a) C. Toniolo, M. Crisma, F. Formaggio, C. Peggion, Wiley Periodicals, Inc. Biopolymers (Pept Sci) 60: 396–419, 2001; (b) Pengo, B.; Formaggio, F.; Crisma, M.; Toniolo, C.; Bonora, G. M.; Broxterman, Q. B.; Kamphius, J.; Saviano, M.; (c) Iacovino, R.; Rossi, F.; Benedetti, E. J. Chem. Soc., Perkin Trans. 2 1998, 1651.

[9] J. Clayden, A. Castellanos, J. Sol and G. A. Morris, *Angew. Chem. Int. Ed.*, 2009, 48, 5962 –5965.

[10] M. De Poli and J. Clayden, *Org. Biomol. Chem.*, 2014, 12, 836.

[11] V. Diemer, J. Maury, B. A. F. Le Bailly, S. J. Webb and J. Clayden, *Chem. Commun.*, 2017,53, 10768.

[12] B. A. F. Le Bailly and J. Clayden, *Chem. Commun.*, 2014, 50, 7949-7952.

[13] J. Sola, G. A. Morris, and J. Clayden, *J. Am. Chem. Soc.*, 2011, 133, 3712–3715.

[14] S. J. Pike, M. De Poli, W. Zawodny, J. Raftery, S. J. Webb and J. Clayden, *Org. Biomol. Chem.*, 2013, 11, 3168-3176.

[15] F. G. A. Lister, N. Eccles, S. J. Pike, R. A. Brown, G. F. S. Whitehead, J. Raftery, S. J. Webb and J. Clayden, *Chem. Sci.*, 2018, 9, 6860-6870.

[16] M. De Poli, L. Byrne, R. A. Brown, J. Sola, A. Castellanos, T. Boddaert, R. Wechsel, J. D. Beadle, and J. Clayden, *J. Org. Chem.,* 2014, 79, 4659−4675.

[17] U. Orcel, M. De Poli, M. De Zotti, and J. Clayden, *Chem. Eur. J.,* 2013, 19, 16357 – 16365.

[18] J. Sola, S. P. Fletcher, A. Castellanos, and J. Clayden, *Angew. Chem. Int. Ed.*, 2010, 49, 6836 –6839.

[19] G. Krauss, Biochemistry of Signal Transduction and Regulation, Fifth, Completely Revised Edition, Wiley-VCH Weinheim, 2014.

[20] D. Mazzier, M. Crisma, M. De Poli, G. Marafon, C. Peggion, J. Clayden, and A. Moretto, *J. Am. Chem. Soc*., 2016, 138, 8007−8018.

[21] R. A. Brown, V. Diemer, S. J. Webb and J. Clayden, Nature Chemistry, 2013, 5, 853-860

[22] N. Eccles, B. A. F. Le Bailly, F. d. Sala, I. J. Vitorica-Yrezabal, J. Clayden and S. J. Webb, *Chem. Commun.,* 2019, 55, 9331.

[23] T. Boddaert, J. Sola, M. Helliwell and J. Clayden, *Chem. Commun.*, 2012, **48**, 3397–3399

[24] L. Byrne, J. Sola, T. Boddaert, T. Marcelli, R. W. Adams, G. A. Morris, and J. Clayden, *Angew. Chem. Int. Ed.* 2014, 53, 151 –155.

[25] B. A. F. Le Bailly, L. Byrne, V. Diemer, M. Foroozandeh, G. A. Morris and J. Clayden, *Chem. Sci.*, 2015, 6, 2313–2322.

[26] F. G. A. Lister, B. A. F. Le Bailly, S. J. Webb and J. Clayden, *Nature Chemistry*, 2017, 9, 420-425.

[27] M. Zagnoni, *Lab Chip*, 2012, 12, 10965--10968

[28] H. T.Tien and E. A. Dawidowicz, *J. Colloid Interface Sci.,* 1966, 22, 438-453.

[29] D. Rousseau and R. R. Rafanan, Microemulsions as Nanoscale Delivery Systems, Comprehensive Biotechnology, Elsevier, 2011, ISBN 978-0-08-088504-9.

[30] A. S. Hauser, S. Chavali, I. Masuho, L. J. Jahn, K. A. Martemyanov, D. E. Gloriam, and M. M. Babu, *Cell*, 2018, 172, 41–54.

[31] T. K. Bjarnadottir, D. E. Gloriam, S. H. Hellstrand, H. Kristiansson, R. Fredriksson, H. B. Schioth, *Genomics*, 2006, 88, 263–273

[32] M. B. Emerit, C. Baranowski, J. Diaz, A. Martinez, J. Areias, J. Alterio, J. Masson, E. Boue-Grabot, and M. Darmon, *The Journal of Neuroscience*, 2016, 36, 1456 –1470.

[33] R. Bekus and T. Schrader, *ChemistryOpen,* 2020, 9, 667–682.

[34] K. Palczewski, *Annu. Rev. Biochem.*, 2006. 75, 743–67.

[35] L. Byrne, J. Sola and J. Clayden, *Chem. Commun.*, 2015, 51, 10965.

[36] J. M. Brown, P. H. Dixneuf, A. Fürstner, L. S. Hegedus, P. Hofmann, P. Knochel, G. van Koten, S.Murai, M. Reetz, Topics in Organometallic Chemistry, Springer-Verlag 2007.

[37] A. T. Biju, N-Heterocyclic Carbenes in Organocatalysis, Wiley-VCH, 2019.

[38] S. Bellemin-Laponnaz and S. Dagorne, *Chem. Rev.* 2014, 114, 8747−8774.

[39] D. Zhang and G. Zi, *Chem. Soc. Rev.*, 2015, 44, 1898.

[40] D. M. Khramov, V. M. Lynch, and C. W. Bielawski, *Organometallics*, 2007**,** *26*, 6042-6049.

[41] M. N. Hopkinson, C. Richter, M. Schedler1 and F. Glorius, *Nature*, 2014, 510, 485-496.

[42] T. J. Seiders, D. W. Ward and R. H. Grubbs, *Org. Lett.*, 2001, **3**, 3225 —3228.

[43] B. A. Arndtsen and L. Gong, Asymmetric Organocatalysis Combined with Metal Catalysis, Springer Nature, 2020.

[44] J. C. Sheehan and D. H. Hunneman, J. Am. Chem. Soc., 1966, 88, 3666–3667.

[45] M. T. Powell, D. R. Hou, M. C. Perry, X. Cui and K. Burgess, *J. Am. Chem. Soc*., 2001, 123, 8878–8879.

[46] M. C. Cassani, M. A. Brucka, C. Femoni, M. Mancinelli, A. Mazzanti, R. Mazzoni and G. Solinas, *New J.Chem.*, 2014, 38, 1768-1779.

[47] Y. Ryu, G. Ahumada and C. W. Bielawski, *Chem. Commun.*, 2019, 55, 4451

[48] Bethany M. Neilson and Christopher W. Bielawski, *Chem. Commun.*, 2013, 49, 5453.

[49] V. W. Yam, J. K. Lee, C. Ko, and N. Zhu, *J. Am. Chem. SOC.*, 2009, *131*, 912–913.

[50] R. Visbal and M. Concepcion Gimeno, *Chem. Soc. Rev.*, 2014, 43, 3551.

[51] M. Basauri-Molina, C. F. Riemersma, M. A. Wurdemann, H. Kleijn and R. J. M. Klein Gebbink, *Chem. Commun.*, 2015, 51, 6792.

[52] Y. Z. Huang, H. Miao, Q. H. Zhang, C. Chen, J. Xu, *Catal. Lett.*, 2008, 122, 344-348.

[53] Z. Q. Zhu, S. Xiang, Q. Y. Chen, Z. Zeng, Y. P. Cui, J. C. Xiao, *Chem. Commun.*, 2008, 0, 5016-5018.

[54] Y. Zhao, S. R. Gilbertson, *Org. Lett.*, 2014, 16, 1033−1035.

[55]. M. Kab, J. Hohenberger, M. Adelhardt, E. M. Zolnhofer, S. Mossin, F. W. Heinemann, J. Sutter, K. Meyer, *Inorg. Chem.*, 2014, 53, 2460−2470.

[56] Staining with iodine, http://umich.edu/~orgolab/Chroma/TLCView2.html (accessed Dec, 12 2020).

[57] B. Yigit, M.Yigit, I. Ozdemir, *Inorganica Chim. Acta*, 2017,75–79.

[58] I. J. B. Lin and C.S. Vasam, *Coord. Chem. Rev.*, 2007, 642–670

[59] M. C. Cassani, M. A. Brucka, C. Femoni, M. mancinelli, A. Mazzanti, R. Mazzoni, G. Solinas, *New J. Chem.*, 2014, **38**, 1768-1779.

[60] C. Balan, R. Pop, V. Comte, D. Poinsot, V. Ratovelomanana-Vidal and P. Gendre, *Appl. Organometal. Chem.*, 2014, 28, 517–522.

[61] K. Yasui, K. Fugami, S. Tanaka, and Y. Tamaru, *J. Org. Chem.*, 1995, 60, 1365-1380.

[62] J. Cipot, R. McDonald, M. J. Ferguson, G. Schatte, and M. Stradiotto, *Organometallics*, 2007, 26, 594-608.

[63] C. A. Swamy P, A. Varenikov, and G. Ruiter, *Organometallics*, 2020, 39, 247−257.

[64] A. L. Blach and D. E. Oram, *J. Organomet. Chem.*, 1988, 245-256.

[65] L. Busetto, M. C. Cassani, C. Femoni, M. Mancinelli, A. Mazzanti, R. Mazzoni, and G. Solinas, *Organometallics*, 2011, 30, 5258–5272.

[66] M. V. Jiménez, J. J. Pérez-Torrente, M. I. Bartolomé, V. Gierz, F. J. Lahoz, and L. A. Oro, *Organometallics*, 2008, *27*, 224–234.

[67] C. Jun and R. H. Crabtree, *Journal of Organometallic Chemistry*, 1993 177-187.

[68] C. Wang, D. Ikhlef, S. Kahlal, J. Saillard and D. Astru, *Coordination Chemistry Reviews*, 2016 1–20.

[69] Recent Advances in the Hydrosilylation of Alkynes, http://www.scientificspectator.com/documents/silicone%20spectator/Alkyne%20Hydrosilylation%20. (accessed 02, 25 2020).

[70] Y. Na and S. Chang, *Org. Lett.* 2000, 2, 13, 1887–1889.

[71] a). Y. Kitano, T. Matsumoto and F. Sato, *Tetrahedron*, 1988, 44, 4073-4086; b). M. G. McLaughlin and M. J. Cook, *Chem. Commun*., 2011, 47, 11104–11106; c). S. Nakamura, M. Uchiyama and T. Ohwada, *J. Am. Chem. Soc.* 2004, 126, 36, 11146–11147.

[72] C. Burstein, C. W.Lehmann, F. Glorius, *Tetrahedron*, 2005, 61, 6207−6217.

[73] A. J. Arduengo, R. Krafczyk, R. Schmutzler, H. A. Craig, J. R. Goerlich and W. J. Marshall, *Tetrahedron* 1999, 55, 14523−14534.

[74] D. Toummini, A. Tlili, J. Berges, F. Ouazzani and M. Taillefer, *Chem. Eur. J*. 2014, 14619 – 14623

[75] A. Szadkowska , E. Zaorska, S. Staszko, R. Pawłowski, D. Trzybiński, K. Woźniak, *Eur. J. Org. Chem.* 2017, 4074–4084.

[76] K. Azouzi, C. Duhayon, I. Benaissa, N. Lugan, Y.Canac, S. Bastin, and V. César, *Organometallics*, 2018, 37, 4726−4735.

[77] D. P. Shelar, D. R. Birari, R. V. Rote, S. R. Patil, R. B. Toche and M. N. Jackak, *J. Phys. Org. Chem.*, 2011. 24. 203-211.

[78] J. P. Morales-Ceron, P. Lara, J. pez-Serrano, L. L. Santos, Ve. Salazar, E. Alvarez, and A. Suarez, *Organometallics*, 2017, 36, 2460−2469

[79] J. Wolf, A. Labande, J. Daran and R. Poli, *Eur. J. Inorg. Chem.* 2007, 5069–5079.

[80] S. P. Nolan, *Acc. Chem. Res.*, 2011, 91-100.

[81] D. Tilly, 2021, *Building catalysts of dynamic chirality for reaction of stimuli controlled enantioselectivities*, Manchester Institute of Biotechnology, University of Manchester, unpublished.